Title	Higher order Effects on the Anisotropic Structures and the Monomer-Dimer Transition of High-Density Hydrogen
Author(s)	蛯名, 邦禎
Citation	大阪大学, 1982, 博士論文
Version Type	VoR
URL	https://hdl.handle.net/11094/441
rights	
Note	

Higher order Effects on the

Anisotropic Structures and

the Monomer-Dimer Transition

of High-Density Hydrogen

Kuniyoshi EBINA

April, 1982

Abstract

In the structural expansion for the ground-state energy of simple metals, the higher-order effects are studied. To take account of the exchange-correlation effects on the higher order polarizations, the effective vertex approximation is examined in the asymptotic forms up to fourth order, with finding its validity region limited by the singularity of the higher order polarizations. A new resummation scheme is presented in a cluster expansion based on the variational principle of Luttinger and Ward. A general method for evaluating the many-point ring diagrams is also presented.

Higher order effects on the high-density hydrogen system are studied. The mechanism for the stability of the filamentary structure is clarified in connection with the singularity of higher order polarizations, where the numerical results are also presented in proof of our theory. It is shown that the resummation effect does not change the situation.

Monomer-dimer transition of hydrogen is studied in the bcc [111] model. It is pointed out that exchange-correlation effects on the fourth order energy are considerable, though a large cancellation occurs with contributions from the Hubbard H-graph. The fifth-order effect is studied for the first time. The transition pressure is predicted to be 2.3Mbar at $r_s = 1.4$ in the fifth-order stage without effect of the zero-point motion of protons.

Acknowledgements

CONTENTS

I   Introductory Part

§1. Phase diagram

Hydrogen is the simplest but most abundant element in the universe. The solar abundances by mass are predicted to be 76% for H and 22% for He.[1] The cosmic abundances are known to be nearly the same. Hydrogen exists in a wide range of circumstances; as the most dilute place we have the intergalactic space and as an extremely dense place the interior of stars and giant planets. According to the variety of circumstances we have the variety of its existing forms; atomic, molecular, plasma and condensed states.

Construction of the phase diagram of hydrogen in the whole p-T plane is a challenging subject. At low pressures and at low temperatures it forms a molecular solid ($\leq$14K at ordinary pressure). At elevated temperatures hydrogen molecules are dissociated and then ionized to form the proton-electron plasma at $10^4 \sim 10^5$K. On the other hand at low temperature and at high pressures, hydrogen is supposed to form a condensed ionized state, namely metallic hydrogen. To such formation of low temperature plasma a crucial role is played by the quantum mechanical nature of electrons.

In Fig.1 we show a global picture for the phase diagram of hydrogen. In drawing the phase diagram we refer mainly to a classic work by Brush, Sahlin and Teller.[2] They drew the phase diagram of Fe, whence we obtain the similar one for H with appropriate modification. In Fig.1 we mention the melting curve of proton

lattice, which is characteristic of hydrogen; the melting occurs even at zero temperature. The cold melting comes out due to the zero-point motion effect of protons, as pointed out first by Abrikosov.[3] We estimate the melting point at 0K from Akrikosov's formula

$$a \sim 5 \cdot 10^{-11} / Z^2 A \text{ cm} \qquad (1)$$

where a denotes the lattice constant, Z the atomic number, and A the atomic weight. We note that the critical lattice constant becomes exceedingly small even for helium. At the side of high temperature the melting curve is drawn with the use of Pollock and Hansen's Monté Carlo result[4]

$$T_M = 1500 \, \rho^{1/3} \text{ K} \qquad (2)$$

where T_M denotes the melting temperature and ρ the density in g cm^{-3}.

For the high density plasma an important parameter is

$$\Gamma = \frac{Z^2 e^2}{a \, k_B T} \quad , \qquad (3)$$

where e denotes the electron charge, k_B the Boltzmann constant, T the absolute temperature and a the radius of ionic sphere. In Fig.1 some of the curves are drawn for Γ = const. For large values of Γ the plasma is strongly coupled. The study for such plasma has been one of developing fields.[5] The critical curves for

the nuclear fusion to occur are also shown roughly in
Fig.1.

§2. Molecular hydrogen

In free state, hydrogen forms diatomic molecule in the ground
state with binding energy [6] -1.1645 Ry. This simplest molecule
has been a touchstone for ensuring our knowledge about the binding
mechanism of molecules. Accordingly, a great deal of theoretical
studies have been done for the binding energy of hydrogen molecule
as well as its properties with considerably high accuracy from
the first principle. [7] If the effect of molecular vibration is
neglected, the ground-state energy of a molecule has been estab-
lished to be [8]

$$- 1.1745 \text{ Ry per atom} \qquad (4)$$

with equilibrium proton distance 0.74 A , that is

$$1.40 \text{ bohr} . \qquad (5)$$

By including the zero-point vibration effect, the measured binding
energy is in agreement with the theoretical one with accuracy of
10^{-4}. The first vibrational level is extremely high and esti-
mated to be about 6000K. [8] Here we note that 1 Ry corresponds
to the termperature 1.58×10^5 K.

In the solid state, molecular hydrogen shows interesting

properties, which mainly come from the quantum nature of the rotational degree of freedom. The H_2 molecules are classified into two species; orthohydrogen with the odd rotational quantum number J and parahydrogen with even J, owing to the Fermi statistics of protons. The first rotational energy level of para H_2 is about 510.K and that for ortho H_2 is much higher.[8] We note that the hydrogen molecule has the highest rotational constant $\hbar^2/2I$ among molecules owing to its smallest moment of inertia I.

For solid hydrogen, the intermolecular interaction is considerably weak at low pressure. Accordingly, valuable informations on the anisotropic intermolecular forces have been obtained from various properties of solid orthohydrogen. The main part of the anisotropic force is the electric quadrupole-quadrupole interaction,[9] whence the Pa3 structure of the solid ortho-hydrogen comes out as the low temperature phase.[10]

At zero pressure, solid hydrogen has a small density $\rho = 0.09$ g/cm^3, which corresponds to about $r_s = 3.1$. Here r_s is the radius of the equivalent sphere to the volume per electron divided by the bohr radius $a_0 = 0.529$ Å. In the low pressure region, the volume v_0 per mole is used as a parameter, which is related to r_s by

$$v_0 = 2 \times 0.374 \, r_s^3 \, \text{cm}^3/\text{mole}.$$

For compressed solid hydrogen, our knowledge about the equation of state (EOS) is very poor. It is because the current

expression for the intermolecular force is based on approximations relevant to the region of low density (de Boer 1942,[11] Evett and Margenau 1953[12]). The assumption of constant separation between protons limits the relevancy. Recent studies with many configurations taken into account show that the effect of the change of proton separation is not small.[13]

We also mention the many-body force, which would bring about larger effect with increasing density. An attempt to evaluate the three-body force has been done by Ree and Bender,[14] who claimed its effect to be important in explaining EOS obtained from the shock wave experiments

§3. Metallic hydrogen

Metallic hydrogen provides us with a unique condensed system which can be treated from the first principle . Furthermore the thermodynamic properties of this system and its mixture with helium play crucial roles in studying the constitution of Jupiter and Saturn.[15]

The first study of metallic hydrogen was done by Wigner and Huntington.[16] One of their motivations was to examine the Wigner= Seitz theory for the cohesive energy of metals. A relevant theory must predict the cohesive energy of metallic hydrogen smaller than that of the molecular hydrogen. For bcc they obtained the ground= state energy -1.05Ry, which is surely higher than that for the

molecular state. Kronig, de Boer and Korringa[17] also treated the same system with main concern in the internal constitution of the Earth.

After appearance of these pioneering works various methods have been developed for calculating the cohesive energy of metals. With the use of these methods, metallic hydrogen was re-attacked by many authors.[18~45] Among them we mention the simple r_s-expansion, which Carr utilized with a result for the ground-state energy nearly indentical to Wigner and Huntington's one.[16] . Almost all the calculations have been confined to the cubic crystal. Eventually the estimates to the ground-state energy are nearly -1.05Ry, Wigner and Huntington's value.

Exceptional study has been done by the Kagan group.[22] They carried out calculations for the structure-dependent energy of metallic hydrogen in a great variety of crystal forms, finding the filamentary structure with considerable lowering of the ground= state energy. Their estimate is close to -1.10Ry.[23]

§4. Molecule-metal transition

The molecule-metal transition is one of the main concerns about our system. This might also be treated from the first principle. However most of the studies employ different methods for two branches, namely metallic and molecular phases. The estimates of the transition pressure show a broad spectrum, 0.5Mbar

∿5Mber. The main reason for such uncertainty may be attributed to our poor knowledge of EOS for the molecular phase. For the metallic phase, however, confinement to cubic phase may be another weak point.

An exceptional study was done by Harris et al,[24∿26] who treated the metallic and molecular phase in a scheme of the Hatree= Fock approximation though they used the different modification of orbitals for different phases. They have shown occurrence of the first-order transition, assuming bcc structure. However their. estimate for the ground-state energy is considerably high, though the r_s-value at the transition may be of reasonable magnitude.

In spite of many efforts with the use of various methods,[46] the metal-molecule transition has not been solved.

Here, we mention the experimental status on the compressed solid hydrogen.[47] The melting point of solid hydrogen rises from 14K to the higher termperature as the pressure increases.[48] According to the recent experiment by Mao and Bell,[49] the solid phase is stable at room termperature under 50kbar. The same authors compressed it up to 600kbar, where they found the refractive index of hydrogen to be comparable to that of ruby. Though their highest pressure attained is still far from the molecule-metal tansition, they observed that the intramolecular vibration begins to soften at 400kbar.[50] A similar experiment has also been done at 5 K by the other authors.[51]

The molecule-metal transition of hydrogen must exist in the

outer layer of Jupiter, which is a giant hydrogen planet. The
pressure ranges from ∿1bar at the surface to ∿100Mbar at the core.
Owing to poor knowledge of the EOS and of the properties of hy-
drogen, both in the vicinity of the transition point, we still
have difficulties in unfolding a complete story about Jupiter.[52]

§5. Scope of the present thesis

The r_s-expansion is a method effective in the high density
region, where the theory starts with the electron gas distributed
uniformly. This is just what happens in the limit of high density.
If the electron-ion interaction is switched on, the electrons
would tend to concentrate around each ion. This tendency may be
treated by the perturbation method with the electron-ion inter-
action as a perturbation, as far as the density is not considerably
low. However a naive treatment of the r_s-expansion would be ef-
fective only in an extremely limited region of validity. Some in-
geneous technique is necessitated to extend the validity region.
This is the structural expansion, as developed by Brovman et al.
and by others.[53]

At this point we are in close contact with the many-body
theory of the electron system. The many-body theory has developed
considerably after the war, where one of the most important tech-
niques consists in the use of the Green's funciton.[54] We shall use
the temperature Green's function in developing our theory. We men-

tion Matsubara,[55]who invented the temperature Green's function.

The key quantities to the structural expansion are the higher order polarizations,which correspond to the many-point diagrams according to the language of the many-body theory. Many-body effect on the higher order polarization is very important to obtain a reliable result in the intermediate density region. For the dielectric function of the electron gas, which reduces to the second order polarization, a great deal of efforts have been devoted to clarify the many-electron effect.[56] It is not the case for the higher order polarizations, though some attempts have been done.[53] A critical study will be presented in Part II for the many-electron effect on the higher order polarizations. The resummation of the perturbation series has also been one of the problems in the structural expansion. For it we also present a new scheme (II).

In III we present a general method for evaluations of the many-point diagrams. This method is simpler and more comprehensive than the previous work.[57] The general formula presented for the anomalous diagrams is entirely new and may be thought valuable for evaluating the fluctuation of spins and of current.

On the basis of these results, we shall study the higher order effect on the ground-state energy of high density hydrogen. The stability of the filamentary structure is also one of our subjects. The mechanism for the occurrence of the above structure will be clarified in connection with the singularity of the third=

order polarization. It may be interesting to see that the stable
structure must be cubic for helium by the same mechanism as the
anisotropic structure is stabilized for hydrogen in the inter-
mediate region of density. The metal-molecule transition will be
discussed with reference to the bcc [111] model,[44] a filamentary
structure. Density at the transition is obtained for each stage
of the approximation , where the true position of the critical
density may be predicted, whithout zero-point motion effect of
protons. The similar data will also be given for the transition
pressure. These are presented in Part IV.

References

1) M. Podlak and A.G.W. Cameron, Icarus 22 (1974), 123.

2) S.G. Brush, H.L. Sahlin and E. Teller, J. Chem. Phys. 45 (1966), 2102.

3) A.A. Abrikosov, Zh. Eksp. Teor. Fiz. 39 (1960), 1797 [Soviet Phys. JETP 12 (1961), 1254].

4) E.L. Pollock and J.P. Hansen, Phys. Rev. A8 (1973), 3110.

5) G. Kalman ed., Strongly Coupled Plasmas (Plenum, New York, 1978).

6) G. Herzberg and A. Monfils, J. Mol. Spectrosc. 5 (1960), 482.

7) For review, I.F. Silvera, Rev. Mod. Phys. 52 (1980), 393.

8) W. Kolos and L. Wolnievicz, J. Chem. Phys. 49 (1968), 404.

9) T. Nakamura, Prog. Theor. Phys. 14 (1955), 135.

10) R.L. Mills and A.F. Schuch, Phys. Rev. Lett. (1965), 1131.

11) J. de Boer, Physica 9 (1942), 363.

12) A.A. Evett and H. Margenau, Phys. Rev. 90 (1953), 1021.

13) F.H. Ree and C.F. Bender, J. Chem. Phys. 71 (1979), 5362.

14) F.H. Ree and C.F. Bender, Phys. Rev. Lett. 32 (1974), 85.

15) T. Gehrels ed. Jupiter (Univ. of Arizona Press, Tucson,1976).

16) E. Wigner and H.B. Huntington, J. Chem. Phys. 3 (1935), 764.

17) R. Kronig, J. de Boer and J. Korringa, Physica 12 (1946), 245.

18) A. Bellemans and M. DeLeener, Phys. Rev. Lett. 6 (1961), 603.

19) W.J. Carr, Jr., Phys. Rev. 128 (1961), 120.

20) T. Schneider, Helv. Phys. Acta $\underline{42}$ (1969), 957.

21) T. Schneider and E. Stoll, Helv. Phys. Acta $\underline{43}$ (1970), 453.

22) E.G. Brovman, Tu. Kagan and A. Kholas, Zh. Eksp. Teor. Fiz. $\underline{61}$ (1971), 2429; $\underline{62}$ (1972), 1942 [Sov. Phys. JETP $\underline{34}$ (1972) 1300; $\underline{35}$ (1972), 783].

23) E.G. Brovman, Yu. Kagan, A. Kholas and V.V. Pushkarev, ZhETF Pis. Red. $\underline{18}$ (1973), 269 [JETP Lett. $\underline{18}$ (1973), 160].

24) F.E. Harris, L. Kumar and H.J. Monkhorst, Phys. Rev. $\underline{B7}$ (1973), 2850.

25) D.E. Ramaker, L. Kumar and E.F. Harris, Phys. Rev. Lett. $\underline{34}$ (1975), 812.

26) F.E. Harris and J. Delhalle, Phys. Rev. Lett. $\underline{39}$ (1977), 1340.

27) J. Hammerberg and N.W. Ashcroft, Phys. Rev. $\underline{B9}$ (1974), 409.

28) H. Beck and D. Straus, Helv. Phys. Acta $\underline{48}$ (1975), 655.

29) D. Straus and N.W. Ashcroft, Phys. Rev. Lett. $\underline{38}$ (1977),415.

30) C. Friedli and N.W. Ashcroft, Phys. Rev. $\underline{B16}$ (1977), 662.

31) J.F. Dobson and N.W. Ashcroft, Phys. Rev. $\underline{B16}$(1977), 5326.

32) L. Caron, Phys. Rev. $\underline{B9}$ (1974), 5025.

33) 1. Caron, Comments Sol. State Phys. $\underline{6}$ (1975), 103.

34) Yu. Kagan, V.V. Pushkarev and A. Kholas, Zh. Eksp. Teor. Fiz- $\underline{73}$ (1977), 967 [Sov. Phys. JETP $\underline{46}$ (1977), 511].

35) M. Ross, J. Chem. Phys. $\underline{60}$ (1974), 3634.

36) H. Nagara, H. Miyagi and T. Nakamura, Prog. Theor. Phys. $\underline{56}$ (1976), 396.

37) H. Miyagi, T. Nakamura and H. Nagara, Phys. Lett. $\underline{62A}$ (1977) 171.

38) V.V. Avilov and S.V. Iordanskii, Fiz. Tverd. Tela $\underline{19}$ (1977), 3516 [Sov. Phys. Solid State $\underline{19}$ (1977), 2054].

39) Yu. Kagan, L.A. Maksimov and A.E. Trenin, Zh. Eksp. Teor. Fiz. $\underline{75}$ (1978), 1729 [Sov. Phys. JETP $\underline{48}$ (1978), 871].

40) V. T. Rajan and C.-W. Woo, Phys. Rev. $\underline{B18}$ (1978), 4048.

41) S. Chacravarty and N. W. Ashcroft, Phys. Rev. B$\underline{18}$ (1978),4048.

42) M.D. Whitmore, J.P. Carbotte and R.C. Shukla, Can. J. Phys.

43) H. Nagara, Thesis, Osaka University, 1979.

44) H. Nagara, H. Miyagi and T. Nakamura, Prog. Theor. Phys. $\underline{64}$ (1980),731.

45) S. Chakravarty, J. H. Rose, D. Wood and N. W. Ashcroft, Phys. Rev. $\underline{B24}$ (1981), 1624.

46) For review, M. Ross and C. Shishkevish, R-2056-ARPA, Rand,1977.

47) For review of earliar works see, A.L. Ruoff, Report#2850, Material Science Center, Cornell Univ. (1977).

48) D.H. Liebenberg, R.L. Mills and J.C. Bronson, Phys. Rev, B$\underline{18}$ (1978), 4526.

49) H.K. Mao and P.M. Bell, Science $\underline{203}$ (1979), 1004.

50) S.K. Sharma, H.K. Mao and P.M. Bell, Phys. Rev. Lett. $\underline{44}$, (1980), 886.

51) J. van Strarten, R.J. Wijngarden and I.F. Silvera, Phys. Rev. Lett. $\underline{48}$ (1982), 97.

52) W. B. Hubbard and R. Smoluchowski, Space Sci. Rev. <u>14</u> (1973), 599; also Ref 15).

53) E. G. Brovman and Yu. Kagan, Uspekhi Fiz. Nauk <u>112</u> (1974), 369 [Sov. Phys. Uspekhi <u>17</u> (1974), 125].

54) A.A.Abrikosov, L.P. Gorkov and I.E. Dzyaroshinski, <u>Method of Quantum Field Theory in Statistical Physics</u>, (Dover, New York, 1963).

55) T. Matsubara, Prog. Theor. Phys. <u>14</u> (1955), 351.

56) For review, V.D. Gorobchenko and E. G. Maksimov, Uspekhi Fiz. Nauk, <u>130</u> (1980), 65 [Sov. Phys. Uspekhi <u>23</u> (1980), 35].

57) E.G. Brovman and A. Kholas, Zh. Eksp. Teor. Fiz. <u>66</u> (1974), 1877 [Sov. Phys. JETP <u>39</u> (1974), 924].

Figure Caption

Fig.1. Global phase diagram for hydrogen. The melting curve
in the molecular region is plotted after Liebenberg et al's
data (Ref. 48). A supposed melting curve in the metallic
region is shown by wavy line. The thin broken lines represent
the isobars, obtained from a rough interpolation between the
low temperature limit and the high temperature one. The elec-
tron degeneracy line in the plasma region is also plotted
(——··——). The adiabat in Jupiter (——·——) is drawn
after Steevenson and Salpeter in Ref. 15. See text for the
other lines.
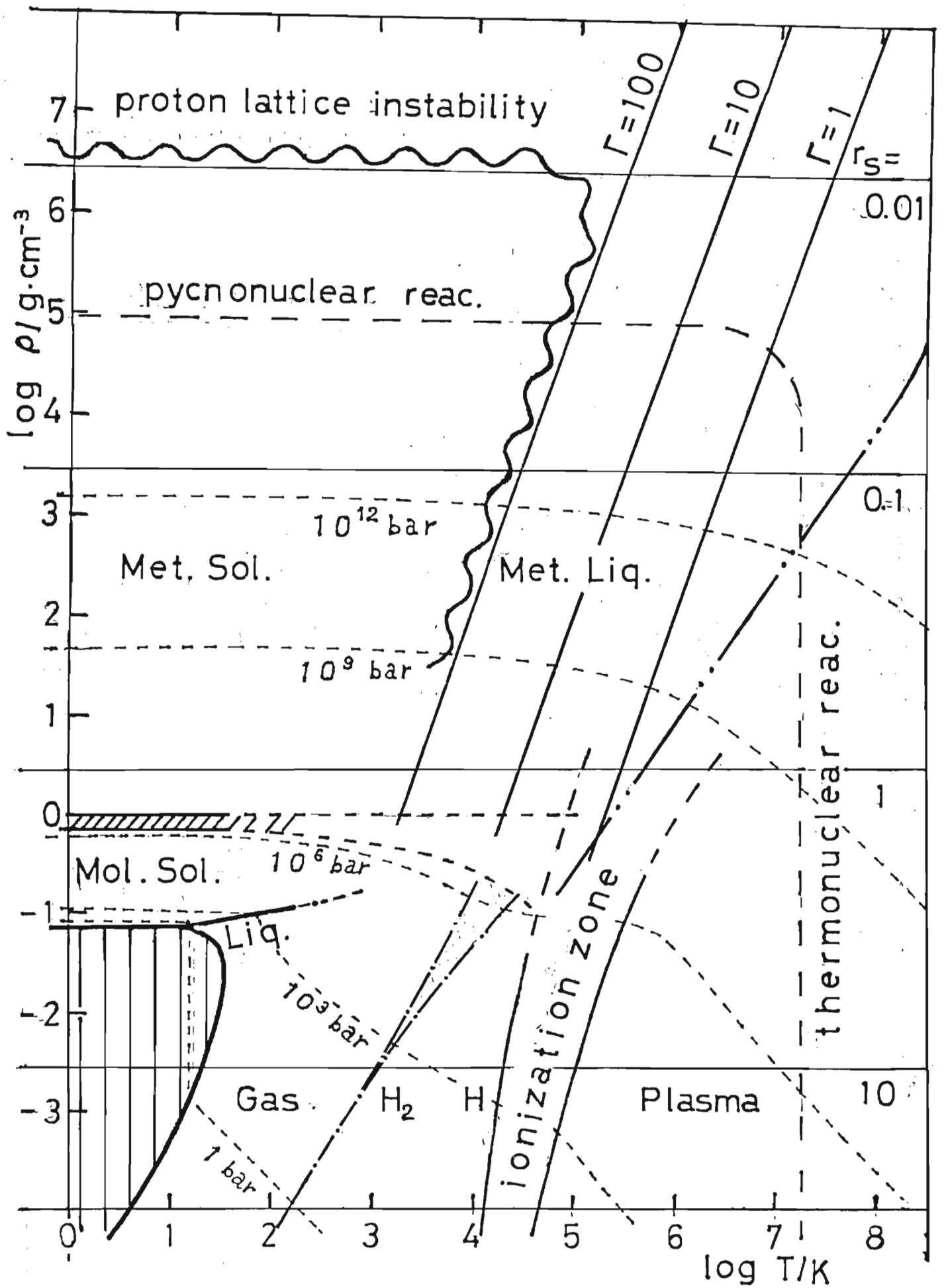
II Structural Expansion, Vertex Function

and Cluster Expansion

§1. Introduction

The structure dependence of the ground-state energy of metals has been studied by many authors.[1] The method of pseudopotential expansion has been successfully used to explain the observed crystal structure of simple metals or their alloys,[1,2] for which the second order perturbation is usually used. Lloyd and Sholl[3] presented a structural expansion in an effective field approach analogous to that of Hohenberg, Kohn and Sham[4,5] and first derived the third order term. Brovman and Kagan[6,7] developed a many particle theory for this problem and extensively applied it to the dynamical properties of non-transition metals.[7] They also attacked the problem of metallic hydrogen[8,9] using the results up to the third order perturbation.

In the case of metallic hydrogen, higher order terms are important. Hammerberg and Ashcroft (HA)[10] used the finite temperature technique and discussed the fourth order effect in the electron-ion interaction, where they considered the relevant diagrams partially. Their scheme is essentially the expanion in terms of the effective electron-ion potential shielded by the Lindhard dielectric function so that the exchange and higher order correlation effects are completely neglected. We mention Yasuhara and Watabe,[11] who pointed out the importance of the correlation effect. We note here that the effect of the Fermi surface distortion was first teken into account by Carr,[12] and later by HA, where the

latter authors also examined the resummation of a partial series
from the higher order terms. On the other hand, Brovman et al.
discussed the singularity of the higher order diagrams[13] and de-
veloped a technique of integrating the many-point ring diagrams[14]
(see part III). They also examined the effect of the choice of
dielectric function[15] and proposed an effective-vertex (T-factor)
approximation[7,16] to the n-point polarization ($n \geq 3$) diagrams.
However the nature of this approximation was not clear.

In a series of papers[17-20], which will hereafter be referred
to as STI, STII, STIII and STIV in order, Nakamura, Miyagi and
Nagara critically studied the higher order effects both in the
electron-ion and electron-electron interactions (See also Ref.
21). All the diagrams up to the fourth order are examined in terms
of RPA-screened interaction line. The first order correction was
evaluated in the Thomas-Fermi approximation up to the three-point
polarization (STII). Dynamical effects were included in the prima-
ry correction to the RPA polarization (STIII), while the second
order corrections were calculated comprehensively in the Thomas=
Fermi approximation to obtain the static dielectric function (STIV).
A resummation of the anomalous terms of higher order in the e-
lectron-ion interaction was also considered with some new result
(STI).

In this part, we shall consider some of the higher order ef-
fects still neglected in STI-IV and examine methods of taking ac-
count of them with application to the high-density hydrogen in

mind.　Method of calculating higher order many-point ring dia-grams will be described in III .

Our Hamiltonian is described in §2 together with the notations. The structural expansion of STII is rederived in somewhat differ-ent manner in §3.　In §4, an approximate treatment for the vertex factor is examined critically.　In §5, a resummation scheme is proposed, in terms of which all the higher order anomalous terms can be absorbed into the primary terms in the expansion.

§2.　Hamiltonian and notations

We shall consider the system　of N electrons, of which in the sea N_0 ions with charge Ze are embedded. The electron Hamiltonian is given by

$$H = \frac{\hbar^2}{2m} \sum_{p\sigma} p^2 a^\dagger_{p\sigma} a_{p\sigma} + \frac{1}{2} \frac{1}{V} \sum_q{}' \frac{4\pi e^2}{q^2} \sum_{p\ p'}$$

$$a^\dagger_{p+q,\sigma}\ a^\dagger_{p'-q,\sigma}\ a_{p',\sigma}\ a_{p,\sigma}$$

$$+ \frac{N}{V} \sum_g{}' \frac{4\pi e^2}{g^2} S(g) \sum_{p,\sigma} a^\dagger_{p+g,\sigma}\ a_{p,\sigma}\ , \tag{1}$$

where the first term represents the kinetic energy, the second one the electron-electron interaction and the third one the electron= ion interaction, with V the volume of the system.　Here $S(g)$ is

the structure factor

$$S(g) \equiv \frac{1}{N_0} \sum_i e^{-ig \cdot R_i}$$

$$= \frac{1}{N} \sum_i Z e^{-ig \cdot R_i} . \tag{2}$$

Here the reciprocal lattice vector is denoted by g, which will be used separately from q, the quasi-continous wave-vector.

In the following, we put $\hbar = 1$, and measure the energy in Ry $= me^4/2\hbar^2$, and the momentum in units of the Fermi momentum $p_F = (3\pi^2 N/V)^{1/3}$. And we introduce the parameter r_s as the radius of the equivalent sphere to the volume per electron devided by the Bohr radius $a_0 = \hbar^2/me^2$. This convention of units is equivalent to putting $e^2 = 2/(\alpha r_s)$, $m = (\alpha r_s)^2/2$, and $N/V = (3\pi^2)^{-1}$, where e is the unit charge, m the electron mass and $\alpha = (4/9\pi)^{1/3} \doteq 0.5211$. Furthermore, we prefer the factor (1/N) to (1/V) for the momentum summation. This is a convenient procedure when we consider the energy per electron.

According to the above conventions Hamiltonian (1) becomes

$$H = H_0 + H_2 + H_1 , \tag{3}$$

$$H_0 = \sum_{p\sigma} \varepsilon_p a_{p\sigma}^\dagger a_{p\sigma} \tag{4-a}$$

$$H_2 = \frac{1}{2} \frac{1}{N} \sum_q{}' v(q) \sum_{\substack{pp' \\ \sigma}} a_{p+q,\sigma}^\dagger a_{p'-q,\sigma}^\dagger a_{p',\sigma}^\dagger a_{p,\sigma} \tag{4-b}$$

$$H_1 = - \sum_g {}' S(g) v(g) \sum_{p\sigma} a^\dagger_{p+g,\sigma} a_{p\sigma} , \qquad (4\text{-c})$$

where

$$\varepsilon_p \equiv \frac{\hbar^2}{2m} p^2 \to \frac{p^2}{(\alpha r_s)^2}$$

$$v(q) \equiv \frac{N}{V} \frac{4\pi e^2}{q^2} \to \frac{1}{(\alpha r_s)} (\frac{8}{3\pi}) \frac{1}{q^2} \qquad (5)$$

Now r_s plays a role of scaling parameter and may be thought as a coupling constant: $(\alpha r_s) \sim v(q)/\varepsilon_p$.

In constructing the Hamiltonian (1), we have taken the usual procedure of treating q = 0 term. Since we neglect the ion motion, the rest of the energy is merely the ion Madelung energy, which can be written as[22,23]

$$E_M = \frac{1}{2} \{ \sum_g {}' v(g) S(g) S(-g) - \frac{Z}{N} \sum_q {}' v(q) \} . \qquad (6)$$

Our main problem is to calculate the total energy E per electron in the ground state as a function of r_s and as a functional of S(g):

$$E = \frac{1}{N} < H_0 + H_2 + H_1 > + E_M \qquad (7)$$

The pressure of the system is obtained from

$$P = - \frac{1}{4\pi r_s^2} \frac{\partial E}{\partial r_s} \qquad (8)$$

in the atomic unit (= 147 Mbar). Equation (8) reflects the fact that the concept of pressure is closely related to a scaling transformation..

§3. Structural expansion

We shall evaluate the ground-state energy E of the electron system under the external potential H_1. To take account of the deformation of the Fermi surface, it is convenient to use the finite-temperature perturbation theory,[24] in which we have the expansion of the thermodynamical potential with respect to the electron-ion interaction. Thus, by the thermodynamic relation we can obtain the ground-state energy of the system.

(A) Thermodynamical potential

According to Luttinger and Ward,[25,26] the thermodynamical potential Ω can be expressed in terms of the temperature Green's function $G_\sigma(p, p'; \zeta_\ell)$, where p denotes the electron momentum, σ the spin state, and $\zeta_\ell = (2\ell+1)\pi i/\beta + \mu$, $\ell = 0, \pm1, \pm2, \cdots$, where μ denotes the electron chemical potential and $\beta = k_B T$. This function is a natural generalization of the free electron thermal propagator

$$G_\sigma^0(p ; \zeta_\ell) = (\zeta_\ell - \epsilon_p)^{-1} , \qquad (9)$$

by which the thermodynamical potential Ω_0 of this system can be

obtained as:[25]

$$\Omega_0 = -2N\int_p \ln[-G^0(p)]^{-1}e^{\zeta 0+}$$

$$= -\frac{2}{\beta}\sum_p \ln[1+e^{\beta(\mu-\varepsilon_p)}]. \tag{10}$$

Here we use the abbreviation $p = (p, \zeta_\ell)$, $\int_p \equiv N^{-1}\sum_p \beta^{-1}\sum_{\zeta_\ell}$ in accord with STII. In Eq.(10), the factor 2 comes from the spin summation, and the summation over frequency ζ_ℓ is performed by the well-known contour integration.[25]

The functional introduced by Luttinger and Ward may be written in the following form:[26,27]

$$\Omega[G] = -\frac{1}{\beta}\sum_\ell \text{tr}\{\ln[-G(\zeta_\ell)]^{-1} + [G^0(\zeta_\ell)]^{-1}G(\zeta_\ell)-1\}+\Phi[G], \tag{11}$$

where the matrices G and G^0 stand for $G(p, p')$ and $G^0(p)\delta_{p,p'}$ respectively, and tr designates the trace of the matrix indices p, p'. The functional $\Phi[G]$ is given by the sum of closed linked skeleton diagrams with weight $1/n$, where n is the number of the Green's function included in each diagram. (Examples of the skeleton diagrams are shown in Fig.1.) Then the functional derivative of $\Phi[G]$ with respect to G gives the self-energy:

$$\Sigma(p,p';\zeta_\ell) = \frac{\delta\Phi[G]}{\delta G(p',p;\zeta_\ell)}. \tag{12}$$

See Fig.2 for the self-energies corresponding to the linked skeletons in Fig.1.

Now the Dyson equation

$$G^{-1} = [G^0]^{-1} - \Sigma \; , \tag{13}$$

may be derived by the variational principle $\delta\Omega/\delta G = 0$. Then the expression for the thermodynamical potential becomes[25]

$$\Omega = \Omega_0 - \frac{1}{\beta} \sum_{\ell} \text{tr}\{ \ell n [1 - G^0(\zeta_\ell)\Sigma(\zeta_\ell)] + \Sigma(\zeta_\ell)G(\zeta_\ell) \} + \Phi[G] \; , \tag{14}$$

where 1 stands for the unit matrix.

Now our problem is how to approximate the functional form of $\Phi[G]$. If we start with the skeletons of b) and c) of Fig.1., an expansion is obtained in terms of the RPA-screened external field given by HA. To take account of the exchange and correlation effect properly, we must include the diagrams a) of Fig.1 and the higher order ones. In the following we restrict our discussion to the effect of the diagrams a). (Higher order effects were considered in STIV.) Thus, from Eq.(12) we have

$$\Sigma(p,p+g) = w(g) + 2v(g) \int_p G(p,p+g)e^{\zeta 0^+}$$

$$- \sum_{g'} \int_q [v(q)\varepsilon^{-1}(q,q+g')]G(p-q,p-q+g-g') \; , \tag{15}$$

where the inverse dielectric tensor $\varepsilon^{-1}(q, q+g')$ is given by the relation

$$\varepsilon(q,q+g) = \delta_{g,0} - v(q)\Pi(q,q+g),$$

$$\Pi(q, q+g) = 2 \sum_{g'} \int_p G(p, p+g') G(p+g'+q, p+g+q) \ . \tag{16}$$

These quantities were utilized by Hubbard.[28~30] In Eq.(15) $w(g)$ stands for the external line (Fig.2 c):

$$w(g) = -v(g)S(g) \ . \tag{17}$$

Now, as in STII we expand G and Σ with respect to the external lines:

$$G(p, p+q) = \sum_{n \geq 0} G^{(n)}(p, p+g) \ ,$$

$$\Sigma(p, p+g) = \sum_{n \geq 0} \Sigma^{(n)}(p, p+g) \ . \tag{18}$$

The zeroth order solution will be taken to be the corresponding functions for the electron gas system:

$$G^{(0)}(p, p+g) = G(p)\delta_{g,0} \ ,$$

$$\Sigma^{(0)}(p, p+g) = \Sigma^{(0)}(p)\delta_{g,0} \ , \tag{19}$$

where

$$G(p)^{-1} = G^0(p)^{-1} - \Sigma^{(0)}(p) \ , \tag{20}$$

and

$$\Sigma^{(0)}(p) = -\int_{p'} \tilde{v}^{(0)}(p-p') G(p') e^{\zeta' 0^+} \tag{21}$$

in our approximation.

Here $\tilde{v}^{(0)}(q)$ denotes the screened internal line given by

$$\tilde{v}^{(0)}(q) = v(q)/[1 - v(q)\tilde{\Pi}^{(0)}(q)] \; ,$$

$$\tilde{\Pi}^{(0)}(q) = 2\int_p G(p)G(p+q) \; . \tag{22}$$

The screened internal line is shown in Fig.2a by double wavy line. If we replace $G(p)$ by $G^0(p)$ in Eqs.(21) and (22), then $\tilde{\Pi}^{(0)}(q)$ reduces to the RPA polarization $\Pi^{(0)}(q)$. In the above approximation the last term of Eq.(14) reduces to the ring diagram contribution:

$$\Phi[G^0] = \frac{1}{2}\int_q \ln[1 - v(q)\Pi^{(0)}(q)] \; . \tag{24}$$

On the other hand the higher order contributions from the self=energy $\Sigma^{(0)}(p)$ is included in the logarithmic term of Eq.(14).

Next, from Eq.(13), $G^{(1)}$ proves to be of the form

$$G^{(1)}(p,p+g) = G(p)\Sigma^{(1)}(p,p+g)G(p+g) \; . \tag{25}$$

Using the above expression we obtain

$$\Sigma^{(1)}(p,p+g) = \tilde{w}(g)\Lambda_g(p) \tag{26}$$

from Eqs.(15) and (16). Here $\tilde{w}(g)$ is given by

$$\tilde{w}(g) = w(g)/\epsilon(g) \; , \tag{27}$$

with $\epsilon(g)$ the static dielectric function of the uniform system:

$$\varepsilon(g) = 1 - v(g)\Pi(g) \ ,$$

$$\Pi(g) = 2\int_{p'} G(p')G(p'+g)\Lambda_g(p') \ . \tag{28}$$

The vertex function $\Lambda_g(p')$ may be obtained from a solution of the integral equation:

$$\Lambda_g(p) = 1 - \int_{p'} \gamma(p,p';g)G(p')G(p'+g)\Lambda_g(p') \ , \tag{29}$$

where the kernel function $\gamma(p,p';g)$[31] is given by

$$\gamma(p,p';g) = -\tilde{v}^{(0)}(p-p')-2\int_{p''}\tilde{v}^{(0)}(p-p'')\tilde{v}^{(0)}(p-p''+g)$$

$$\times G(p'')[G(p''-p+g') + G(p-p''+p'+g)] \ . \tag{30}$$

Contributions to $\Pi(g)$ are given explicitly by Eqs.(3.13) to (3.16) of STⅡ up to second order in $\tilde{v}^{(0)}$. We note that the present approximation does not include the term $\tilde{\Pi}_{2,2}^{(b)}$ of STⅡ.

For the higher order terms, Eq.(13) gives

$$G^{(n)}(p,p+g) = G(p)[v_g^{(n)}(p) + \Sigma^{(n)}(p,p+g)]G(p+g) \ ,$$

$$n \geqq 2 \ , \tag{31}$$

where the proper self-energy parts $\Sigma^{(n)}$ of higher order are obtained by replacing thin lines in Fig.2a,b by the higher order propagators:

$$\Sigma^{(n)}(p,p+g) = 2v(g) \int_{p'} G^{(n)}(p',p'+g)$$

$$- \int_{p'} \tilde{v}^{(0)}(p-p')G^{(n)}(p',p'+g) + \cdots . \qquad (32)$$

In Eq.(31) the function $v_g^{(n)}(p)$ stands for the improper self=
energy, which is of the form

$$v_g^{(n)}(p) = [G(p+g)]^{-1} \sum_{g'} \sum_{s=1}^{n-1} \Sigma^{(s)}(p,p+g')G^{(n-s)}(p+g',p+g) . \quad (33)$$

Examples of $\Sigma^{(n)}$ are given in Fig.3.

By using these quantities, the thermodynamical potential is
obtained from Eq.(14) with substitution of Eq.(18),in the ex-
panded form:

$$\Omega = \Omega_{eg} + \Omega_2 + \Omega_3 + \Omega_4 + \cdots , \qquad (33)$$

where Ω_{eg} is the contribution from the system of uniform electron
gas and may be written as

$$\Omega_{eg} = -N \int_p \ln[-G^{(0)}(p)]^{-1} + [\Phi_0 - N \int_p \Sigma^{(0)}(p)G^{(0)}(p)] ,$$

$$\Phi_0 \equiv \Phi[G^{(0)}] . \qquad (34)$$

The structure dependent part $\Omega_{st} = \Omega - \Omega_{eg}$ may be expanded from

$$\Omega_{st} = -\frac{1}{\beta} \sum_{\ell} \text{tr } \ln\{1 - G^{(0)}(\zeta_\ell)[\Sigma(\zeta_\ell) - \Sigma^{(0)}(\zeta_\ell)]\}$$

$$+ \{\Phi[G] - \Phi_0\} - \{\frac{1}{\beta} \sum_{\ell} \text{tr}[\Sigma(\zeta_\ell)G(\zeta_\ell) - \Sigma^{(0)}(\zeta_\ell)G^{(0)}(\zeta_\ell)]\} . \quad (35)$$

Here the logarithmic term is a single-particle like contribution, where the correlation effects are absorbed in the self-energy, while the remaining terms may be thought as a correction for double counting which comes in ordinarily in the single-particle description.

We write down straightforwardly the expansion of the first and last terms of Eq.(35), which we denote by $\Omega^{(i)}$ and $\Omega^{(iii)}$ respectively. The result is

$$\Omega^{(i)} = \frac{1}{\beta} \sum_{\ell} tr\{\frac{1}{2}[G^{(0)}\Sigma^{(1)}]^2\}$$

$$+ \frac{1}{\beta} \sum_{\ell} tr\{\frac{1}{3}[G^{(0)}\Sigma^{(1)}]^3 + [G^{(1)}\Sigma^{(2)}]\}$$

$$+ \frac{1}{\beta} \sum_{\ell} tr\{\frac{1}{4}[G^{(0)}\Sigma^{(1)}]^4 + \frac{1}{2}[G^{(0)}\Sigma^{(2)}]^2$$

$$+ G^{(0)}\Sigma^{(1)}G^{(0)}\Sigma^{(3)} + [G^{(0)}\Sigma^{(1)}]^2 G^{(0)}\Sigma^{(2)}\}$$

$$+ \cdots , \tag{36}$$

$$\Omega^{(iii)} = -\frac{1}{\beta} \sum_{\ell} tr\{G^{(2)}\Sigma^{(0)} + [G^{(0)}\Sigma^{(1)}]^2\}$$

$$- \frac{1}{\beta} \sum_{\ell} tr\{G^{(3)}\Sigma^{(0)} + 2G^{(1)}\Sigma^{(2)}\}$$

$$- \frac{1}{\beta} \sum_{\ell} tr\{G^{(4)}\Sigma^{(0)} + 2G^{(1)}\Sigma^{(3)} + G^{(2)}\Sigma^{(2)}\}$$

$$- \cdots . \tag{37}$$

In writing down Eqs.(36) and (37) some terms have been dropped out, since they cancel each other in the resultant of $\Omega^{(i)}$ and $\Omega^{(ii)}$.

The expansion of the term $\Omega^{(iii)}$ may be obtained by a diagramatic analysis, or by expanding $\Phi[G]$ in a Taylor series

$$\Phi[G] = \Phi_0 + \frac{\delta\Phi}{\delta G}\bigg|_{G=G(0)}\Delta G + \frac{1}{2}\frac{\delta^2\Phi}{\delta G\delta G}\bigg|_{G=G(0)}\Delta G\Delta G + \cdots \qquad (38)$$

with the help of the relation

$$\frac{\delta\Phi}{\delta G} = \Sigma \ , \qquad \delta\Sigma = G^{-1}\delta G G^{-1} \ . \qquad (39)$$

The result is as follows.

$$\Omega^{(ii)} = \frac{1}{\beta}\sum_{\ell} \mathrm{tr}\{G^{(2)}\Sigma^{(0)} + \frac{1}{2}[G^{(1)}(\Sigma^{(1)}-w)] + G^{(1)}w\}$$

$$+ \frac{1}{\beta}\sum_{\ell} \mathrm{tr}\{G^{(3)}\Sigma^{(0)} + [G^{(1)}(\Sigma^{(2)}-\Sigma_F^{(2)})] + \frac{1}{3}G^{(1)}\Sigma_F^{(2)}\}$$

$$+ \cdots \ , \qquad (40)$$

where $(w)_{p,p+g} \equiv w(g)$ and $\Sigma_F^{(2)}$ corresponds to the diagram F of Fig.3.

Collecting terms from $\Omega^{(i)}$, $\Omega^{(ii)}$ and $\Omega^{(iii)}$, we obtain the series:

$$\Omega_2 = \frac{1}{\beta}\sum_{\ell} \mathrm{tr}\{\frac{1}{2}G^{(0)}\Sigma^{(1)}G^{(0)}w\}$$

$$\Omega_3 = \frac{1}{\beta} \sum_{\ell} \text{tr}\{\frac{1}{3}[G^{(0)}\Sigma^{(1)}]^3 - \frac{2}{3} G^{(1)}\Sigma_F^{(2)}\} . \qquad (41)$$

The above result is essentially identical with that of STⅡ apart from the second term of Ω_3 (See Fig.4a), which was not explicitly written down previously. This term comes in naturally in our procedure. Though we shall not treat it, the following may be interesting to note. The mentioned term is analogous to a second order term shown in Fig.4b, whose importance was pointed out by Geldart and Vosko[31], and analysed by Geldart and Taylor[32,33]. Such terms would be necessary in the scheme of expansion with respect to a screened internal line in order to keep the consistency[31].

The following may also be worth noting. According to our procedure, a peculiar form of the second order term Ω_2 comes out as a result of the correction of double counting. This characteristic feature of our formalism will be useful in treating both of an effective approximation to the vertex factor (§4) and the resummation of the perturbation series (§5) so as to avoid overcounting. Moreover, such a term does not appear in the third order term Ω_3. This fact is closely related to the " H-reducibility" argument by Hubbard.[28,30] A H-type diagram appears in fourth order as pointed out by HA[10]. It is because the factor attached to the skeleton b) of Fig.1 does not cancel that of the self-energy contribution.

In Eq.(41), the matrix products in trace reduces to the sum over reciprocal lattice vectors. The frequency and momentum sum-

mations may be performed beforehand to give sturcture independent quantities. These quantities were called Π_n in STII, where n stands for the power of the external potential. In the actual calculation, these quantities are further expanded with respect to the free electron propagator $G^0(p)$ and the RPA screened interacion $\tilde{v}^0(q)$. Here the latter is the primary term of $\tilde{v}^{(0)}(q)$ and given by

$$\tilde{v}^0(q) = v_2(q)/\varepsilon^0(q) , \qquad (42)$$

with

$$\varepsilon^0(q) = 1 - v_2(q)\Pi^{(0)}(q) ,$$

$$\Pi^{(0)}(q) = 2 \int_p G^0(p)G^0(p+q) . \qquad (42a)$$

The resulting contributions are shown diagramatically in Fig.5.

(B) Ground-state energy

By the procedure described above, we can calculate the thermodynamical potential Ω under a constant value of the chemical potential μ. However, simple use of the perturbation procedure does not conserve the particle number N.[32] This problem was treated in STI[17] and also in HA[10] in connection with the deformation of the Fermi surface. We shall below look into this problem briefly.

Assume that the thermodynamical potential Ω is given as a function of μ and of a parameter λ.

$$\Omega = \Omega(\mu;\lambda) \ , \ 0 \le \lambda \le 1 \ . \tag{43}$$

then the condition

$$- \left(\frac{\partial\Omega}{\partial\mu}\right)_\lambda = \bar{N} \ (= \text{constant}) \tag{44}$$

gives a curve $\mu = \mu_{\bar{N}}(\lambda)$ in the $\lambda - \mu$ plane (Fig.6.), which is determined by the differential equation

$$\frac{d\mu_{\bar{N}}}{d\lambda} = - \left(\frac{\partial^2\Omega}{\partial\mu\partial\lambda}\right) \Big/ \left(\frac{\partial^2\Omega}{\partial\mu^2}\right) \tag{45a}$$

with the initial condition

$$\mu_{\bar{N}}(\lambda=0) = \mu_0 \ . \tag{45b}$$

Here Eq.(45) is obtained by the differentiation of Eq.(44) with respect to λ.

Now the Legendre transformation at zero-temperature gives us

$$\bar{N}E(\bar{N},\lambda) = \Omega(\mu_{\bar{N}}(\lambda),\lambda) + \bar{N}\mu \ , \tag{46a}$$

where E is the energy per electron. From the above expression we get

$$\bar{N} \left.\frac{dE}{d\lambda}\right|_{\bar{N}} = \left.\frac{\partial\Omega}{\partial\lambda}\right|_{\mu=\mu_{\bar{N}}(\lambda)} \tag{46b}$$

under the condition of Eq.(41). If Ω is given as a power series

with respect to λ at $\mu = \mu_0$ and if the μ-derivatives of Ω are well behaved , then $\mu_{\bar{N}}(\lambda)$ and $E(\bar{N}, \lambda)$ may also be expanded in Taylor series with respects to λ:

$$\mu = \mu_0 + \lambda\mu_1 + \lambda^2\mu_2 + \cdots ,$$

$$E = E_0 + \lambda E_1 + \lambda^2 E_2 + \cdots . \tag{47}$$

Then

$$\mu_1 = -\, \Omega_1' / \Omega_0'' \quad .$$

$$\mu_2 = -(\Omega_2' + \Omega_1''\mu_1 + \tfrac{1}{2}\Omega_0'''\mu_1) / \Omega_0'' \tag{48a}$$

and

$$\bar{N}E_0 = \Omega_0 + \bar{N}\mu_0$$

$$\bar{N}E_1 = \Omega_1 ,$$

$$\bar{N}E_2 = \Omega_2 - \tfrac{1}{2}(\Omega_1')^2 / \Omega_0 ,$$

$$\bar{N}E_3 = \Omega_3 - \Omega_1'\Omega_2' / \Omega_0'' + \tfrac{1}{3}(\Omega_1')^2\Omega_1'' / (\Omega_0'')^2 . \tag{48b}$$

Here, primes denote the derivative with respect to μ at $\mu = \mu_0$. If Ω has no linear term in λ, then the result is much simplified:

$$\mu_1 = 0 , \quad \mu_2 = -\Omega_2' / \Omega_0'' , \quad \mu_3 = -\Omega_3' / \Omega_0'' ,$$

$$\mu_4 = -(\Omega_4' + \Omega_2'' \mu_2 + \tfrac{1}{2} \Omega_0''' \mu_2{}^2) / \Omega_0'' , \qquad (49a)$$

and

$$NE_1 = 0 , \quad NE_2 = \Omega_2 , \quad NE_3 \doteq \Omega_3 ,$$

$$NE_4 = \Omega_4 - \tfrac{1}{2}(\Omega_2')^2 / \Omega_0'' ,$$

$$NE_5 = \Omega_5 - \Omega_3' \Omega_2' / \Omega_0'' . \qquad (49b)$$

In accordance with the present problem, let us multiply the electron-ion potential $w(g)$ by λ. Then μ_0 and Ω_0 are the corresponding quantities for the system of the uniform gas μ_{eg} and Ω_{eg}. Thus Ω_0'' appearing in Eq.(49a,b) as the denominator reduces to the $q = 0$ limit of the static dielectric function defined by Eq.(28)

$$\Omega_{eg}'' / N = \Pi(0) . \qquad (50a)$$

The above expression may be derived from the differentiation of

$$N = 2 \sum_p \frac{1}{\beta} \sum_\ell G(p) e^{\zeta 0^+} \qquad (50b)$$

with respect to μ, where the Ward identity[27]

$$1 - \frac{d\Sigma^{(0)}(p)}{d\mu} = \Lambda_{g=0}(p) \qquad (51)$$

is to be used.

Finally we note that the power series method discribed above may break down when the denominator $\partial^2\Omega / \partial\mu^2$ in Eq.(45a) becomes small as λ increases. This quantity is related to q = 0 limit of the polarization tensor for the crystal given by Eq.(16), which might become small if the crystal undergoes the metal-insulator transition.

§4. Exchange and correlation effects
on the many-point polarization

In the previous section, a structural expansion of the ground= state energy has been described. The primary term in the structure dependent part E_{st} is of the form:

$$E_2 = \frac{1}{2} \sum_g' |w(g)|^2 \frac{\Pi_2(g)}{\epsilon(g)} \tag{52}$$

Here the two-point polarization $\Pi_2(g)$ is written simply as $\Pi(g)$ in §3, which is related to $\epsilon(q)$ by Eq.(28). The leading term in Π_2 is the Lindhard function $\Pi^{(0)}(q)$, which gives us the dielectric function $\epsilon^0(q)$ in RPA (Eq.(43)).

Many attempts have been done to take account of the exchange and correlation effects on $\Pi_2(q)$ (Refs. 29),31)∿33),35∿38) and STIII , STIV), and certain progress has been achieved, though the available results may still be somewhat far from the reliable knowledge about $\Pi(q)$ and $\epsilon(q)$ at metallic densities $(3 \leq \gamma_s \leq 6)$,

and particularly in the region of $|q| \sim 2$.   A current procedure is based on the Hubbard from

$$\Pi_2(q) = \frac{\Pi^{(0)}(q)}{1+\phi(q)\Pi^{(0)}(q)} \, , \qquad (53)$$

with modifications of the local field factor $\phi(q)$ from the original Hubbard's one.[29]

For n-th order energy E_n, the n-point polarization Π_n is the relevant quantity.   For example, the third order energy is of the form:

$$E_3 = \frac{1}{3} \sum_{\substack{g_1,g_2 \\ g_1 \neq g_2}}' \tilde{w}(g_1)\tilde{w}(g_2-g_1)\tilde{w}(-g_2)\Pi_3(g_1,g_2) \, . \qquad (54)$$

The primary contribution to Π_n comes from the n-point ring diagram $\Pi_n^{(0)}$.   This quantity was extensively studied by Brovman, Kagan and Kholas,[13,14] who have presented its evaluation method.   The treatment has been improved recently by Nakamura et al. (STI) and by the present auther (part III).

To take account of the exchange and correlation effects on Π_n ($n \geq 3$) is much more difficult than in the case of Π_2.   In STII, Miyagi et al studied the primary correction $\Pi_3^{(1)}$ to $\Pi_3^{(0)}$, by including the screened internal line in the Thomas-Fermi approximation.   The results indicate the importance of the exchange=correlation effects especially in the region of Brovman and Kagan's singularity.   This singularity occurs when the radius of circle

circumscribing a triangle formed by reciprocal lattice vectors g_1, g_2 coincides with the Fermi radius. The results applied to the problem of high-density hydrogen [39] show significant effects of the term $\Pi_3^{(1)}$. This fact may indicate that the exchange-correlation effects would be considerable also in the fourth order energy E_4. However any direct calculation of the mentioned correction to Π_n ($n \geq 4$) seems to be a formidable work, even in the first order. It is also the case for the higher order correction to Π_3. Thus an approximate procedure is needed to take into account the exchange-correlation effect.

For this problem, Brovman et al[7,15] proposed an effective vertex approximation. Their approximation is based on the following observation for the Hubbard approximation of the two-point polarization, $\Pi_2(g)$ given by Eq.(53). The mentioned approximation comes out with replacement of the exact vertex function in Eq.(28) by an approximate one

$$T(g) = \frac{1}{1+\phi(g)\Pi^0(g)} , \qquad (55)$$

where the momentum dependence of $\Lambda_g(p)$ is neglected. Further approximation lies in the replacement of the exact Green's function $G(p)$ by the free electron one $G^0(p)$. With these approximations the Hubbard formula (53) is obtained, according to Brovman et al. Now, by generalizing the above observation to the higher order polarization, they proposed an approximation of the form:

$$\Pi_3(g_1, g_2) = T(g_1)T(g_2-g_1)T(-g_2) \, \Pi_3^{(0)}(g_1, g_2) , \qquad (56)$$

with $T(g)$ given by Eq.(55).

However the replacement $\Lambda_g(p) \rightarrow T(g)$ and $G(p) \rightarrow G^0(p)$ cannot be separate approximations. This is because in Eq.(56) $\Pi_3^{(0)}(g_1, g_2)$ refers to the free propagator. Therefore, besides the vertex correction one must have the self-energy correction, coming from the replacement of $G(p)$ by $G^0(p)$, to be taken account of in the factor of $T(g)$. The self-energy correction may be considerable since the quasiparticle renormalization factor for $G^0(p)$ has proved substantially important.[11b] However, the vertex function $\Lambda_g(p)$ is known to have a strong momentum dependence, as pointed out by Yasuhara and Watabe.[11a] In actuality the error due to the neglect of the momentum dependence may be reduced largely as a result of momentum summations.

In spite of the above argument we agree with the approximation, on the basis of our analysis to be described later. However, Brovman et al[15] determined the T-factor by comparing both sides of Eq.(56) in the limiting case when one of g_i's approaches zero. In the above limit they use an identity

$$\frac{\Pi_3(g,0)}{[\epsilon(g)]^2} = -\frac{1}{2}\frac{d}{d\mu}\frac{\Pi_2(g)}{\epsilon(g)} \qquad (56a)$$

We shall examine the approximation from the opposite side since all g-vectors are of considerable length in the region of interest.

Let us now consider the primary terms bringing the T-factor, which stand for the first order terms in the electron-electron interaction. These primary contributions to $\Pi^{(0)}(g)$ may be of the form:

$$T^{(1)}(g) = - \phi(g) \, \Pi^{(0)}(g), \qquad (57)$$

in conformity with the original Hubbard argument. Accordingly the primary correction $\Pi_2^{(1)}$ to $\Pi^{(0)}$ may be written as

$$\Pi_2^{(1)}(g) = - \Pi^{(0)}(g)\phi(g)\Pi^{(0)}(g). \qquad (58)$$

Thus, if the approximation: Eq.(56) is relevant, the primary correction, $\Pi_3^{(1)}$, to $\Pi_3^{(0)}$ must be approximated by

$$\Pi_3^{(1)}(g_1,g_2) = - \{ \Pi^{(0)}(g_1)\phi(g_1) + \Pi^{(0)}(g_2)\phi(g_2)$$

$$+ \Pi^{(0)}(g_2-g_1)\phi^{(0)}(g_2-g_1) \} \Pi_3^{(0)}(g_1,g_2), (59)$$

with

$$\phi(g) = - \Pi_2^{(1)}(g)/[\Pi^{(0)}(g)]^2. \qquad (60)$$

See Fig.7, where the value of $\Pi_3^{(1)}(g_1,g_2)/ \Pi_3^{(0)}(g_1,g_2)$ is compared with the same ratio calculated by Eq.(59), both in the Thomas-Fermi approximation. The result shows a good agreement, unless the radius of circle circumscribing the triangle $<g_1,g_2>$ determined by g_1 and g_2 is smaller than the Fermi readius.

Let us then examine the asymptotic form of the considered ratio, expecting that the above agreement may hold for $\Pi_3^{(1)}$ even with the dynamically screened interaction, for which we have no available datum. We shall then write down $\Pi_3^{(1)}$ as

$$\Pi_3^{(1)}(g_1,g_2) = \Pi_3^{(1,a)}(g_1,g_2) + \Pi_3^{(1,b)}(g_1,g_2), \qquad (61)$$

where

$$\Pi_3^{(1,a)}(g_1,g_2) = - 2\int_p\int_{p'} G^0(p)G^0(p+g_1)G^0(p+g_2)\ \tilde{v}^0(p-p')$$

$$\times [G^0(p')G^0(p'+g_1) + G^0(p'+g_1)G^0(p'+g_2)$$

$$+ G^0(p'+g_2)G^0(p')],$$

$$\Pi_3^{(1,b)}(g_1,g_2) = - 2\int_p\int_{p'} G^0(p)G^0(p+g_1)G^0(p+g_2)\ \tilde{v}^0(p-p')$$

$$\times [G^0(p)G^0(p') + G^0(p+g_1)G^0(p'+g_1)$$

$$+ G^0(p+g_2)G^0(p'+g_2)]. \qquad (62)$$

In the above expressions, $\Pi_3^{(1,a)}$ corresponds to the first order correction to the vertex function and $\Pi_3^{(1,b)}$ to the correction from the self-energy insertions. (See Fig.5)

Now we examine the asymptotic form of $\Pi_3^{(1)}$. Here the following formula will be very useful:

$$\prod_{i=1}^{n} G^0(p+g_i) = \sum_{i=1}^{n} G^0(p+g_i) \prod_{j \neq i} \frac{1}{\varepsilon_{p+g_i} - \varepsilon_{p+g_j}},$$

$$g_i \neq g_j \quad \text{for} \quad i \neq j. \tag{63}$$

In addition to the above formula we also use

$$[G^0(p)]^2 = (\partial/\partial\varepsilon_p) \, G^0(p). \tag{64}$$

Then we obtain the expression for $\Pi_3^{(1)}$ as follows

$$\Pi_3^{(1)}(g_1, g_2) = J(g_1, g_2) + J(g_2 - g_1, -g_1) + J(-g_2, g_1 - g_2)$$

$$+ \tilde{J}_{g_2 - g_1}(g_1, -g_2) + \tilde{J}_{-g_2}(g_2 - g_1, g_1) + \tilde{J}_{g_1}(-g_2, g_2 - g_1)$$

$$+ R. \tag{65}$$

Here we put

$$J(g_1, g_2) = \frac{-2}{N^2} \sum_{p,p'} F_{p-p'}(p,p') \frac{1}{\varepsilon_p - \varepsilon_{p+g_1}} \cdot \frac{1}{\varepsilon_p - \varepsilon_{p+g_2}}$$

$$\times \left\{ \left[\frac{1}{\varepsilon_{p'} - \varepsilon_{p'+g_1}} - \frac{1}{\varepsilon_p - \varepsilon_{p+g_1}} \right] + \left[\frac{1}{\varepsilon_{p'} - \varepsilon_{p'+g_2}} - \frac{1}{\varepsilon_p - \varepsilon_{p+g_2}} \right] \right\}, \tag{66}$$

$$J_{g_3}(g_1, g_2) = \frac{-2}{N^2} \sum_{p,p'} F_{p+p'+g_3}(p,p') \frac{1}{\varepsilon_p - \varepsilon_{p+g_3}}$$

$$\times \{ [\frac{1}{\varepsilon_p - \varepsilon_{p+g_3}} + \frac{1}{\varepsilon_{p'} - \varepsilon_{p'+g_3}}] \cdot [\frac{1}{\varepsilon_p - \varepsilon_{p+g_1}} + \frac{1}{\varepsilon_p - \varepsilon_{p+g_2}}]$$

$$+ [\frac{1}{\varepsilon_p - \varepsilon_{p+g_1}} \cdot \frac{1}{\varepsilon_{p'} - \varepsilon_{p'+g_2}} + \frac{1}{\varepsilon_p - \varepsilon_{p+g_2}} \cdot \frac{1}{\varepsilon_{p'} - \varepsilon_{p'+g_1}}] , \quad (67)$$

$$R = \frac{-2}{N^2} \sum_{p,p'} [\frac{\partial}{\partial \varepsilon_p} F_{p-p'}(p,p')] \cdot [\frac{1}{\varepsilon_p - \varepsilon_{p+g_1}} \cdot \frac{1}{\varepsilon_p - \varepsilon_{p+g_2}}$$

$$+ \frac{1}{\varepsilon_p - \varepsilon_{p+g_2-g_1}} \cdot \frac{1}{\varepsilon_p - \varepsilon_{p-g_1}} + \frac{1}{\varepsilon_p - \varepsilon_{p-g_2}} \cdot \frac{1}{\varepsilon_p - \varepsilon_{p+g_2-g_1}}] , \quad (68)$$

where

$$F_q(p,p') = \frac{1}{\beta^2} \sum_{\ell,\ell'} \frac{v(q) \ G^0(p;\zeta_\ell) \ G^0(p';\zeta_{\ell'})}{\varepsilon^0(q,\zeta_\ell - \zeta_{\ell'})} . \quad (69)$$

In the above expressions R includes an anomalous contribution, which cancels the contribution from the first order shift of chemical potential. In Eqs.(66)∿(68) we shall neglect the contribution from the imaginary part of $1/\varepsilon^0(q,\varepsilon_p - \varepsilon_{p'}, -i0^+)$, which may be considered as a higher order term (see STII). Then the term R in Eq.(65) may be neglected and Eq.(69) becomes

$$F_q(p,p') = f(\varepsilon_p)f(\varepsilon_{p'}) \, \text{Re}[\frac{v(q)}{\varepsilon^0(q,\varepsilon_p-\varepsilon_{p'},-i0^+)}] . \quad (70)$$

Now the momenta p and p' appearing in Eqs.(66) and (67) are always inside the Fermi sphere, so that we may expand the energy denominator as

$$\frac{1}{\varepsilon_p-\varepsilon_{p+g}} = \frac{-1}{g^2} \{ 1 - \frac{2p \cdot g}{g^2} + (\frac{2p \cdot g}{g^2})^2 - \cdots \} \quad (71)$$

for large g. For a moment we put $\alpha r_s = 1$ for the sake of brevity, since the neglected factor can easily be taken into account in the final expression.

In this way we obtain the asymptotic form for the factor $\Pi_3^{(1)}(g_1,g_2)/\Pi_3^{(0)}(g_1,g_2)$ as follows:

$$\frac{\Pi_3^{(1)}(g_1,g_2)}{\Pi_3^{(0)}(g_1,g_2)} \simeq \tilde{T}^{(1)}(g_1) + \tilde{T}^{(1)}(g_2) + \tilde{T}^{(1)}(g_2-g_1) + R',$$

$$g_1, g_2, |g_2-g_1| \to \infty, \quad (72)$$

where $\tilde{T}^{(1)}(g)$ is the asymptotic form of $T^{(1)}(g) = \Pi_2^{(1)}(g)/\Pi^{(0)}(g)$ obtained in the same manner as described above:

$$\tilde{T}^{(1)}(g) = \mu^{3/2} \frac{\tilde{I}_0 - \tilde{I}_1}{g^4} . \quad (73)$$

Here $\tilde{I}_0$ is the asymptotic value of

- 46 -

$$I_0 = \frac{1}{\mu^3} \frac{4}{N^2} \sum_{p,p'} F_g(p,p')\, g^2 , \qquad (74)$$

and I_1 is given by

$$I_1 = \frac{1}{\mu^3} \frac{4}{N^2} \sum_{p,p'} F_{p-p'}(p,p')\frac{(p-p')^2}{3} . \qquad (75)$$

The remainder R' is given by

$$R' = \frac{\mu^{1/2} I_1\, A}{g_1^{\,4} g_2^{\,4} |g_2-g_1|^4 (g_1^{\,2}+g_2^{\,2}+|g_2-g_1|^2)} ,$$

$$A = g_1^{\,2} g_2^{\,2} |g_2-g_1|^2 [g_1^{\,2} g_2^{\,2} + g_1^{\,2}|g_2-g_1|^2 + g_2^{\,2}|g_2-g_1|^2]$$

$$- \{ |g_2-g_1|^6(g_1^{\,2}+g_2^{\,2})g_1 \cdot g_2 + g_1^{\,6}(g_2^{\,2}+|g_2-g_1|^2)g_1 \cdot (g_1-g_2)$$

$$+ g_2^{\,6}(g_1^{\,2}+|g_2-g_1|^2)g_2 \cdot (g_2-g_1) \} . \qquad (76)$$

In the expressions for R', there appear terms of scalar product $g_1 \cdot g_2$, which indicates that the ratio $\Pi_3^{(1)}/\Pi_3^{(0)}$ depends actually upon the shape of the triangle determined by g_1 and g_2. Then the term $\Pi_3^{(1)}$ is not completely factorized as premised in Eq.(59) even in the asymptotic form. However we note that R' vanishes exactly for the regular triangle.

Now let us go into more details of the constants $\tilde{I}_0$ and I_1 which appear in Eqs.(73) and (76). The first one, $\tilde{I}_0$, comes

from the matrix element $\tilde{v}(q)$ of large momentum transfer $|q| \sim$ g. Since $\tilde{v}(q)$ approaches $v(q)$ for large q, the constant $\tilde{I}_0$ may easily be evaluated with the following result:

$$\tilde{I}_0 = \frac{8}{3\pi} (\alpha r_s) . \qquad (77)$$

On the other hand I_1 comes from the term J in Eq.(65), which includes the matrix elements $\tilde{v}(p-p')$, with p and p' both inside the Fermi sphere. In the Hatree-Fock approximation, where the bare interaction $v(p-p')$ replaces the shielded one $\tilde{v}(p-p')$, the momentum summation in Eq.(75) becomes trivial. For this case we have

$$I_1 = \frac{1}{3} \tilde{I}_0 \qquad (78)$$

in accord with Geldart and Taylor.[33] For the shielded interaction the factor (1/3) will somewhat be reduced; particularly in the Thomas-Fermi approximation, we estimate $I_1 \sim (1/7) \tilde{I}_0$ for $\alpha r_s = 1$. Thus, we may conclude that because of the factor, I_1 , in Eq.(76) the shape dependent term R' is of smaller magnitude than the remaining terms, $T^{(1)}(g_1)$ etc., of Eq.(72), unless the triangle constructed by g_1 and g_2 distorts extremely from the regular one. However the failure is due to such expansion procedure as given by Eq.(71), according to the numerical analysis. This is shown in Fig. 8 for the case of g_1 and g_2 which are parallel to each other.

Thus we have proved that Eq.(59) is a good approximation. However the considered approximation breaks down for triangles $<g_1,g_2>$ whose circumscribing spheres have radii smaller than the Fermi radius; an important fact overlooked by Brovman et al. [7] The characteristic behavior of $\Pi_3^{(1)}/\Pi_3^{(0)}$ just pointed out can be observed in Figs.7,8 for triangles with and without Brovman and Kagan's singularity. The mentioned failure could not be analyzed according to the present method, which relies on the expansion effective only for large transfer momenta.

The similar analysis has been done for Π_4 (See Appendix). The result indicates that the approximation (56) may also hold for Π_4 with some modifications. The following form for Π_4 would be more consistent than a simple generalization of Eq.(56), accoding to our analysis.

$$\Pi_4(g_1,g_2,g_3) = T(g_1)T(g_2-g_1)T(g_3-g_2)T(-g_3)$$

$$\times \{ \Pi_4^{(0)}(g_1,g_2,g_3) - \Pi_3^{(0)}(g_1,g_2)\phi(g_2)T(g_2)\Pi_3^{(0)}(g_2,g_3)$$

$$- \Pi_3^{(0)}(g_2-g_1,g_3-g_1)\phi(g_3-g_1)T(g_3-g_1)\Pi_3^{(0)}(g_3-g_1,-g_1) \}. \quad (79)$$

Let us consider a tetrahedron which is determined by g_1,g_2 and g_3. We then expect that the above approximation is a good one unless the smallest radius of four circles circumscribing the sides of the tetrahedron is smaller than the Fermi radius. This conjecture seems reasonable in view of the numerically analyzed

results for Π_3. It is also quite reasonable that the considered approximation may hold for the higher order polarization in the similar region of validity.

Finally we note that the last two terms in the brace of Eq. (79) include a contribution from the diagram shown in Fig.9c as a primary term. This is the 'exchange conjugate' to the H-type diagram shown in Fig.9d, according to the terminology by Hubbard.[29] He introduced the above concept in his discussion on the Hubbard approximation. Thus it seems natural that such terms in Eq.(79) appear in a generalization of the Hubbard type approximation (53).

§5. Systematic method of resummation
— a cluster expansion

In the structural expansion we meet various kinds of divergence, if the shortest reciprocal lattice vector is smaller than the Fermi diameter. Then the partial summation of perturbation series is needed to eliminate the divergence. The resummation procedure becomes much more complicated for finding out an appropriate perturbation series if the primary term is of higher order, because the series is further from simple series of geometric progression. Though the resummation has been dicussed by HA[10] and in STI,[17] there still remain some ambiguities in collecting the higher order terms. In this section we shall show that for a specific set of diagrams there exists a systematic

method of resummation, by which all of the terms included in the set can unambiguously absorbed into a single resummed term. Extention of our method to more general set of diagrams would be straightforward.

In the expansion for Ω_{st} given in §3, we may obtain a series of terms from the logarithmic part $\Omega^{(i)}$, Eq.(36), which does not contain any higher-order self-energy $\Sigma^{(n)}$ than the first-order one $\Sigma^{(1)}$. These terms may be collected into a logarithmic form:

$$\Omega^{(1)} = -\frac{1}{\beta} \sum_{\ell} \sum_{k \in Bz} tr_g [1 - G^{(0)}(k,\zeta_\ell) \Sigma^{(1)}(k,\zeta_\ell)] . \quad (80)$$

Here we introduce a quasimomentum k by

$$p = k + g \quad (81)$$

for convenience' sake. In Eq.(80), the matrix elements $G(k)_{g,g'}$, $\Sigma(k)_{g,g'}$, etc. stand respectively for $G(k+g,k+g')$, $\Sigma(k+g,k+g')$ etc, and tr_g designates the diagonal sum over g with fixed quasi-momentum k. And the summation over k is to be taken in a Brillouin zone.

According to the discussion in the previous section, Eq.(80) is effectively equivalent to

$$\Omega^{(1)} = -\frac{1}{\beta} \sum_{\ell} \sum_{k \in Bz} tr_g \, \ell n [1 - G^0 \tilde{\Sigma}] , \quad (82)$$

where the effective field $\tilde{\Sigma}$ is independent of k and ζ_ℓ, and is

given by

$$\tilde{\Sigma}_{g,g'} = \tilde{w}(g'-g)T(g'-g) \ . \tag{83}$$

Here G^0 is the free electron propagator matrix $G^0(k)_{g,g'} = G^0(k+g)\delta_{g,g'}$, $\tilde{w}(g)$ the shielded external potential given by Eq. (27), and $T(g)$ the effective vertex factor given by Eq.(55).

In order to obtain the rearranged series, we rewrite Eq.(82) as

$$\Omega^{(1)} = -\frac{1}{\beta} \sum_{\ell} \sum_{k\epsilon Bz,\ell} \text{tr}_g\{ \ell n[\tilde{\Sigma}-(G^0)^{-1}] - \ell n[-(G^0)^{-1}] \} \ . \tag{84}$$

Here we choose the branch cut for the logarithmic singularity to be along the negative real axis with $\ell n\ 1 = 0.$[25,31a] Then we use the following theorem of linear algebra:[41]

$$\text{tr } \ell nA = \ell n\ \det A \ . \tag{85}$$

Here A is an arbitrary matrix, whose logarithm is well-defined. Thus Eq.(84) becomes

$$\Omega^{(1)} = -\frac{1}{\beta} \sum_{\ell} \sum_{k\epsilon Bz} \{ \ell n\ D - \ell n \prod_i D_1(i) \} \ , \tag{86}$$

where we put

$$D_1(i) \equiv -[G^0(k+g_i,\zeta_\ell)]^{-1}$$

$$= \varepsilon_{k+g_i} - \zeta_\ell \,, \tag{87}$$

and

$$D = \begin{vmatrix} -[G^0(k+g_1)]^{-1} & \tilde{\Sigma}_{1,2} & \tilde{\Sigma}_{1,3} & \cdots \\ \\ \tilde{\Sigma}_{2,1} & -[G^0(k+g_2)]^{-1} & \tilde{\Sigma}_{2,3} & \cdots \\ \\ \tilde{\Sigma}_{3,1} & \tilde{\Sigma}_{3,2} & -[G^0(k+g_3)]^{-1} & \cdots \\ \\ \cdot \quad \cdot \quad \cdot \quad \cdot \quad \cdot \quad \cdot \quad \cdot \quad \cdot \quad \cdot \quad \cdot \quad \cdot \quad \cdot \quad \cdot \quad \cdot \\ \\ \cdot \quad \cdot \quad \cdot \quad \cdot \quad \cdot \quad \cdot \quad \cdot \quad \cdot \quad \cdot \quad \cdot \quad \cdot \quad \cdot \quad \cdot \quad \cdot \end{vmatrix} , \tag{88}$$

where the components of the determinant refer to reciprocal lattice vectors. Let us confine ourselves to a set consisting of a certain number M of reciprocal lattice vectors. And introcuce a n × n determinant D_n by

$$D_1(\{i\}) \equiv D_1(i) \,,$$

$$D_2(\{i,j\}) \equiv \begin{vmatrix} -[G^0(k+g_i)]^{-1} & \tilde{\Sigma}_{i,j} \\ \\ \tilde{\Sigma}_{j,i} & -[G^0(k+g_j)]^{-1} \end{vmatrix} ,$$

$$D_3(\{i,j,k\}) \equiv \begin{vmatrix} -[G^o(k+g_i)]^{-1} & \tilde{\Sigma}_{i,j} & \tilde{\Sigma}_{j,k} \\ \tilde{\Sigma}_{j,i} & -[G^0(k+g_j)]^{-1} & \tilde{\Sigma}_{j,k} \\ \tilde{\Sigma}_{k,i} & \tilde{\Sigma}_{k,j} & -[G^0(k+g_k)]^{-1} \end{vmatrix},$$

$$\circ \; \cdot \; \cdot \; \circ \; \cdot \; \cdot \; \cdot \; \cdot \; \cdot \; \cdot \; \cdot \; \cdot \; \cdot \qquad (89)$$

Let us now apply the meothod of cluster expansion[42] to $\ln D$. The result becomes

$$\ln D = \sum_i \ln D_1(\{i\}) + \sum_{i<j} \ln \frac{D_2(\{i,j\})}{D_1(\{i\})D_1(\{j\})}$$

$$+ \sum_{i<j<k} \ln \frac{D_3(\{i,j,k\})D_1(\{i\})D_1(\{j\})D_1(\{k\})}{D_2(\{i,j\})D_2(\{j,k\})D_2(\{k,i\})}$$

$$+ \sum_{i<j<k<\ell} \ln \{ \frac{D_4(\{i,j,k,\ell\})}{D_3(\{i,j,k\})D_3(\{i,j,\ell\})D_3(\{i,k,\ell\})D_3(\{j,k,\ell\})}$$

$$\times \frac{D_2(\{i,j\})D_2(\{k,\ell\})D_2(\{i,k\})D_2(\{j,\ell\})D_2(\{i,\ell\})D_2(\{j,k\})}{D_1(\{i\})D_1(\{j\})D_1(\{k\})D_1(\{\ell\})} \}$$

$$+ \; \cdot \; \cdot \; \cdot \; \cdot \; \cdot \; \cdot \; \cdot \; \cdot \qquad (90)$$

Substituting the above expression into Eq.(86), we get the cluster expansion of $\Omega^{(1)}$. After substitution the first term in Eq.(90) disappears as a result of cancellation.

The above result contains all of the anomalous diagrams, if we confine ourselves to simple ones which take account of the electron-electron interactions by means of the vertex function. However we must mention the effect of the chemical potential shift. In the original perturbation series the anomalous terms are largely cancelled by another energy contribution coming from the chemical potential shift, leaving a small residual as a deformation energy of the Fermi surface (STI). However the anomalous terms are of considerable magnitude. It means that the effect of the chemical potential shift is also considerable. This effect must not be neglected if we use our expansion scheme.

In the present scheme the number of electrons does not conserve if the chemical potential is fixed (§3.B). The deviation of the number $\delta N^{(1)}$ due to $\Omega^{(1)}$ is given by

$$\delta N^{(1)}(\mu) = -\frac{\partial \Omega^{(1)}}{\partial \mu} \quad . \tag{91}$$

Then the true value $\bar{\mu}$ of the chemical potential is determined from

$$-\frac{\partial \Omega^{(1)}}{\partial \mu}\Bigg|_{\mu=\bar{\mu}} = \delta N^{(1)}(\bar{\mu}) = -\frac{\partial \Omega_0}{\partial \mu}\Bigg|_{\mu=\mu_0} + \frac{\partial \Omega_0}{\partial \mu}\Bigg|_{\mu=\bar{\mu}} \ , \tag{92}$$

if we disregard the other contribution than $\Omega^{(1)}$. Here Ω_0 and μ_0 are the thermodynamical potential and the chemical potential for the free electron system, respectively. If we expand the quantities in Eq.(92) at $\mu = \mu_0$, the energy change δE due to the chemical potential shift is approximately given by

$$N \delta E \simeq - \frac{1}{2} \{ \frac{\partial^2 \Omega_0}{\partial \mu^2} + \frac{\partial^2 \Omega^{(1)}}{\partial \mu^2} \}^{-1}_{\mu=\mu_0} [\delta N^{(1)}(\mu_0)]^2 . \qquad (93)$$

At this point we note that the derivative $\partial \Omega^{(1)}/\partial\mu$ comes out only through the μ-dependence of the free propagator G^0. It is because the term arising from the derivative of the self=energy $\tilde{\Sigma}$ are cancelled by those from $\Omega^{(ii)}$ and $\Omega^{(iii)}$, Eqs.(40) and (37), owing to our variation principle (§3); the expression (14) for the thermodynamical potential is stationary with respect to the change of the self-energy.[24] In this way we get

$$\frac{\partial \Omega^{(1)}}{\partial \mu} = - \frac{1}{\beta} \sum_{\ell} \sum_{k \in Bz} \{ \sum_{i<j} [- \frac{D_1(\{i\})+D_1(\{j\})}{D_2(\{i,j\})}$$

$$+ \frac{1}{D_1(\{i\})} + \frac{1}{D_1(\{j\})}]$$

$$+ \sum_{i<j<k} [- \frac{D_2(\{i,j\})+D_2(\{j,k\})+D_2(\{i,k\})}{D_3(\{i,j,k\})}$$

$$+ \frac{D_1(\{i\})+D_1(\{j\})}{D_2(\{i,j\})} + \frac{D_1(\{j\})+D_1(\{k\})}{D_2(\{j,k\})}$$

$$+ \frac{D_1(\{i\})+D_1(\{k\})}{D_2(\{i,k\})} - \frac{1}{D_1(\{i\})} - \frac{1}{D_2(\{j\})} - \frac{1}{D_2(\{k\})}]$$

$$+ \cdots \cdots \quad \} \, , \tag{94}$$

where the use is made of

$$\frac{\partial D_n(\{1,2,\cdots,n\})}{\partial \mu} = - \sum_i D_{n-1}(\{1,\cdots,i-1,i+1,\cdots,n\}) \, . \tag{95}$$

- 57 -

Appendix

———— Analysis of Π_4 ————

Before going into the analysis of Π_4 we note the following fact. Both of the primary terms in $\Pi_2^{(1,a)}(g)/\Pi^{(0)}(g)$ and $\Pi_2^{(1,b)}(g)/\Pi^{(0)}(g)$ are of order of $1/g^2$ for large g. However these terms cancel each other with the resultant asymptotic form of $T^{(1)}(g) = \Pi_2^{(1)}(g)/\Pi^{(0)}(g)$ proportional to $1/g^4$ (See Eq.(73)), as pointed out by Geldart and Taylor.[33] The similar cancellation occurs between the primary terms of $\Pi_3^{(1,a)}$ and $\Pi_3^{(1,b)}$. Otherwise we could not get such asymptotic behavior as Eq.(72) and accordingly the factorization in Eq.(56). The similar cancellation is expected to occur for the case of $\Pi_4^{(1)}$. Let us then consider collectively the contributions to $\Pi_4^{(1)}$, which consists of $\Pi_4^{(1,a)}$, $\Pi_4^{(1,b)}$ and $\Pi_4^{(1,c)}$ as follows.

$$\Pi_4^{(1,a)}(g_1,g_2,g_3)$$

$$= -2 \int_p \int_{p'} G^0(p)G^0(p+g_1)G^0(p+g_2)G^0(p+g_3)$$

$$\times \tilde{v}^{(0)}(p-p')[G^0(p')G^0(p'+g_1) + G^0(p'+g_1)G^0(p'+g_2)$$

$$+ G^0(p'+g_2)G^0(p'+g_3) + G^0(p'+g_3)G^0(p')] , \qquad (A.1)$$

$$\Pi_4^{(1,b)}(g_1,g_2,g_3)$$

$$= -2 \int_p \int_{p'} G^0(p) G^0(p+g_1) G^0(p+g_2) G^0(p+g_3)$$

$$\times \tilde{v}^{(0)}(p-p')[\, G^0(p) G^0(p') + G^0(p+g_1) G^0(p'+g_1)$$

$$+ G^0(p+g_2) G^0(p'+g_2) + G^0(p+g_3) G^0(p'+g_3) \,] \quad , \qquad \text{(A.2)}$$

$$\Pi_4^{(1,c)}(g_1,g_2,g_3)$$

$$= -2 \int_P \int_{P'} [\, G^0(p) G^0(p+g_1) G^0(p+g_2)$$

$$\times \tilde{v}^{(0)}(p-p') G^0(p') G^0(p'+g_3) G^0(p'+g_2)$$

$$+ G^0(p+g_1) G^0(p+g_2) G^0(p+g_3)$$

$$\times \tilde{v}^{(0)}(p-p') G^0(p'+g_1) G^0(p') G^0(p'+g_3) \,] \quad . \qquad \text{(A.3)}$$

These terms correspond to the diagrams shown in Fig.9 , where the superscript a, b, c in Π_4 are also in accord with the labels in the figure.

Let us now examine the asymptotic behavior of

$$\Pi_4^{(1)}(g_1,g_2,g_3) = \Pi_4^{(1,a)}(g_1,g_2,g_3) + \Pi_4^{(1,b)}(g_1,g_2,g_3)$$

$$+ \Pi_4^{(1,c)}(g_1,g_2,g_3) \quad . \qquad \text{(A.4)}$$

Similarly as in the case for $\Pi_3^{(1)}$, we use the formula (63) and

(64) to obtain the following expression for $\Pi_4^{(1)}$:

$$\Pi_4^{(1)}(g_1,g_2,g_3)$$

$$= J(g_2;g_1,g_3) + J(g_3-g_1;g_2-g_1,-g_1)$$

$$+ J(-g_2;g_3-g_2,g_1-g_2) + J(g_1-g_3;-g_3,g_2-g_3)$$

$$+ K(g_2,g_1;g_2,g_3) + K(g_2,g_2-g_1;g_2,g_2-g_3)$$

$$+ K(g_3-g_1,g_2-g_1;g_3-g_1,-g_1) + K(g_3-g_1,g_3-g_2;g_3-g_1,g_3)$$

$$+ \tilde{J}_{g_1}(g_3,g_2;g_2-g_1,g_3-g_1) + \tilde{J}_{g_2-g_1}(g_3-g_1,-g_1;-g_2,g_3-g_2)$$

$$+ \tilde{J}_{g_3-g_1}(-g_2,g_1-g_2;g_1-g_3,-g_3) + \tilde{J}_{-g_3}(g_1-g_3,g_2-g_3;g_2,g_1)$$

$$+ \tilde{K}_{g_2}(g_1,g_2;g_1-g_2,g_3-g_2) + \tilde{K}_{g_3-g_1}(-g_1,g_2-g_1;-g_3,g_2-g_3)$$

$$+ R . \tag{A.5}$$

Here we put

$$J(g_1;g_2,g_3) = - \frac{2}{N^2} \sum_{p,p'} F_{p-p'}(p,p')(\Delta_{g_1})^{-1}(\Delta_{g_2})^{-1}(\Delta_{g_3})^{-1}$$

$$\times [(\Delta'_{g_2})^{-1} -(\Delta_{g_2})^{-1} +(\Delta'_{g_3})^{-1} -(\Delta_{g_3})^{-1}] ,$$

$$\tag{A.6}$$

$$K(g_1,g_2;g_1,g_3)$$

$$= - \frac{2}{N^2} \sum_{p,p'} F_{p-p'}(p,p')(\Delta_{g_1})^{-1}(\Delta_{g_2})^{-1}$$

$$\times [(\Delta'_{g_1})^{-1}(\Delta'_{g_3})^{-1} - (\Delta_{g_1})^{-1}(\Delta_{g_3})^{-1}] , \qquad (A.7)$$

$$\tilde{J}_{g_1}(g_2,g_3;g_4,g_5)$$

$$= - \frac{2}{N^2} \sum_{p,p'} F_{p+p'+g_1}(p,p')[(\Delta'_{g_1})^{-1} + (\Delta_{g_1})^{-1}]$$

$$\times [(\Delta_{g_1})^{-1}(\Delta_{g_2})^{-1}(\Delta_{g_3})^{-1} + (\Delta_{-g_1})^{-1}(\Delta_{g_4})^{-1}(\Delta_{g_5})^{-1}$$

$$+ (\Delta'_{g_4})^{-1}(\Delta_{g_2})^{-1}(\Delta_{g_3})^{-1} + (\Delta'_{g_2})^{-1}(\Delta_{g_4})^{-1}(\Delta_{g_5})^{-1}] , \quad (\Lambda.8)$$

$$\tilde{K}_{g_1}(g_2,g_3;g_4,g_5)$$

$$= - \frac{2}{N^2} \sum_{p,p'} F_{p+p'+g_2}(p,p')\{(\Delta_{g_2})^{-1}(\Delta_{g_3})^{-1}(\Delta'_{g_4})^{-1}(\Delta'_{g_5})^{-1}$$

$$+ (\Delta_{g_1})^{-1}(\Delta'_{g_1})^{-1}[(\Delta_{g_4})^{-1}(\Delta'_{g_3})^{-1} + (\Delta_{g_2})^{-1}(\Delta'_{g_5})^{-1}]$$

$$+ (\Delta_{g_1})^{-1}(\Delta_{g_2})^{-1}(\Delta_{g_3})^{-1}[(\Delta'_{g_4})^{-1} + (\Delta'_{g_5})^{-1}]$$

$$+ (\Delta_{g_1})^{-1}(\Delta_{g_4})^{-1}(\Delta_{g_5})^{-1}[(\Delta'_{g_2})^{-1} + (\Delta'_{g_3})^{-1}]$$

$$+ (\Delta_{g_1})^{-2}[(\Delta_{g_2})^{-1}(\Delta_{g_3})^{-1} + (\Delta_{g_4})^{-1}(\Delta_{g_5})^{-1}]\} , \qquad (A.9)$$

with

$$\Delta_g \equiv \varepsilon_p - \varepsilon_{p+g} ,$$

$$\Delta'_g \equiv \varepsilon_{p'} - \varepsilon_{p'+g} . \qquad (A.10)$$

The remainder R in Eq.(A.5) includes contributions from the anomalous term as well as those from the imaginary part of $1/\varepsilon^o(q, \varepsilon_p - \varepsilon_{p'} - i0^+)$. We shall neglect the remainder by the same reason as in §4. Then we may expand the energy denominator $(\Delta_g)^{-1}$ to obtain the asymptotic form of $\Pi_4^{(1)}(g_1, g_2, g_3)$ as follows:

$$\tilde{\Pi}_4^{(1)}(g_1, g_2, g_3)$$

$$= \tilde{\Pi}_4^{(0)}(g_1, g_2, g_3)\{\tilde{T}^{(1)}(g_1) + \tilde{T}^{(1)}(g_2 - g_1)$$

$$+ \tilde{T}^{(1)}(g_3 - g_2) + \tilde{T}^{(1)}(-g_3)\} - \tilde{\Pi}_3^{(0)}(g_1, g_2)\tilde{\phi}(g_2)\tilde{\Pi}_3^{(0)}(g_2, g_3)$$

$$- \tilde{\Pi}_3^{(0)}(g_2 - g_1, g_3 - g_1)\tilde{\phi}(g_3 - g_1)\tilde{\Pi}_3^{(0)}(g_3 - g_1, -g_1)$$

$$+ R' . \qquad (A.11)$$

Here $\tilde{T}^{(1)}(g)$ denotes the asymptotic expression for $T^{(1)}(g) =$

$\Pi_2^{(1)}(g)/\Pi^{(0)}(g)$ which is given by Eq.(73). And $\tilde{\phi}(g)$ is the similar expression for $\phi(g) = -\Pi_2^{(1)}(g)/[\Pi^{(0)}(g)]^2$:

$$\tilde{\phi}(g) = \frac{\tilde{I}_0 - I_1}{2g^2} \tag{A.12}$$

with I_0 and I_1 given by Eqs.(77) and (74). And $\tilde{\Pi}_3^{(0)}$ and $\tilde{\Pi}_4^{(0)}$ are the asymptotic expressions for $\Pi_3^{(0)}$ and $\Pi_4^{(0)}$ respectively given by

$$\tilde{\Pi}_3^{(0)}(g_1,g_2) = \mu^{1/2} \frac{g_1^2 + g_2^2 + |g_2 - g_1|^2}{g_1^2 \, g_2^2 \, |g_2 - g_1|^2} \quad , \tag{A.13}$$

$$\tilde{\Pi}_4^{(0)}(g_1,g_2) = -\mu^{1/2} \{ \frac{1}{g_1^2 g_2^2 g_3^2} + \frac{1}{g_1^2 |g_2 - g_1|^2 |g_3 - g_1|^2}$$

$$+ \frac{1}{g_2^2 |g_1 - g_2|^2 |g_3 - g_2|^2} + \frac{1}{g_3^2 |g_1 - g_3|^2 |g_2 - g_3|^2} \} \quad . \tag{A.14}$$

In Eq.(A.11) the remainder R' consists of two terms, R_0' and R_1', which include respectively I_0 and I_1 as a factor. The term R_0' is given simply by

$$R_0' = I_0 \{ h(g_1; g_2, g_3) + h(g_1 - g_2; g_1 - g_3, g_1)$$

$$+ h(g_2 - g_3; g_2, g_2 - g_1) + h(g_3; g_3 - g_1, g_3 - g_2) \} \tag{A.15}$$

where

$$h(g_1;g_2,g_3) = \frac{1}{g_1{}^4} \{ \frac{1}{g_2{}^2|g_2-g_1|^2} (\frac{1}{g_3{}^2} - \frac{1}{|g_3-g_2|^2})$$

$$+ \frac{1}{g_3{}^2|g_3-g_1|^2} (\frac{1}{|g_3-g_1|^2} - \frac{1}{|g_3-g_2|^2}) \} . \quad (A.16)$$

The expression for $R_1{}'$ is much more complicated and may be omitted here, since the factor I_1 is fairly smaller than I_0. Now, $R_0{}'$ vanishes identically if the tetrahedron $[g_1,g_2,g_3]$ determined by g_1, g_2 and g_3 is the regular one, in conformity with the case for Π_3. It appears that the other term $R_1{}'$ does not exactly vanish for the above tetrahedron. However the contribution of $R_1{}'$ may be thought small as mentioned before.

By the foregoing analysis Eq.(79) has proved to be a relevant approximation. The proof is apparently in parallel with that for Π_3. However the result for Π_4 is much more involved than the other. It is because an entirely new diagram comes in for Π_4 as shown in Fig.9c. Though that diagram cannot be taken account of in a single vertex function it is indispensable in ensuring the proper behavior of the asymptotic form. It is also the mentioned diagram which produces the last two terms in Eq.(79).

References

1) V. Heine and D. Weaire, Solid State Phys. $\underline{24}$ (1970), 249.

2) W.A. Harrison, <u>Pseudopotentials in the Theory of Metals</u>
    (Benjamin, Reading, 1966).

3) P. Lloyd and C.A. Sholl, J. of Phys. $\underline{C1}$ (1968), 1620.

4) P. Hohenberg and W. Kohn, Phys. Rev1 $\underline{136}$ (1964), B864.

5) W. Kohn and L.J. Sham, Phys. Rev. $\underline{140}$ (1965), A1133.

6) E.G. Brovman and Yu. Kagan, Zh. Eksp. Teor. Fiz. $\underline{57}$ (1967),
    557 [Soviet Phys. -JETP $\underline{25}$ (1967), 365].

7) E.G. Brovman and Yu. Kagan, in <u>Dynamical Properties of Solids,</u>
    Vol. 1. ed. by G.k. Horton and A.A. Maradudin (North-Holland,
    Amsterdam, (1974), also 7a).

7a) E.G. Brovman and Yu. Kagan, Uspekhi Fiz. Nauk SSSR $\underline{112}$ (1974),
    369 [Soviet Phys. -Uspekhi $\underline{17}$ (1974), 924].

8) E.G. Brovman, Yu. Kagan and A. Kholas, Zh. Eksp. Teor. Fiz.
    $\underline{61}$ (1971), 2429 [Soviet Phys. -JETP 34 (1972), 1300].

9) E.G. Brovman, Yu. Kagan and A. Kholas, Zh. Eksp. Teor. Fiz.
    $\underline{62}$ (1972), 1492 [Soviet Phys. -JETP $\underline{35}$ (1972), 783].

10) J. Hammerberg and N.W. Ashcroft, Phys. Rev. $\underline{B9}$ (1974), 409.

11) M. Watabe and H. Yasuhara, Phys. Lett. $\underline{28A}$ (1968), 329.

11a) H. Yasuhara and M. Watabe, Prog. Theor. Phys. $\underline{49}$ (1973), 1785.

11b) V. Heine, P. Nozieres and J. Wilkins, Phil.Mag. $\underline{13}$(1966),741.

12) W.J. Carr, Jr., Phys. Rev. $\underline{128}$ (1962), 120.

13) E.G. Brovman and Yu. Kagan, Zh. Eksp. Teor. Fiz. 63 (1972), 1973 [Soviet Phys. -JETP 36 (1973), 1025].

14) E.G. Brovman and A. Kholas, Zh. Eksp. Teor. Fiz. 66 (1974), 1877 [Soviet Phys. -JETP 39 (1974), 924].

15) E.G. Brovman, Yu. Kagan, A. Kholas and V.V. Pushkarev, ZhETF Pis. Red. 18 (1973), 269 [JETP Lett. 18 (1973), 160].

16) Yu. Kagan, V.V. Pushkarev and A. Kholas, Zh. Eksp. Teor. Fis. 73 (1977), 967 [Soviet Phys. -JETP 46 (1977), 511].

17) T. Nakamura, H. Nagara and H. Miyagi, Prog. Theor. Phys. 63 (1980), 368.

18) H. Miyagi, H. Nagara and T. Nakamura, Prog. Theor. Phys. 63 (1980), 1509.

19) H. Miyagi and H. Nagara, Prog. Theor. Phys. 64 (1980), 747.

20) H. Miyagi, Prog. Theor. Phys. 65 (1981), 66.

21) H. Nagara, Thesis (Osaka University, 1979).

22) A.A. Abrikosov, Zh. Eksp. Teor. Fiz. 39 (1960), 1797 [Soviet Phys. -JETP, 12 (1961), 1254].

23) H. Nagara, H. Miyagi and T. Nakamura, Prog. Theor. Phys. 56 (1976), 396.

24) A.A. Abrikosov, L.P. Gorkov and I.E. Dzyaloshinski, Method of Quantum Field Theory in Statistical Physics, (Dover, New York, 1963).

25) J.M. Luttinger and J.C. Ward, Phys. Rev. 118 (1960), 1417)
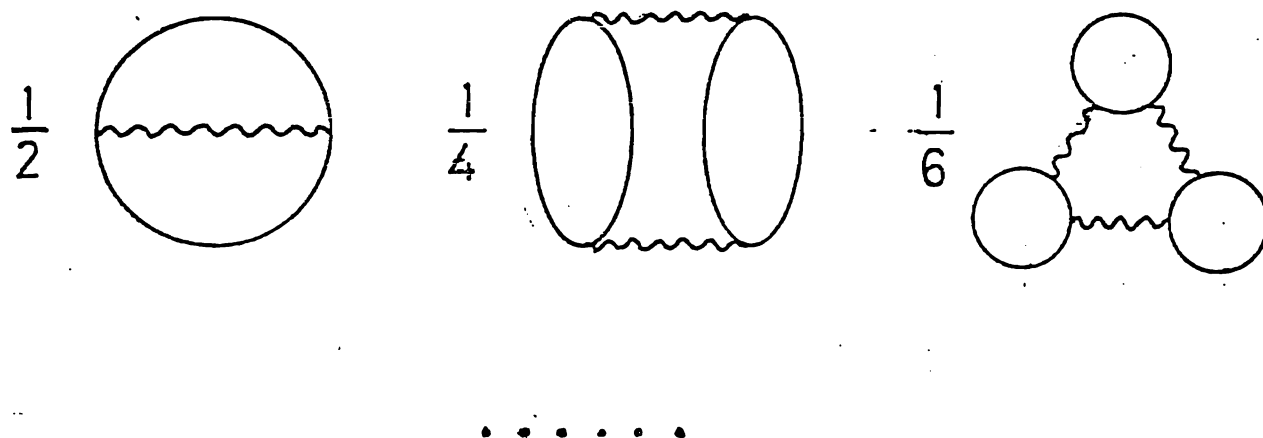
26) J.M. Luttinger , Phys. Rev. 119 (1960), 1153.

27) P. Nozières, Theory of Interacting Fermi Systems, (Benjamin, New York, 1964).

28) J. Hubbard, Proc. Roy. Soc. A, 240, 539.

29) J. Hubbard, Proc. Roy. Soc. A, 243, 336.

30) J. Hubbard, Proc. Roy. Soc. A, 244, 199.

31) D.J.W. Geldart and S.H. Vosko, Can. J. Phys. 44 (1966), 2137. See also 31a).

31a) G. Baym, Phys. Rev. 127 (1962), 1391.

32) D.J.W. Geldart and R. Taylor, Can. J. Phys. 48 (1970), 155.

33) D.J.W. Geldart and R. Taylor, Can. J. Phys. 48 (1970), 167.

34) W. Kohn and J.M. Luttinger, Phys. Rev. 118 (1960), 41.

35) F. Toigo and T.O. Woodruff, Phys. Rev. B2 (1970), 3958.

36) P. Vashishta and K.S. Singwi, Phys. Rev. B6 (1972), 875.

37) H. Yasuhara, J. Phys. Soc. Japan 36 (1974), 361.

38) D.N. Lowy and G.E. Brown, Phys. Rev. B12 (1975), 2138.

39) H. Nagara, H. Miyagi and T. Nakamura, Prog. Theor. Phys. 64 (1980), 731.

40) D.J.W. Geldart and R. Taylor, Solid State Commun. 9 (1971), 7.

41) I. Satake, Gyôretu to Gyôretusiki (Japanese; Matrices and Determinants, Syôkabo, Tokyo, 1958).

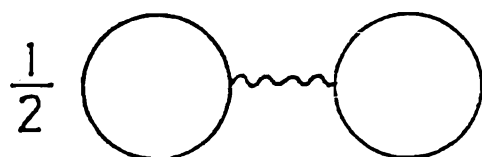42) R. Kubo, J. Phys. Soc. Japan 17 (1962), 1100.

Figure Captions

Fig.1. Skeleton diagrams for the functional $\Phi[G]$. Solid lines
represent the electron propagator, wavy lines the electron=
electron interaction and the broken line the electron-ion one.

Fig.2. Skeleton diagrams for the self-energy Σ. The double
wavy lines represent the renormalized electron-electron inter-
action.

Fig.3. Illustrations showing the first and second order self=
energies, $\Sigma^{(1)}$ and $\Sigma^{(2)}$. The presented diagrams are typical
ones obtained by expanding the integral equations (29) or (32).

Fig.4. Diagram illustrating a third order polarization (a) as
a generalization of the second order one (b).

Fig.5. Lower order diagrams contributing to the thermodynamical
potential Ω. The shown diagrams appear in the expansion of Ω
with respect to the free electron propagator.

Fig.6. Schematic curve of the chemical potential μ vs. a cou-
pling constant λ.

Fig.7. Comparison of $\Pi_3^{(1)}(g_1,g_2)/\Pi_3^{(0)}(g_1,g_2)$ with $3\Pi_2^{(1)}(g)/$
$\Pi_2^{(0)}$, for the regular triangles $|g_1| = |g_2| \equiv g$. Their values
multiplied by r_s^{-1} are plotted as a function of R, the radius
of the circle circumscribing the triangle $<g_1,g_2>$. The data
are owing to H.Miyagi.

Fig.8. The similar plot to Fig.7 in the limmitting case when
g_1 and g_2 are antiparallel to each other with $|g_1| = |g_2|$.

Fig.8. Primary corrections to $\Pi_4^{(0)}$. (a) incluedes a vertex
part, (b) a self-energy part, (c) a part irreducible to the
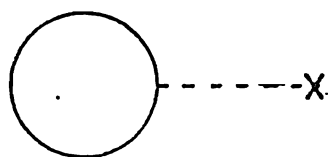vertex one.   (d) rpresents the Hubbard H-diagram.
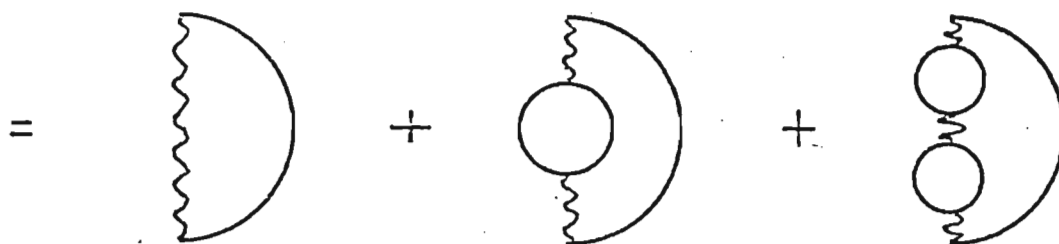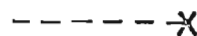
(a)

$\frac{1}{2}$ $\frac{1}{4}$ $-\frac{1}{6}$

(b)

$\frac{1}{2}$

(c)

Fig. 1

(a)

(b)

(c)

Fig. 2

Fig. 3

(a)   (b)

Fig. 4

2nd

(a)

(b)

3rd

(a)

(b)

Fig. 5

Fig. 6

Fig. 7

$$\Pi_3^{(1)} / \Pi_3^{(0)} \, r_s$$

$$2 \, \Pi_2^{(1)}(g) / \Pi_2^{(0)}(g) \, r_s + \Pi_2^{(1)}(2g) / \Pi_2^{(0)}(2g) \, r_s$$

$$r_s = 1.5$$

Fig. 8

(a)

(b)

(c)

(d)

Fig. 9

- 78 -
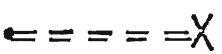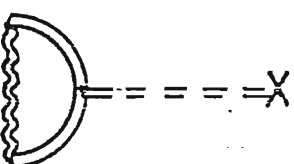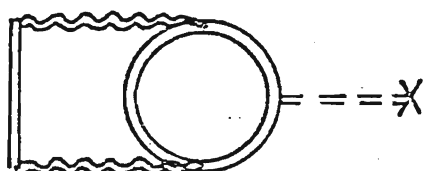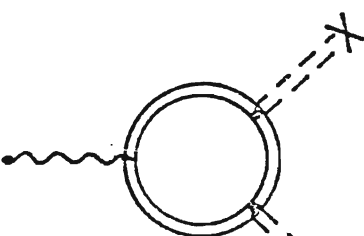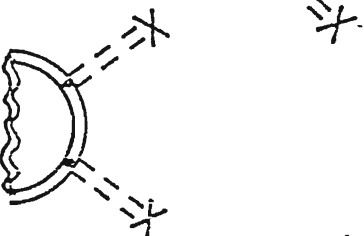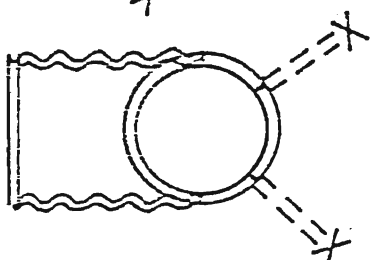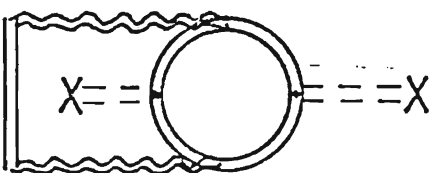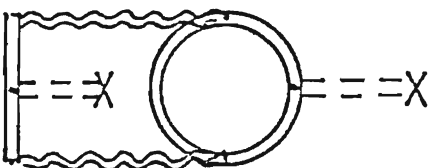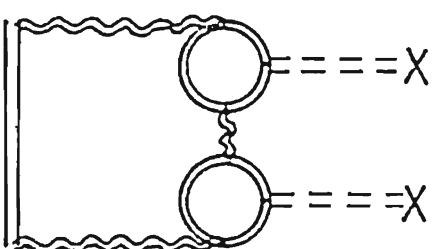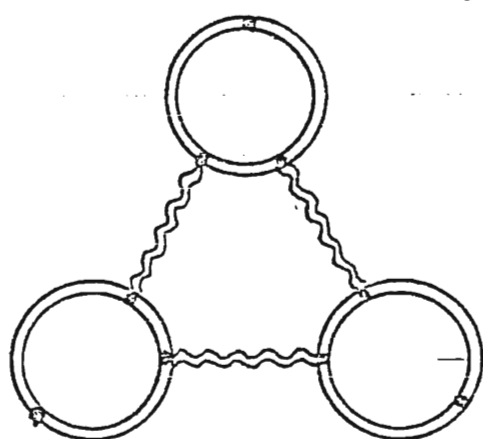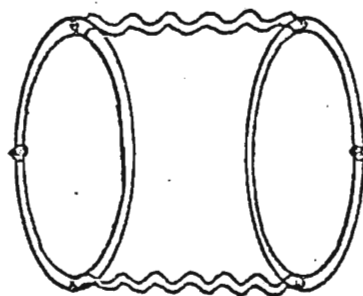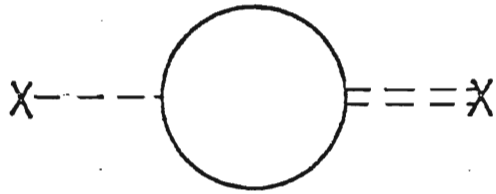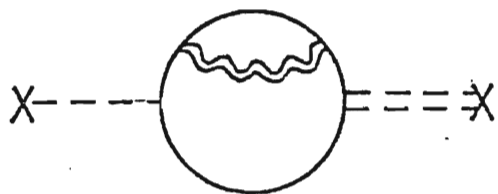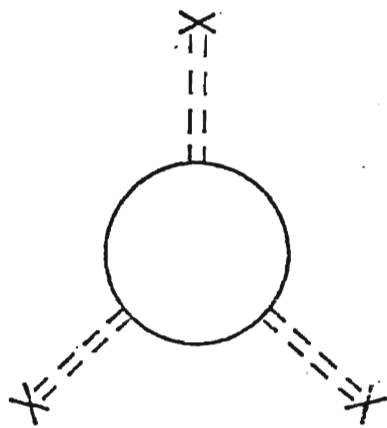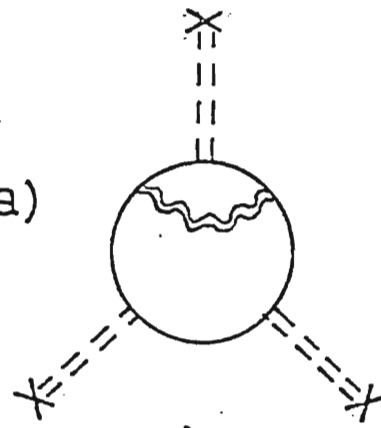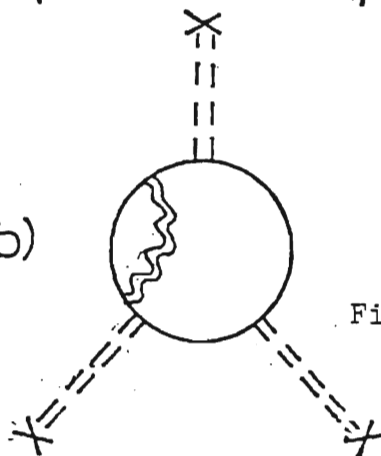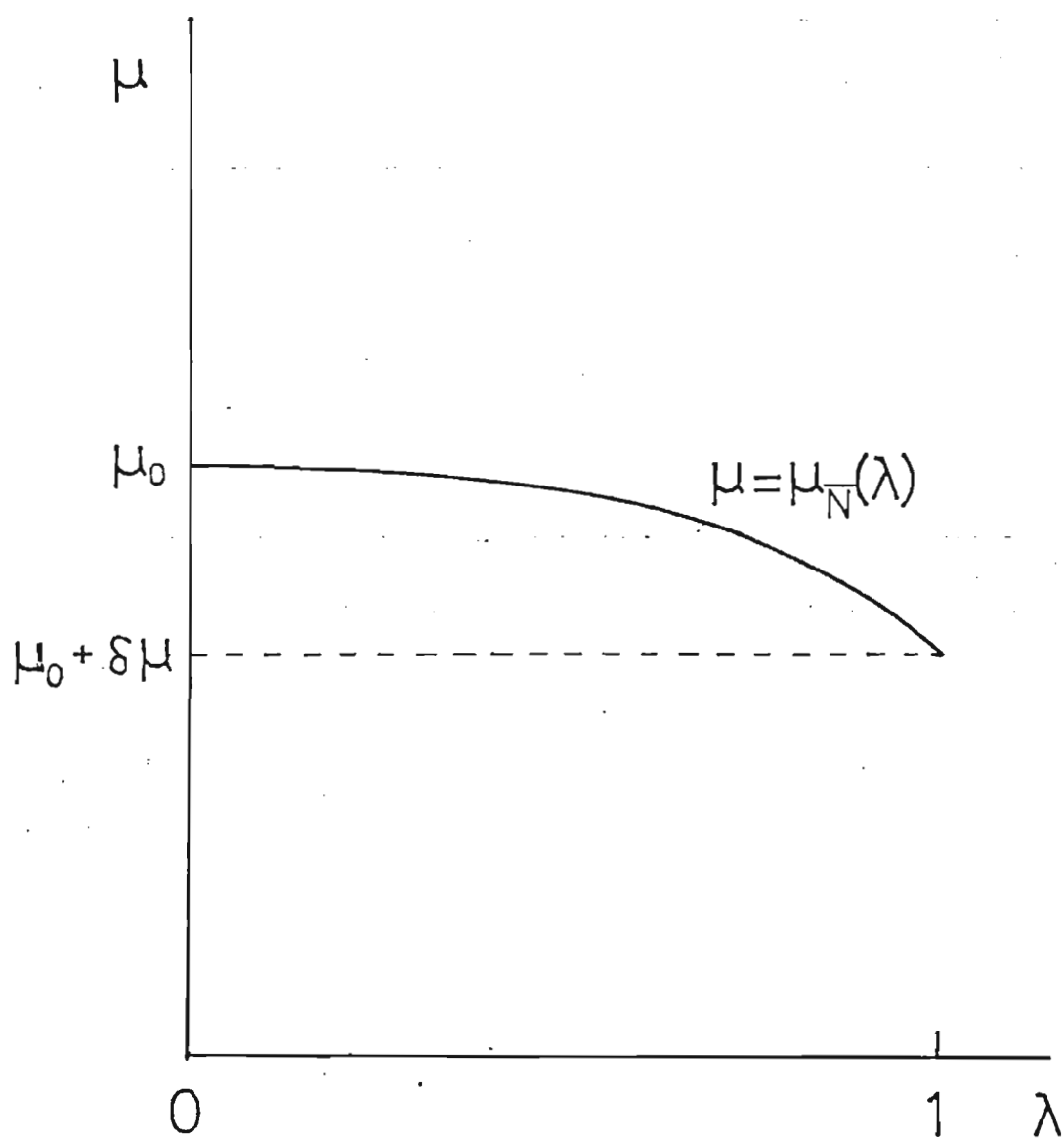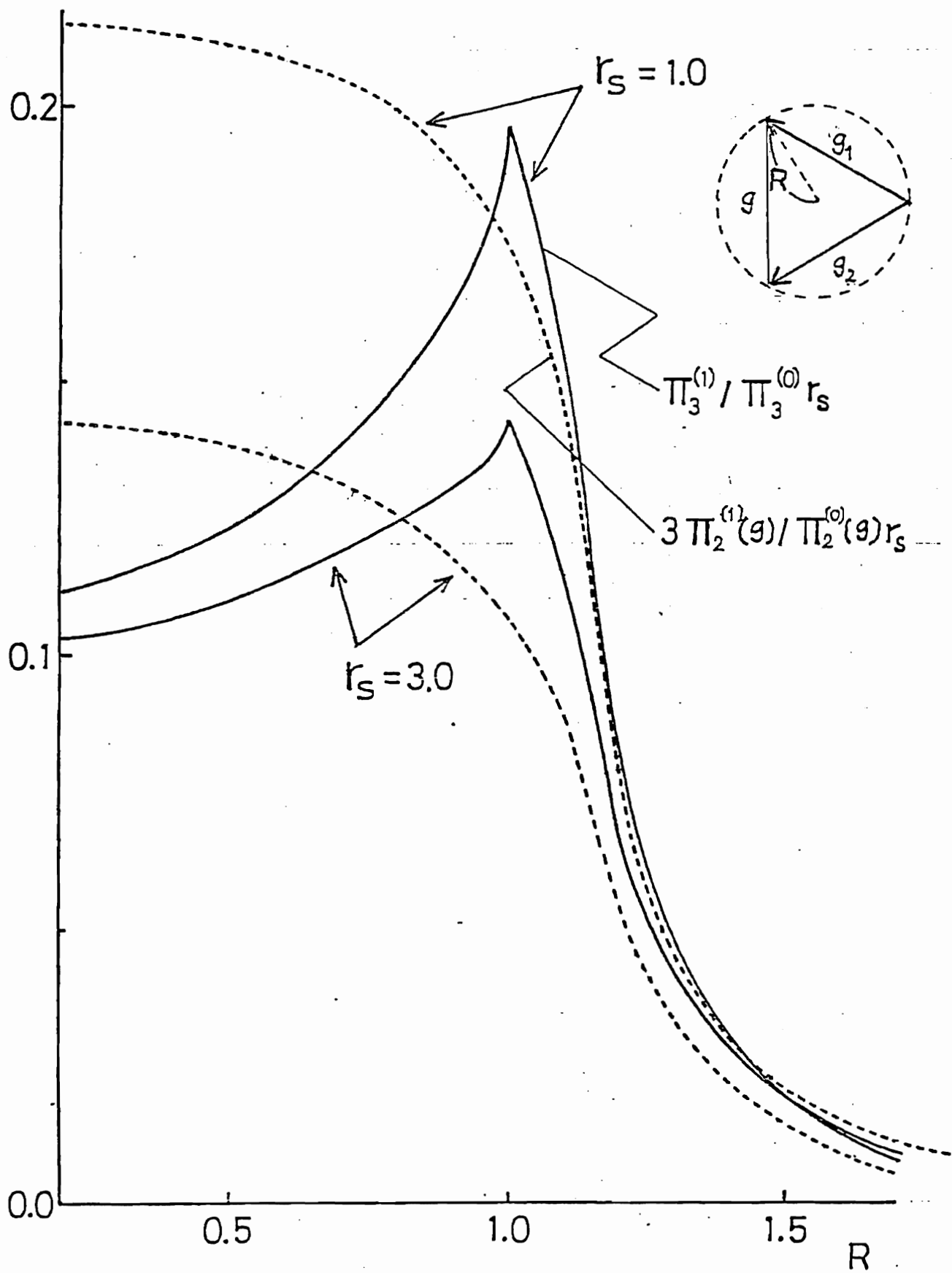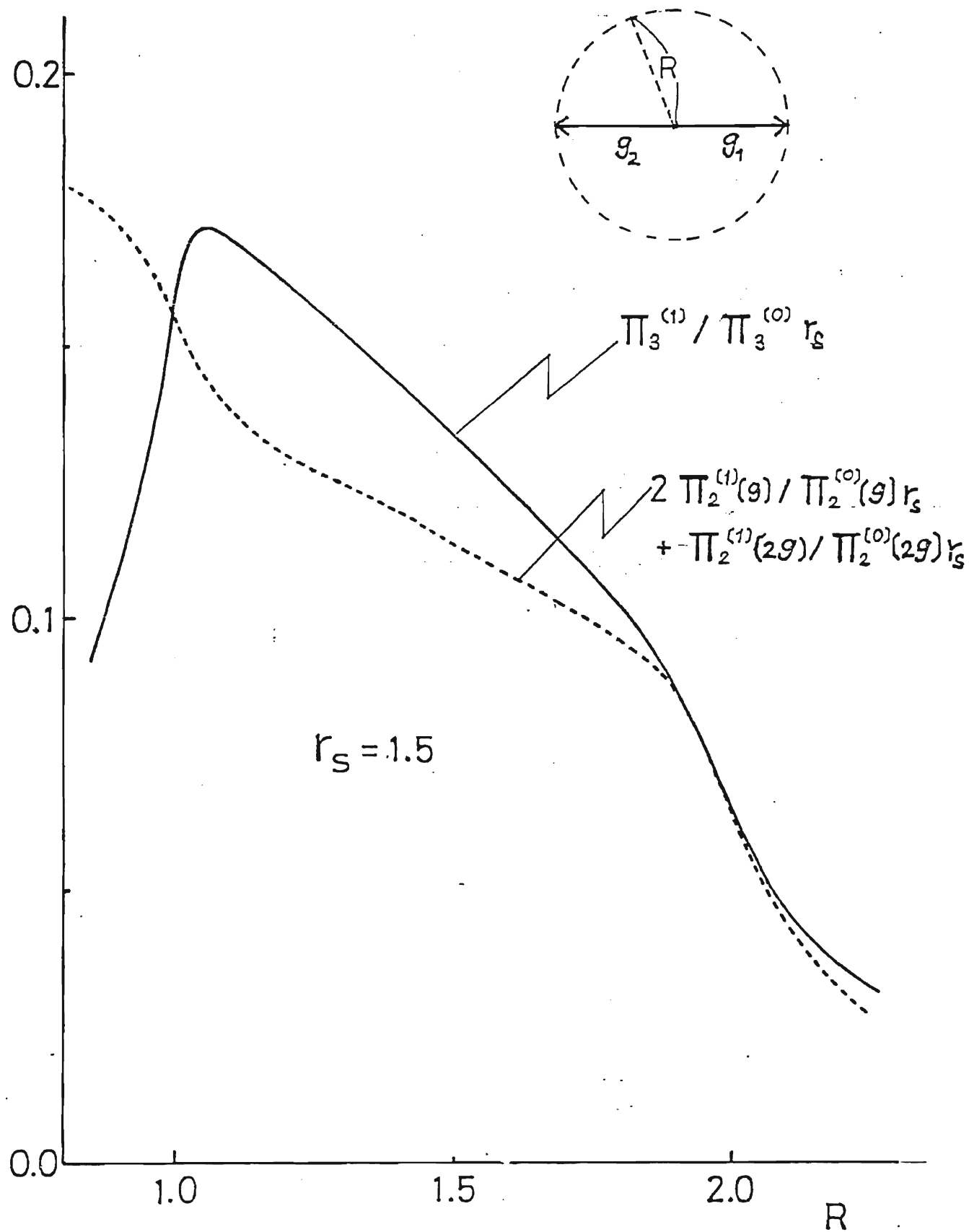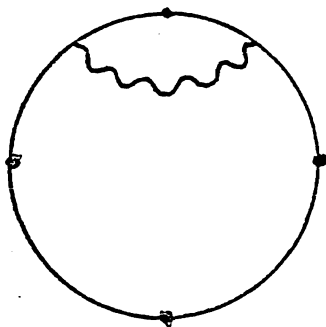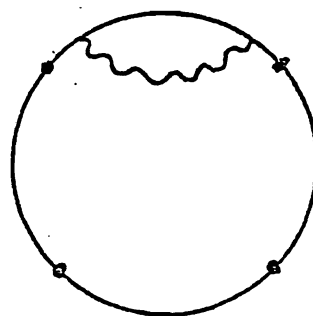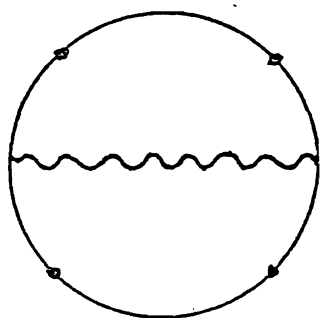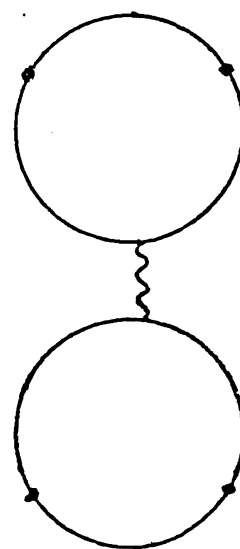
III Method for Evaluating Many-Point Ring Diagrams

in the Degenerate Case

§1. Introduction

In the structural expansion for the thermodynamical poten-
tial of metals,[1~3] the most important contributions come from
many-point ring diagrams(Fig.1). These are of the form

$$\Pi_n(g_1, \cdots g_n) = N^{-1} \sum_{p\sigma} \beta^{-1} \sum_{\ell} G_\sigma^0(p+g_1, \omega_\ell) \cdots \cdot G_\sigma^0(p+g_n, \omega_\ell), \quad (1)$$

where $G_\sigma^0(p, \omega_\ell)$ is the thermal Green's function for a free electron
with spin state σ:

$$G_\sigma^0(p, \omega_\ell) = (i\omega_\ell + \mu - \varepsilon_p)^{-1} \quad (2)$$

with $\qquad \omega_\ell = (2\ell+1)\pi/\beta, \ell = 0, \pm 1, \pm 2, \cdots$

$$\varepsilon_p = p^2/(\alpha r_s)^2. \quad (2a)$$

Here p denotes the momentum reduced in units of the Fermi momentum,
g_i the reciprocal lattice vector $(\hbar=1)$, μ the chemical potential,
N the number of electrons, $\beta = 1/k_B T$, and the other notations are also
the standard ones.

For the evaluation of Eq.(1), a systematic method was pro-
posed by Brovman and Kholas (BK),[4] where an integral represen-
tation with the Feynman prametrization was used for the n-point
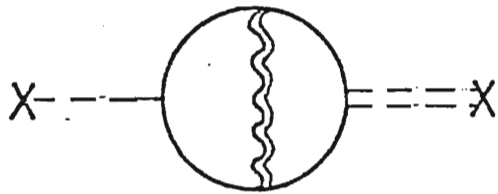diagram Π_n.[5,6] They also analyzed in detail the four-point ring
diagrams, giving expressions for all possible cases.[4] Nakamura
et al. also examined this case and presented more tractable ex-

pression for Π_4.[6] This paper will be referred to as STI.

Although BK's method of integration is general and in principle makes it possible to calculate Π_n for any specific cases, it is complicated especially for the degenerate case; a particular analysis is needed for each specific case in order to get the final expression. Here, by the degenerate case we mean the case when the vectors

$$\underset{\sim}{g}'_1 \equiv \underset{\sim}{g}_1 - \underset{\sim}{g}_n, \; \underset{\sim}{g}'_2 \equiv \underset{\sim}{g}_2 - \underset{\sim}{g}_n, \; \cdots, \; \underset{\sim}{g}'_{n-1} \equiv \underset{\sim}{g}_{n-1} - \underset{\sim}{g}_n \qquad (3)$$

are lineaaly dependent. (We introduce a redundant vector for the sake of symmetry.) Accordingly, one has exclusively the degenerate case for $n \geq 5$. Thus, in the higher order calculation BK's argument would be extremely cumbersome.

On the other hand, in STI a simple recurrence relation has been given together with a formula which connects a degenerate Π_4 to $\partial\Pi_n/\partial\mu$ with $n < 4$. However the treatment is not comprehensive for the case $n \geq 5$. In this paper three fundamental recurrence relations are presented for general cases. The obtained formulas constitute an algorithm for evaluating the higher-order diagrams, with the help of the existing lower order results.

The recurrence formulas are generally given in §2 and some of their applications to evaluation of the five-point diagrams are described in §3. The results will be utilized in part IV.

§2. Recurrence formulas

Let us consider

$$\Pi_n([\underset{\sim}{g_1}]^{k_1}, \cdots, [\underset{\sim}{g_m}]^{k_m})$$

$$\equiv \Pi_n(\overbrace{\underset{\sim}{g_1}, \cdots, \underset{\sim}{g_1}}^{k_1}, \cdots, \overbrace{\underset{\sim}{g_m}, \cdots, \underset{\sim}{g_m}}^{k_m}) \tag{4}$$

with $n = k_1 + k_2 + \cdots + k_m$, where all of the vectors $\underset{\sim}{g_1}$, $\underset{\sim}{g_2}$, $\cdots$, $\underset{\sim}{g_m}$ are assumed distinct. The exponent k_i will be called the multiplicity of the vector $\underset{\sim}{g_i}$. We shall use the following quantities

$$\mu^* = (\alpha r_s)^2 \mu,$$

$$\overset{\sim}{\Pi}_n = \Pi_n/(\alpha r_s)^{2n-2} \tag{5}$$

We shall consider two kinds of cases separately. The one is the case when the set of g-vectors $\{\underset{\sim}{g_1}, \cdots, \underset{\sim}{g_m}\}$ is degenerate irrespectively of the multiplicity. The other is the case when the set of g-vectors is non-degenerate but includes at least one vector with higher multiplicity than one. In accordance with the two cases considered above, we shall below look for two kinds of recurrence formulas separately.

(A) <u>Case when the set of g-vectors is degenerate.</u>

For this case, we have

$$\sum_{i=1}^{m-1} \gamma_i (\underset{\sim}{g}_i - \underset{\sim}{g}_m) = 0$$

with the coefficients $\gamma_1, \cdots, \gamma_{m-1}$, which do not vanish simultaneously. Introducing the m-th constant γ_m by $\gamma_m = -(\gamma_1 + \cdots + \gamma_{m-1})$, we rewrite the above relation as

$$\sum_{i=1}^{m} \gamma_i = 0, \qquad \sum_{i=1}^{m} \gamma_i \underset{\sim}{g}_i = 0. \tag{6}$$

For the sake of brevity we shall write $G(p)$ in place of $G_\sigma^0(\underset{\sim}{p}, \omega_\ell)$. And consider a quantity defined by

$$C = (\alpha r_s)^2 \sum_{i=1}^{m} \gamma_i [G(\underset{\sim}{p} + \underset{\sim}{g}_i)]^{-1}. \tag{7}$$

It is a simple matter to prove that C is a constant as given by

$$C = -\sum_{i=1}^{m} \gamma_i \, g_i^2. \tag{8}$$

Let us now rewrite Eq.(7) as

$$C[G(\underset{\sim}{p} + \underset{\sim}{g}_1)]^{k_1} \cdots [G(\underset{\sim}{p} + \underset{\sim}{g}_m)]^{k_m}$$

$$= (\alpha r_s)^2 \sum_{i=1}^{m} \gamma_i [G(\underset{\sim}{p} + \underset{\sim}{g}_1)]^{k_1} \cdots [G(\underset{\sim}{p} + \underset{\sim}{g}_i)]^{k_i - 1}$$

$$\cdots [G(\underset{\sim}{p} + \underset{\sim}{g}_m)]^{k_m}. \tag{9}$$

Assuming $C \neq 0$ and summing both sides of Eq.(9) over $\underset{\sim}{p}$, σ and ω_ℓ, we obtain the <u>first recurrence formula</u>

$$\overset{\sim}{\Pi}_n ([\underset{\sim}{g}_1]^{k_1} \cdots, [\underset{\sim}{g}_m]^{k_m})$$

$$= C^{-1} \sum_{i=1}^{m} \gamma_i \, \overset{\sim}{\Pi}_{n-1} ([\underset{\sim}{g}_1]^{k_1}, \cdots, [\underset{\sim}{g}_i]^{k_i - 1}, \cdots, [\underset{\sim}{g}_m]^{k_m}). \tag{10}$$

with the help of Eqs.(1) and (4). This is a generalization of Eq.(5.17) of STI. The formula (10) may be used successively until one of the Green's functions is eliminated from each term on the right-hand side of it. It is machinary to write down the expression thus obtained.

In the case when $C = 0$, Eq.(10) does not work. For this case we may assume $\gamma_1 \neq 0$ without loss of generality. Then we multiply Eq.(9) by $G(\underset{\sim}{p}+\underset{\sim}{g}_1)$ and perform the summation over $\underset{\sim}{p}$, σ, ω_ℓ. The result is the <u>second recurrence formula</u>

$$\underset{n}{\overset{\sim}{\Pi}}([\underset{\sim}{g}_1]^{k_1}, \cdots, [\underset{\sim}{g}_m]^{k_m})$$

$$= -\gamma_1^{-1} \sum_{i=2}^{m} \gamma_i \, \underset{n}{\overset{\sim}{\Pi}}([\underset{\sim}{g}_1]^{k_1+1}, [\underset{\sim}{g}_2]^{k_2}, \cdots, [\underset{\sim}{g}_i]^{k_i-1}, \cdots, [\underset{\sim}{g}_m]^{k_m}). \quad (11)$$

The case $C = 0$ occurs when heads of the vectors $\underset{\sim}{g}_1, \cdots, \underset{\sim}{g}_m$ are lying on the same sphere whose dimension is less than or equal to m-2 (See §3.). This case was called the still more degenerate one by BK. They treated it as an exceptional case, though an expression was derived for a specific case of Π_4 by the limiting procedure. Some examples will be given in §3 together with another geometrical meaning.

In Eq.(11) the multiplicity of $\underset{\sim}{g}_1$ becomes higher by one in the right-hand side. In the structural expansion only Π_n's with single multiplicities $k_1 = \cdots = k_n = 1$ come out in the normal term. However, if the condition $C = 0$ happens to be satisfied by some set of the reciprocal lattice vectors $\underset{\sim}{g}_1, \cdots, \underset{\sim}{g}_n$, the corres-

ponding Π_n is decomposed into the anomalous terms.

(B) Reduction of the multiplicity

The recurrence relations obtained above work when a set of g-vectors is degenerate. The reduction procedures are performed successively until any set of g-vectors contained in Π_n becomes non= degenerate , where the multiplicity of each g-vector may still remain. Let us then look for another recurrence relation which reduces Π_n to that of lower multiplicity.

Now, Brovman and Kagan[5] gave an integral representation for $\Pi_n(\underset{\sim}{g}_1, \underset{\sim}{g}_2, \cdots, \underset{\sim}{g}_n)$, using the Feynman parametrization procedure.[7] Following the same procedure we start with

$$\underset{\sim}{\Pi}_n([\underset{\sim}{g}_1]^{k_1}, \cdots, [\underset{\sim}{g}_m]^{k_m}) = (-\frac{d}{d\mu^*})^{n-1} \int_0^1 d\alpha_1 \cdots \int_0^1 d\alpha_m \, \delta(1-\sum_{i=1}^m \alpha_i)$$

$$\times \frac{\alpha_1^{k_1-1} \cdots \alpha_m^{k_m-1}}{(k_1-1)! \cdots (k_m-1)!} [\xi_m(\underset{\sim}{g}_1, \cdots, \underset{\sim}{g}_m)]^{3/2}, \qquad (12)$$

where we put

$$\xi_m = \mu^* + (\sum_{i=1}^m \alpha_i \underset{\sim}{g}_i)^2 - \sum_{i=1}^m \alpha_i g_i^2. \qquad (13)$$

Expression (12) can be derived by a generalized Feynman procedure (Appendix·A). In the same expression we carry out the integration in the last parameter α_m and introduce $\underset{\sim}{g}'_1, \cdots, \underset{\sim}{g}'_{m-1}$ by Eq.(3) to write down

$$\tilde{\Pi}_n([\underset{\sim}{g}_1]^{k_1}, \cdots, [\underset{\sim}{g}_m]^{k_m}) = (- \frac{d}{d\mu^*})^{n-1} \int_0^1 d\alpha_1 \cdots \int_0^{1-\sum_{i=1}^{m-2} \alpha_i} d\alpha_{m-1}$$

$$\times \frac{\alpha_1^{k_1-1} \cdots \alpha_{m-1}^{k_{m-1}-1} (1-\sum_{i=1}^{m-1} \alpha_i)^{k_m-1}}{(k_1-1)! \cdots (k_{m-1}-1)!(k_m-1)!}$$

$$\times [\xi_{m-1}(\underset{\sim}{g}_1', \cdots, \underset{\sim}{g}_{m-1}')]^{3/2}. \tag{14}$$

Here $\underset{\sim}{g}_1', \cdots, \underset{\sim}{g}_{m-1}'$ may be assumed linearly independent, since the alternative case has been treated already.

Now a useful recurrence relation may be obtained from Eq.(14) by partial integration in α_i. In the partial integration we meet

$$\partial \xi_{m-1}/\partial\alpha_i = 2 \sum_{j=1}^{m-1} g_{ij}\alpha_j - g_{ii} ,$$

$$i = 1, \cdots, m - 1 , \tag{15}$$

where in accordance with STI we put

$$g_{ij} = \underset{\sim}{g}_i' \cdot \underset{\sim}{g}_j' , \quad i,j = 1, \cdots, m - 1 . \tag{16}$$

Since the Gram determinant $D_{m-1} = \det(g_{ij})$ does not vanish, Eq. (15) is solved to be

$$\alpha_i = \tilde{\alpha}_i + \frac{1}{2} \sum_{j=1}^{m-1} \bar{g}_{ij} \frac{\partial \xi_{m-1}}{\partial \alpha_j} , \qquad i = 1, \cdots, m - 1, \tag{17}$$

where $\bar{g}_{ij}$ denotes ij-element of the inverse matrix to (g_{ij}) and

$$\tilde{\alpha}_i = \frac{1}{2} \sum_{j=1}^{m-1} \bar{g}_{ij} g_{jj}, \qquad i = 1, \cdots, m - 1 . \qquad (18)$$

It is convenient to introduce $\tilde{\alpha}_m$ by

$$\alpha_m = 1 - \sum_{i=1}^{m-1} \alpha_i, \qquad \tilde{\alpha}_m = 1 - \sum_{i=1}^{m-1} \tilde{\alpha}_i . \qquad (19)$$

Then Eq.(17) holds for i = m by introducing

$$\bar{g}_{mj} = \bar{g}_{jm} = -\sum_{i=1}^{m-1} \bar{g}_{ij}, \qquad j = 1, \cdots, m. \qquad (20)$$

Now, we utilize Eq.(17) in the partial integration (Appendix B). The result is the <u>third recurrence formula</u>

$$\tilde{\Pi}_{n+1}([\underset{\sim}{g_1}]^{k_1}, \cdots, [\underset{\sim}{g_i}]^{k_i+1}, \cdots, [\underset{\sim}{g_m}]^{k_m})$$

$$= - \frac{d}{d\mu^*} \{ \frac{\tilde{\alpha}_i}{k_i} \tilde{\Pi}_n([\underset{\sim}{g_1}]^{k_1}, \cdots, [\underset{\sim}{g_m}]^{k_m})$$

$$+ \frac{1}{2k_i} \sum_{j=1}^{m} \bar{g}_{ij} \tilde{\Pi}_{n-1}([\underset{\sim}{g_1}]^{k_1}, \cdots, [\underset{\sim}{g_j}]^{k_j-1}, \cdots, [\underset{\sim}{g_m}]^{k_m}) \},$$

$$\qquad\qquad\qquad i = 1, \cdots, m \qquad (21)$$

with $n = \sum_{j=1}^{m} k_j$. This formula is a generalization of Eq.(5.29) in STI. Note that the maximum number of g-vectors in Eq.(21) is four.

Recurrence Eq.(21) satisfies an identity

$$\sum_{i-1}^{m} k_i \tilde{\Pi}_{n+1}([\underset{\sim}{g_1}]^{k_1}, \cdots, [\underset{\sim}{g_i}]^{k_i+1}, \cdots, [\underset{\sim}{g_m}]^{k_m})$$

$$= - \frac{d}{d\mu^*} \overset{\sim}{\Pi}_n([\underset{\sim 1}{g_1}]^{k_1}, \cdots, [\underset{\sim m}{g_m}]^{k_m}),\qquad (22)$$

which is also derived easily from Eq.(4). This identity is essentially equivalent to BK's one, though the latter uses the sum of Π_n symmetrized in the transfer momenta.

§3. Evaluation of the five-point diagrams

In this section we shall go into some details of the computation procedure with particular reference to the five-point diagrams. Of the three recurrence formulas, the first one will be applied in the subsection (A), the second one in (B), and the third one in (C).

(A) The first recurrence formula.

We shall apply Eq.(10) to the five-point diagrams. For this case, we conveniently choose γ_i by

$$\sum_i \gamma_i t_i = \frac{1}{6} \begin{vmatrix} t_1 & t_2 & t_3 & t_4 & t_5 \\ 1 & 1 & 1 & 1 & 1 \\ g_{1x} & g_{2x} & g_{3x} & g_{4x} & g_{5x} \\ g_{1y} & g_{2y} & g_{3y} & g_{4y} & g_{5y} \\ g_{1z} & g_{2z} & g_{3z} & g_{4z} & g_{5z} \end{vmatrix}, \qquad (23)$$

where (g_{ix}, g_{iy}, g_{iz}) denote the components of g_i in a Cartesian coordinate system. The γ_i's thus chosen satisfy Eq.(6), as is easily observed from Eq.(23) by substituting 1 or g_i for t_i. We note here that, for instance, $|\gamma_1|$ is equal to the volume of a tetrahedron with heads of g_2, g_3, g_4 and g_5 as vertices. The above procedure works unless all of the vertices are lying on the same plane. For the coplanar case, we set $\gamma_5 = 0$ and determine the other coefficients by the current method.

Most of the five-point normal diagrams can be treated by utilizing Eq.(10). A computed example is shown in Fig.2. For the shown case, a set of four g-vectors chosen from $\{g_1, \cdots, g_5\}$ is degenerate. Even for this case $\Pi_5(g_1, \cdots, g_5)$ can be expressed in terms of Π_4, since C does not vanish. The singular behavior of Π_5 shown in Fig.2 comes from that of Π_4.[5] No more singularity comes in through decomposition.

(B) The second recurrence formula

This formula works for the case C = 0, namely

$$\sum_i \gamma_i g_i^2 = 0. \qquad (24)$$

As mentioned already, the above case occurs when heads of g_1, $\cdots$, g_5 are lying in a spherical surface. This follows directly from $\sum_i \gamma_i(g_i - P)^2 = 0$, which is satisfied by an arbitrary vector P owing to Eqs.(6) and (24).

Such singular case often appears among diagrams in the structural expansion. Some examples are shown in Fig.3. With refer-

ence to the figure, case (a) occurs in sc lattice, where eight reciprocal lattice points are lying in a spherical surface. Similar case also occurs in the orthorhombic lattice. In the body centered tetragonal lattice there exists the case when five reciprocal lattice points are lying in a spherical surface. Another reciprocal lattice point falls into the same surface paricularly for bcc lattice. This is shown in (b). Some of the other cases are also shown in (c) and (d), which appear in rhombohedral and hexagonal lattices respectively.

Now the physically significant vectors are such as $\underset{\sim}{g}_1' = \underset{\sim}{g}_1 - \underset{\sim}{g}_5$, $\cdots$, $\underset{\sim}{g}_4' = \underset{\sim}{g}_4 - \underset{\sim}{g}_5$ in accord with Eq.(3). All of the planes bisecting each of these vectors meet at the center of the sphere circumscribing such polyhedrons as shown in Fig.3. If the meeting point touches the Fermi surface, the relevant integral might be singular.

As an example let us consider the following set:

$$\underset{\sim}{g}_1 = (g,\ g,\ 0),\ \underset{\sim}{g}_2 = (g,\ 0,\ g),\ \underset{\sim}{g}_3 = (g,\ 0,\ -g),$$

$$\underset{\sim}{g}_4 = (2g,\ 0,\ 0),\ \underset{\sim}{g}_5 = (0,\ 0,\ 0). \tag{25}$$

For this set we choose γ_i by Eq.(23) as $\gamma_1 = 0$, $\gamma_2 = \gamma_3 = -\gamma_4 = -\gamma_5 = g^3/3$. Then we use Eq.(11) with γ_1 replaced by γ_5 to get

$$\overset{\sim}{\pi}_5(\underset{\sim}{g}_1,\ \cdots,\underset{\sim}{g}_4,\ 0)$$

$$= 2\overset{\sim}{\pi}_5(\underset{\sim}{g}_1,\ \underset{\sim}{g}_2,\ \underset{\sim}{g}_4,\ [0]^2) - \overset{\sim}{\pi}_5(\underset{\sim}{g}_1,\ \underset{\sim}{g}_2,\ \underset{\sim}{g}_3,\ [0]^2), \tag{26}$$

where $[0]^2$ stands for square of the Green's function $G(\underset{\sim}{p})$. The computed result is shown in Fig.4. Of the singularities included in each term of the right-hand side of Eq.(26), the two are weakened as a result of cancellation while the main one survives, being of the form $(\mu^\# - R)^{-1}$ with R the radius of the circumscribing sphere.[5]

(C) <u>The third recurrence formula</u>

The simplest terms, to which Eq.(21) is applied, are $\overset{\sim}{\Pi}_5([\underset{\sim}{g_1}]^2,$ $[\underset{\sim}{g_2}]^3)$, $\overset{\sim}{\Pi}_5(\underset{\sim}{g_1}, [\underset{\sim}{g_2}]^4)$ for m = 2 and $\overset{\sim}{\Pi}_5(\underset{\sim}{g_1}, \underset{\sim}{g_2}, [\underset{\sim}{g_3}]^3)$ for m = 3. We may leave the above terms out of consideration, since they do not appear in the fifth order calculation.

Let us then consider $\overset{\sim}{\Pi}_5(\underset{\sim}{g_1}, [\underset{\sim}{g_2}]^2, [\underset{\sim}{g_3}]^2)$ for m = 3. By applying twice Eq.(21) to the considered term, we obtain

$$\overset{\sim}{\Pi}_5(\underset{\sim}{g_1}, [\underset{\sim}{g_2}]^2, [\underset{\sim}{g_3}]^2)$$

$$= \overset{\sim}{\alpha}_2 \overset{\sim}{\alpha}_3 \overset{\sim}{\Pi}_3''(\underset{\sim}{g_1}, \underset{\sim}{g_2}, \underset{\sim}{g_3}) - (1/2)\bar{g}_{23}\overset{\sim}{\Pi}_3'(\underset{\sim}{g_1}, \underset{\sim}{g_2}, \underset{\sim}{g_3})$$

$$+ (1/8)\{[(2\overset{\sim}{\alpha}_2+1)\bar{g}_{31}+(2\overset{\sim}{\alpha}_3+1)\bar{g}_{21}]\overset{\sim}{\Pi}_2''(\underset{\sim}{g_2}, \underset{\sim}{g_3})$$

$$+ [(2\overset{\sim}{\alpha}_3+1)\bar{g}_{22}+2\overset{\sim}{\alpha}_2\bar{g}_{32}]\overset{\sim}{\Pi}_2''(\underset{\sim}{g_1}, \underset{\sim}{g_3})$$

$$+ [(2\overset{\sim}{\alpha}_2+1)\bar{g}_{33}+2\overset{\sim}{\alpha}_3\bar{g}_{23}]\overset{\sim}{\Pi}_2''(\underset{\sim}{g_1}, \underset{\sim}{g_2})\} \qquad (27)$$

after symmetrization, where we use the abbrreviatious: $\overset{\sim}{\Pi}_2' = d\overset{\sim}{\Pi}_2/d\mu^\#$, etc.

For m = 4, we similarly have

$$\Pi_5(\underset{\sim}{g}_1, \underset{\sim}{g}_2, \underset{\sim}{g}_3, [\underset{\sim}{g}_4]^2) = - \tilde{\alpha}_4 \hat{\Pi}'_4(\underset{\sim}{g}_1, \underset{\sim}{g}_2, \underset{\sim}{g}_3, \underset{\sim}{g}_4)$$

$$- (1/2)\{\bar{g}_{41}\hat{\Pi}'_3(\underset{\sim}{g}_2, \underset{\sim}{g}_3, \underset{\sim}{g}_4) + \bar{g}_{42}\hat{\Pi}'_3(\underset{\sim}{g}_1, \underset{\sim}{g}_3, \underset{\sim}{g}_4)$$

$$+ \bar{g}_{43}\hat{\Pi}'_3(\underset{\sim}{g}_1, \underset{\sim}{g}_2, \underset{\sim}{g}_4) + \bar{g}_{44}\hat{\Pi}'_3(\underset{\sim}{g}_1, \underset{\sim}{g}_2, \underset{\sim}{g}_3)\}. \quad (28)$$

Here $\hat{\Pi}'_4(\underset{\sim}{g}_1, \underset{\sim}{g}_2, \underset{\sim}{g}_3, \underset{\sim}{g}_4)$ can be evaluated similarly as in STI. However we note that the differentiated term does not include a single integral which remains in Π_4.

Appendix   A

— Generalized Feynman Procedure —

.

We shall derive Eq.(12) of text.   In the Feynman parametriza-
tion formula[7]

$$\frac{1}{A_1 A_2 \cdots A_m} = (m-1)! \int_0^1 d\alpha_1 \cdots \int_0^1 d\alpha_m \frac{\delta(1-\sum \alpha_i)}{(\sum_{i=1}^m \alpha_i A_i)^m} , \qquad (A1)$$

we substitute $A_i - \lambda_i$ for each of A_i's.   On the substituted ex-
pression we operate

$$\prod_{i=1}^m \left[\frac{1}{(k_i-1)!} \left(\frac{\partial}{\partial \lambda_i} \right)^{k_i-1} \right] , \qquad (A2)$$

and then put $\lambda_i = 0$ after differentiation.   Thus we get

$$\frac{1}{A_1^{k_1} A_2^{k_2} \cdots A_m^{k_m}} = \frac{(n-1)!}{(k_1-1)! \cdots (k_m-1)!} \int_0^1 d\alpha_1 \cdots \int_0^1 d\alpha_m$$

$$\times \delta(1-\sum \alpha_i) \frac{\alpha_1^{k_1-1} \cdots \alpha_m^{k_m-1}}{(\sum \alpha_i A_i)^n} , \qquad \sum k_i = n. \qquad (A3)$$

In the above expression we substitute $G(\underset{\sim}{p}+\underset{\sim}{g}_i)$ for each of A_i^{-1}'s.
The remaining procedures for the derivation are the same as given
in STI.

Appendix B

— Derivation of the third recurrence formula —

For the sake of simplicity, let us replace $\overset{\sim}{\Pi}_n([\underset{\sim}{g}_1]^{k_1}, \cdots,$
$[\underset{\sim}{g}_m]^{k_m})$ by $\overset{\sim}{\Pi}_{n+1}([\underset{\sim}{g}_1]^{k_1}, \cdots, [\underset{\sim}{g}_m]^{k_m+1})$ in Eq.(14) of text. Into
the resulting expression we substitute Eq.(17) of text to get

$$\overset{\sim}{\Pi}_{n+1}([\underset{\sim}{g}_1]^{k_1}, \cdots, [\underset{\sim}{g}_m]^{k_m+1})$$

$$= - \frac{d}{d\mu^*} \{ \frac{\overset{\sim}{\alpha}_m}{k_m} \overset{\sim}{\Pi}_n([\underset{\sim}{g}_1]^{k_1}, \cdots, [\underset{\sim}{g}_m]^{k_m}) + \frac{1}{2k_m} \sum_{j=1}^{m-1} \bar{g}_{mj} F_{mj} \}, \quad (B1)$$

where we put

$$F_{mj} = (- \frac{d}{d\mu^*})^{n-1} \int_0^1 d\alpha_1 \cdots \int_0^{1-\sum_{i=1}^{m-2}\alpha_i} d\alpha_{m-1}$$

$$\times \frac{2}{5} \frac{\alpha_1^{k_1-1} \cdots \alpha_{m-1}^{k_{m-1}-1} (1-\sum_{i=1}^{m-1}\alpha_i)^{k_m-1}}{(k_1-1)! \cdots (k_{m-1}-1)!(k_m-1)!} \frac{\partial}{\partial\alpha_j} \xi_{m-1}^{5/2} . \quad (B2)$$

It is now proved that

$$F_{mj} = \overset{\sim}{\Pi}_{n-1}([\underset{\sim}{g}_1]^{k_1}, \cdots, [\underset{\sim}{g}_i]^{k_i-1}, \cdots, [\underset{\sim}{g}_m]^{k_m})$$

$$- \overset{\sim}{\Pi}_{n-1}([\underset{\sim}{g}_1]^{k_1}, \cdots, [\underset{\sim}{g}_i]^{k_i}, \cdots, [\underset{\sim}{g}_m]^{k_m-1}) . \quad (B3)$$

For the proof we notice that Eq.(12) of text is symmetric in

permutation of $\alpha_1, \cdots, \alpha_m$. This symmetry is partially broken

after the first integration is performed with respect to α_m. However the permutation symmetry must be conserved in a set of $\alpha_1, \cdots, \alpha_{m-1}$. Owing to this observation we replace the integral in Eq.(B2) by

$$\int_0^1 d\alpha_1 \cdots \int_0^{1-\Sigma'' \alpha_i} d\alpha_j \cdots \qquad (B4)$$

where $\sum'' \alpha_i$ indicates the sum over α_i with exclusion of α_m and α_j. With the above replacement in mind, we integrate the right-hand side of Eq.(B2) by part with respect to α_j to eliminate the differentiation of $\xi_{m-1}^{5/2}$. In the resultants, the integrated term vanishes unless $k_j = 1$ and/or $k_m = 1$. After differentiating the resulting expressions once with respect to μ^*, one gets Eq.(B3) by using Eq.(12) of text. We note here that Eq.(B3) is valid even in the case when $k_j = 1$ and/or $k_m = 1$. For the mentioned case, with the help of Eq.(13) of text the integrated terms prove to bring about both or one of the two terms on the right-hand side of Eq.(B3) according as $k_j = 1$ and/or $k_m = 1$.

By inserting Eq.(B3) into Eq.(B1), we get Eq.(21) for $i = m$. This result must be independent of choice of the last parameter. Note that both $\bar{g}_{ij}$ and $\tilde{\alpha}_i$ are dependent only on the geometrical configuration of $\underset{\sim}{g}_1, \cdots, \underset{\sim}{g}_m$.

References

1) P. Lloyd and C.A. Sholl, J. of Phys. C1 (1968), 1620.

2) E.G. Brovman and Yu. Kagan, Uspekhi Fiz. Nauk SSSR 112 (1974), 369 [Soviet Phys.-Uspekhi 17 (1974), 125].

3) J. Hammerberg and N.W. Ashcroft, Phys. Rev. B9 (1974), 409.

4) E.G. Brovman and A. Kholas, Zh. Eksp. Teor. Fiz. 66 (1974), 1877 [Soviet Phys.-JTEP 39 (1974), 924].

5) E.G. Brovman and Yu. Kagan, Zh. Eksp. Teor. Fiz. 63 (1972), 1937 [Soviet Phys. -JETP 36 (1973), 1025].

6) T. Nakamura, H. Nagara and H. Miyagi, Prog. Theor. Phys. 63 (1980), 368.

7) J.D. Bjorken and S.D. Drell, *Relativistic Quantum Mechanics* (McGraw - Hill, 1964).

Figure Captions

Fig.1. Illustration showing many-point diagram. The symbols attached to broken lines represent momentum transfer.

Fig.2. Curve for $\tilde{\Pi}_5(g_1, \cdots, g_5)$ as a function of the scaling parameter g. In this ease $\tilde{\Pi}_5$ is decomposed into three distinct $\tilde{\Pi}_4'$s, which are shown in broken, dotted and dot-broken lines.

Fig.3. Illustration showing the cases when heads of g-vectors are lying on a sphere. (a) appears in sc, (b) in bcc, (c) in rhombohedral lattice, and (d) in hexagonal one.

Fig.4. Curve for $\tilde{\Pi}_5(g_1, g_2, g_3, g_4, 0)$ with heads of all g-vectors lying on a sphere. The broken and dotted curves represent the decomposed terms.

Fig.1

$$g_1 = (\ 0,g,g\ )$$
$$g_2 = (\ g,0,g\ )$$
$$g_3 = (\ g,g,0\ )$$
$$g_4 = (-g,g,0\ )$$
$$g_5 = (\ 0,0,0\ )$$

—— $\tilde{\Pi}_5(g_1,g_2,g_3,g_4,g_5)$

– – – $\tilde{\Pi}_4(g_2,g_3,g_4,g_5)$

········ $\tilde{\Pi}_4(g_1,g_3,g_4,g_5)$

–·–·– $\tilde{\Pi}_4(g_1,g_2,g_3,g_5)$

Fig.2

(b)

(d)

(a)

(c)

Fig.3

- 100 -

$$\tilde{\Pi}_5(g_1,g_2,g_3,g_4,0)$$

$$\tilde{\Pi}_5(g_1,g_2,g_4,[0]^2)$$

$$\tilde{\Pi}_5(g_1,g_2,g_3,[0]^2)$$

$$g_1 = (g,g,0)$$
$$g_2 = (g,0,g)$$
$$g_3 = (g,0,-g)$$
$$g_4 = (2g,0,0)$$

- 101 -

Fig.4
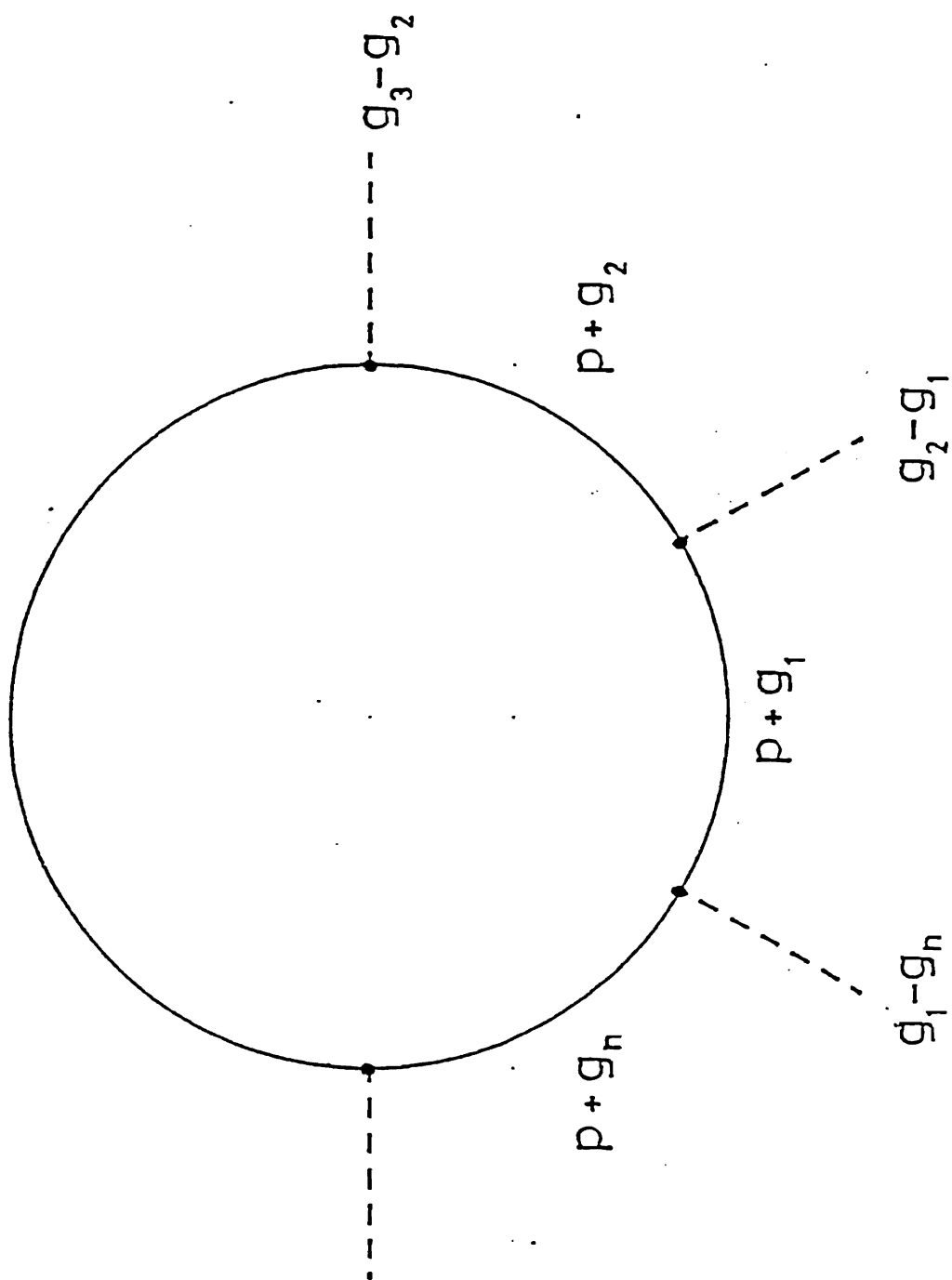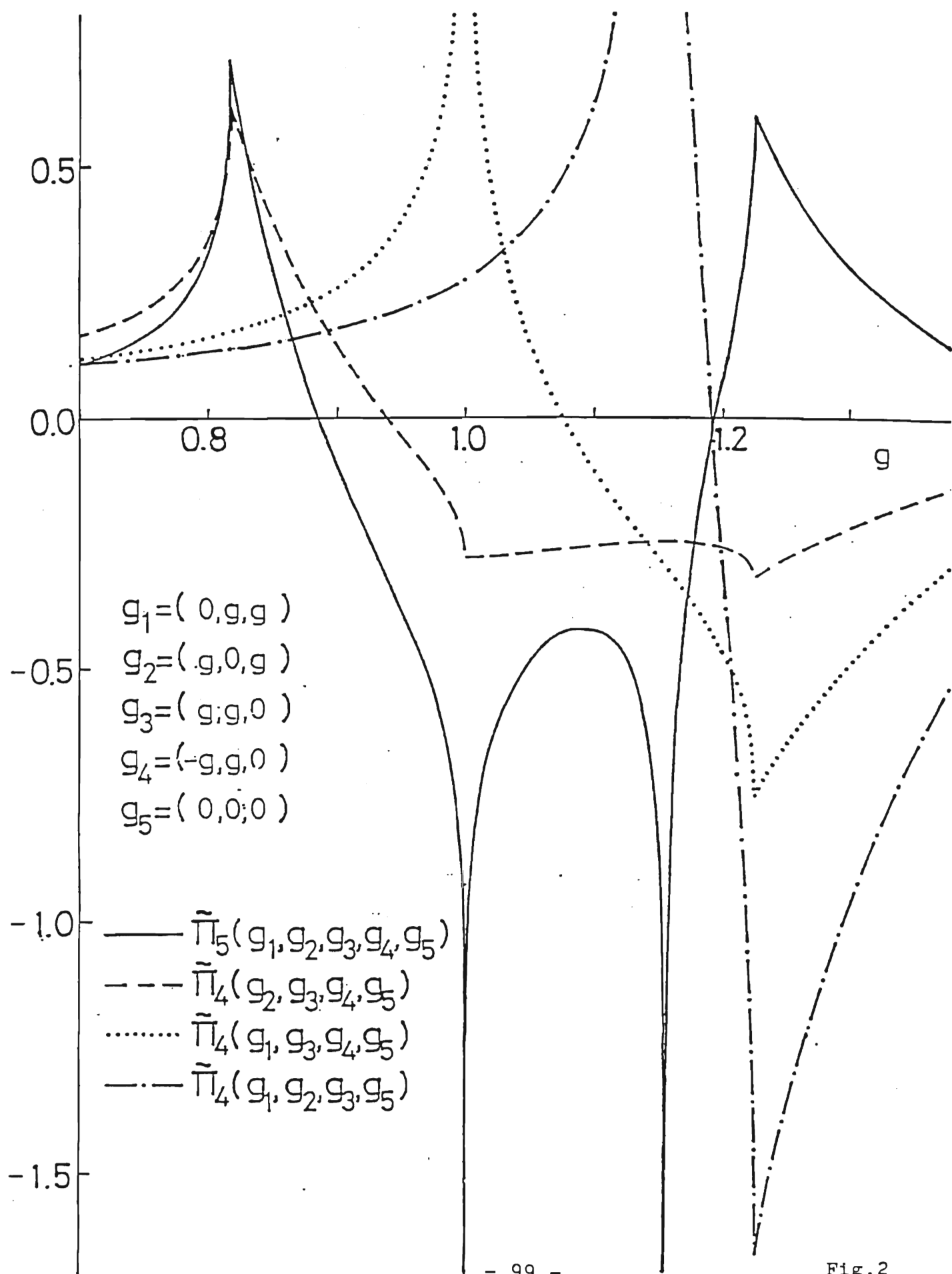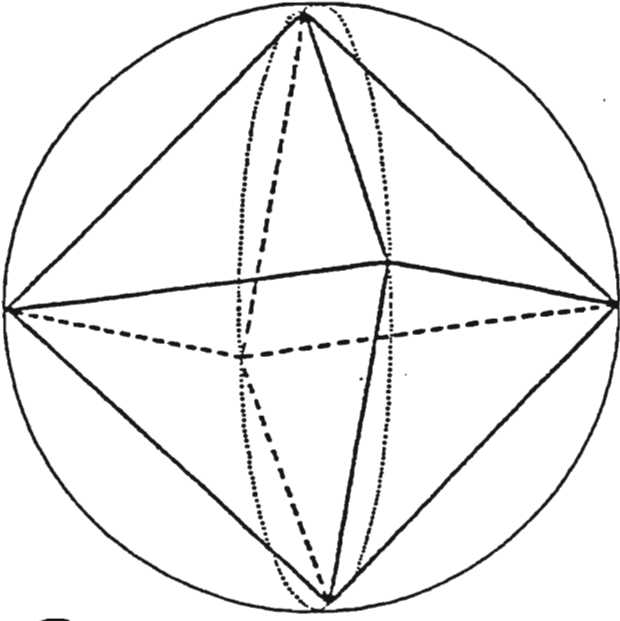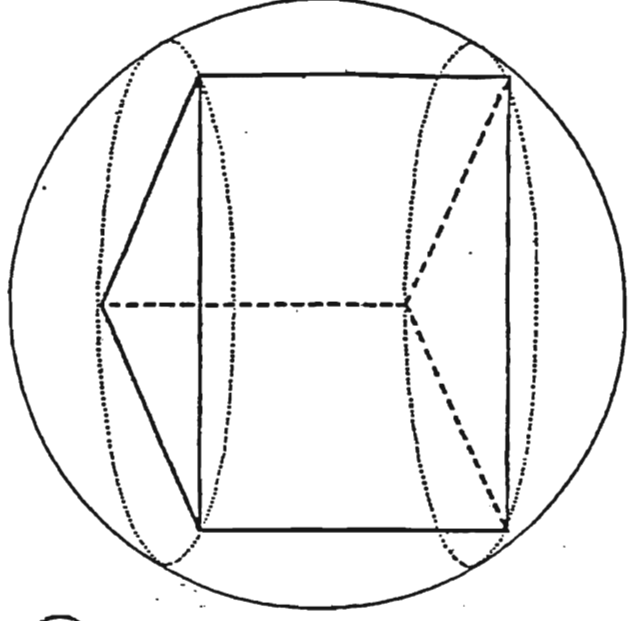
IV Stability of the Filamentary Structure of

Hydrogen and Its Monomer-dimer Transition

§1. Introduction

At extremely high pressures, any material would have an iso-
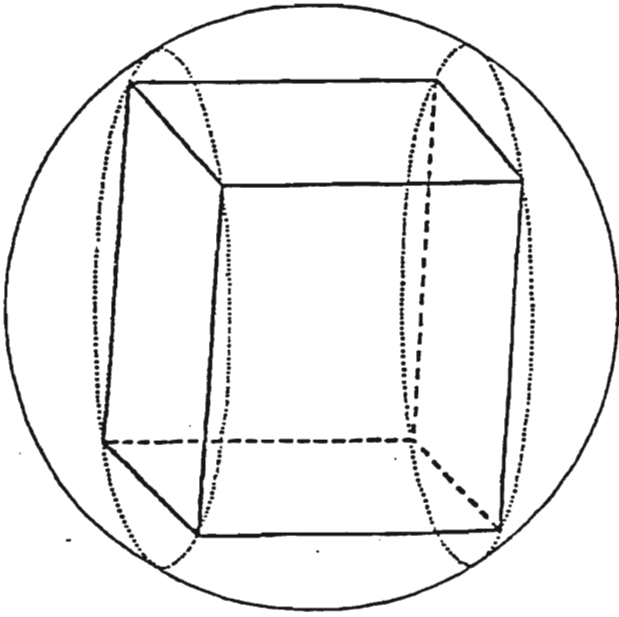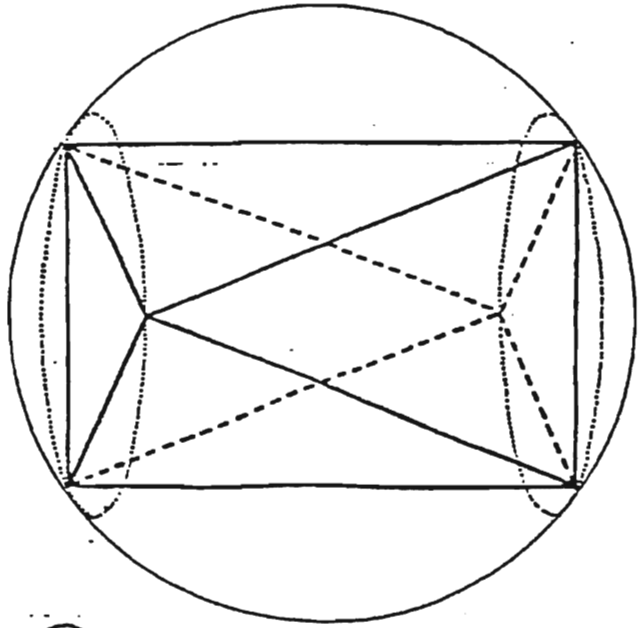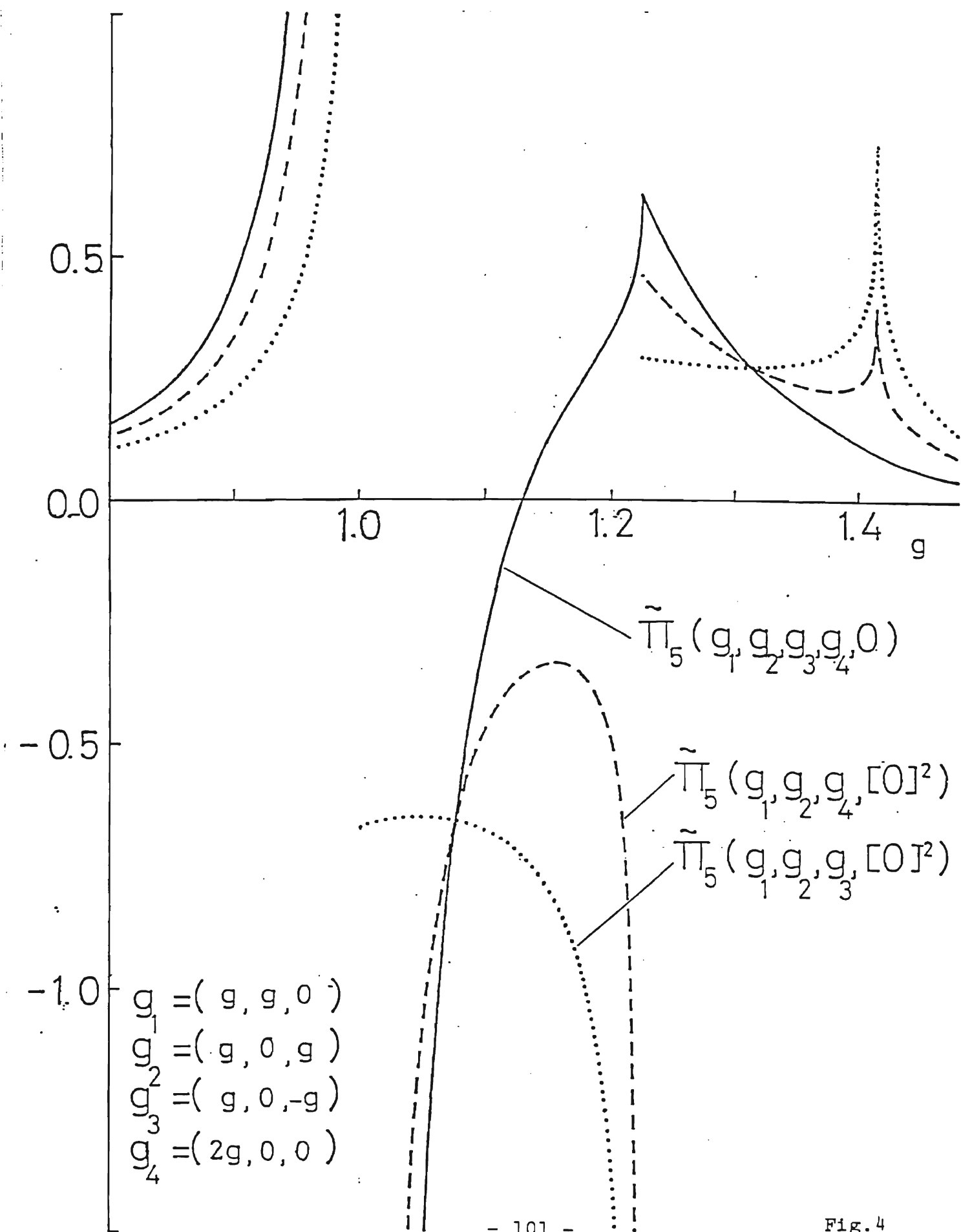tropic structure such as body-centered cubic (bcc) or face-centered
cubic (fcc), because of the strong repulsion between bare ions.
For the case of hydrogen, these highly symmetric structures become
unstable with decreasing density; strikingly anisotropic structures
may arise in the intermediate density regions. This possibility was
pointed   out by Brovman, Kagan and Kholas (BKK),[1~3] who investi-
gated extensively the structures of metastable phase of metallic
hydrogen over wide range of Bravais lattice structures in the
third-order perturbation. According to them, the prolate structures,
in which two-dimensional arrays of protons are stacked, are the
most stable one at intermediate densities (r_s~1), while the oblate
structures, in which a system of proton filaments forms a trian-
gular or quadratic lattice, are more favored at the lower density.

In a previous paper,[4] hereafter refered to as I, Nagara,
Miyagi and Nakamura looked for the stable phase of the same system
among cubic structures of more than one atom in a unit cell. This
approach is complementary to that by BKK. It was found in I that
the "bcc [111] monomer" structure is the lowest one in the third=
order stage. The mentioned structure is obtained from the simple
bcc lattice by putting an additional atom at every midpoint be-
tween the neighboring atoms along the body diagonal [111] and is
nearly identified with BKK's filamentary structure.[2] It was also

proved that the above structure transforms into a dimer one at a fairly low density in the fourth-order stage. The transition was found to be of the second order and the transition pressure was estimated to be $\sim$0.9Mbar ($r_s \sim 1.55$). In the dimer phase, the proton distance approaches a value nearly equal to but smaller than that of the free-molecule with decreasing density.

The predicted formation of anisotropic structures may be a characteristic feature of hydrogen, in which the anisotropy increases with decreasing density. However BKK's anisotropic structure is controversial.[5~8] Thus it may be important to look into the mechanism for the formation of anisotropic struc-tures: It is somewhat puzzling that the strongly anisotropic structures appear in such simple system as hydrogen. A qualitative consideration on the second order perturbation effect was made by Beck and Straus ,[9] in connection with the dynamical instability of phonons in metallic hydrogen. They attributed the phonon instability to the Kohn anomalies, which was thought responsible for the occurrence of BKK's structure. However this is not the whole story, though the occurrence for the planar structure may be related to their mechanism. The third- and higher-order effects are more essential to the formation of the filamentary structures. It is also interesting to elucidate whether such a strongly anisotropic stuctures might occur for the other simple elements, e.g. helium in the intermediate densities.

The aim of this part is two-fold. The first one is to ana-

lyse the mechanism of the formation of anisotropic structure. It is proved that the anisotropic structures result from the characteristic behavior in the momentum dependence of the n-point polarization Π_n. The same mechanism works to stabilize the cubic structures of helium. These qualitative results are confirmed by the numerical calculation for virtual crystals with nuclear charge $Z(1 \leq Z \leq 2)$.

The second purpose is to study the higher order effects on the monomer-dimer transition in the high-density hydrogen. In I, contrary to most of the other theoretical studies, Ref.10 and references therein, the ground-state energies for both monomer and dimer phases were calculated in the same scheme of the expansion, by utilizing the structural expansion given in Refs.[11~14] However, for the dimer phase the convergence of the series was rather slow. In order to clarify the nature of the transition it seems necessary to go beyond the approximations adopted in I.

This part is organized as follows. In IV-A, the mechanism for the formation of the anisotropic structure is analysed. Characteristics of the expansion terms are clarified in §2 for each order. The numerical results are described in §3 for the rhombohedral structures. An application of the result to the system of hydrogen-helium mixture is also discussed.

In IV-B, the higher-order effects on the monomer-dimer transition is studied with the use of the method described in parts II and III. This is done on the basis of the bcc [111] model. The

numerical result for the monomer-dimer transition is described in
§4. The fifth-order energy is included for the first time by
utilizing the result of part III. Higher-order effects with re-
spect to the electron-electron interaction are taken into account
by the effective vertex approximation proposed in part II. The
effect of the resummation is examined in Appendix A. Some techni-
cal aspects of the calculations are also described in the Appendices
B, C and D.

A.   Anisotropic stuctures of high-density hydrogen

§2.   Mechanisms by which the stable structure occurs

Let us consider the system with nuclear charge Z and write
down its total average energy, E per electron, as

$$E = E_{eg} + E_M + E_{st} , \qquad (1)$$

where E_{eg} denotes the electron gas energy, E_M the Madelung energy
and E_{st} the structural part of the electronic energy. We shall
consider the role of the structure dependent energies, E_M and E_{st},
which have different functions as factors for determining the
stable structure of crystals.

In this section our discussion will be confined to the Bravais
lattice structures with particular reference to the rhombohedral
family.

(a) Family of the rhombohedral lattices as a self-reciprocal
system

Rhombohedral lattices are obtained by stretching or shrinking
the simple cubic (sc) lattice along the body diagonal [111].[15]
The obtained lattice is described by a single uniaxial parameter
c/a. This family of lattices has an interesting symmetry; the
reciprocal lattice of its member also belongs to the family.
Structures having such a symmetry is called self-reciprocal by
Heine and Weaire.[16] The present case provides us with another
one than discussed by them. A fascinating feature of the rhombo-
hedral family consists in the fact that all of the three cubic
lattices, sc, bcc and fcc, are its members. It is convenient to
use the parameter $\gamma = \sqrt{6}$ c/a instead of c/a. The values of γ are
1/2, 1 and 2 respectively for bcc, sc and fcc. This parameter
has a property such that a lattice described by $1/\gamma$ coincides with
the reciprocal lattice of a crystalline lattice described by γ.

In Fig.1 we show the Madelung energy E_M as a function of γ.
A noticeable point is its symmetry with respect to the change
$\gamma \leftrightarrow 1/\gamma$. This symmetric character of the Madelung energy in a
self-reciprocal structure was pointed out by Weaire and Williams[17]
for the case of simple hexagonal structure. In the present case
two minima occur at bcc and fcc for which the numerical values of
E_M are fairly close to each other. We also observe in Fig.1 that
E_M increases steeply as the anisotropy of lattice becomes larger
both for the planar structure ($\gamma > 2$) and the filamentary one

$(\gamma < 1/2)$.

(b) Stability of the isotropic structures

In the high density region, the most dominant part of the structure dependent energy is E_M:

$$E_M = \alpha_M(\gamma) \, z^{2/3} \, r_s^{-1} \, . \tag{2}$$

The constant $\alpha_M(\gamma)$ is given by[18]

$$\alpha_M(\alpha) = \frac{4}{3\pi\alpha} \left\{ \sum_g{}' \frac{1}{(z^{1/3}g)^2} - \frac{1}{N_0} \sum_q{}' \frac{1}{(z^{1/3}q)^2} \right\} \tag{3}$$

for the Bravais lattice structures. In Eq.(3), N_0 is the total number of ions and $\alpha = (4/9\pi)^{1/3}$. And the second term in braces stands for the self-potential correction with q denoting the quasi= continuous wave vectors.

For the Madelung constants in the rhombohedral family, the appearance of minima at bcc and fcc may be proved by the following simple analysis.

Let us consider a sum over reciprocal lattice points defined by

$$I = \sum_g{}' f(g) \, , \tag{4}$$

where $f(g)$ is a function of the magnitude of g. The change of I under the volume conserving distortion may be expanded with respect to the change of g:

$$\Delta I = \sum_{g}' \left\{ (g'-g)f'(g) + \frac{(g'-g)^2}{2} f''(g) + \cdots \right\} . \qquad (5)$$

Then we expand $g' - g$ in the distortion parameter δ as

$$g' - g = g \left[A(g)\delta + B(g)\delta^2 + \cdots \right] . \qquad (6)$$

Let us look into what happens for the coefficients $A(g)$ and $B(g)$ at positions of bcc, sc and fcc. We first note that for the three structures under consideration the first, second and third neighbors form the cubic lattices, respectively. The first neighbor contribution to $A(g)$ vanishes for the three structures. And, for the similar contributions to $B(g)$ we have

$$\sum_{n.n.} B(g) = \begin{cases} \dfrac{63}{4} & \text{bcc} \\ 12 & \text{sc} \\ \dfrac{32}{3} & \text{fcc} \end{cases} \qquad (7)$$

Similarly we estimate

$$\sum_{n.n.} [A(g)]^2 = \begin{cases} 12 & \text{bcc} \\ 0 & \text{sc} \\ \dfrac{32}{3} & \text{fcc} \end{cases} \qquad (8)$$

Now for the Madelung constant we have $f(g) = \text{const}/g^2$. Then ΔI becomes

$$\Delta I = \sum_{g}' \frac{\text{const}}{g^2} [\, 3A(g)^2 - 2B(g) \,] \delta^2 + \cdots \quad . \qquad (9)$$

Thus by Eqs.(7) and (8) we can see that the first neighbor contributions to ΔI are positive for bcc and fcc and negative for sc.

Let us go further into what happens. In Fig.2 the magnitudes of short reciprocal lattice vectors are shown as a function of γ. Two baranches of the shortest reciprocal lattice vectors and the next ones cross at the positions of bcc and fcc, while sc is the minimum point of a single branch. According to the analysis described before, the contribution to the Madelung energy increases if the shortest vectors split into shorter and longer ones by the lattice distortions. The above observation for bcc and fcc will be important on considering the screening effect to be described shortly.

(c) Formation of the planar structures. —— Effect of the screening.

With decreasing density, the electronic part E_{st} of the structure dependent energy becomes more effective. Because of the Coulomb matrix element $\propto 1/g^2$ in the electron-ion interaction, contributions to E_{st} become larger for structures having smaller reciprocal lattice vectors. Since E_{st} is negative in sign, the isotropic structure may be less stabilized.

In the simple r_s-expansion, it is proved that the cubic

structures become unstable in the intermediate density region. Moreover, any structure can hardly be stabilized for r_s larger than certain value of it unless extremely anisotropic sturctures are taken into account.[18] At this point the screening effects on the electron-ion interaction come into play. It is very important to take proper account of the dielectric function.

Adding the second order energy in the structural expansion (part II) to the Madelung energy, we have

$$\tilde{E}_M = E_M + E_2$$

$$= \frac{1}{2} \sum_g{}' \tilde{v}(g) - \text{(self potential correction)}, \tag{10}$$

$$\tilde{v}(g) = v(g) / \varepsilon(g) \tag{11}$$

for the Bravais lattice sturctures, where $v(g)$ is the Coulomb matrix element

$$v(g) = \frac{8}{3\pi} \frac{1}{\alpha r_s} \frac{1}{g^2} \tag{12}$$

and $\varepsilon(g)$ the dielectric function for the electron gas.

Since Eq.(10) is of the same form as Eq.(4), we may use the similar analysis as in (b) to discuss the stability of crystals for the region with $\tilde{E}_M$ as a dominant contribution. The only difference from the previous analysis is the functional form of $f(g)$ for $g \lesssim 2$. In Fig.3 we show $\tilde{v}(g)$ as a function of g for $g \sim 2$.

The dotted line is the result with use of the RPA dielectric function $\varepsilon^0(g)$. And the full line corresponds to that with $\varepsilon(g)$ calculated by Miyagi,[14] which will be used throughout our calculation. The characteristic feature of $\tilde{v}(g)$ is the change of the curvature near $g = 2$, where the length of the shortest g-vector coincides with the Fermi diameter. This was already pointed out by Miyagi.[14]

Now, let us consider the first neighbor contribution ΔI to the energy difference of $\tilde{E}_M$ with lattice distortion taken into account. If the shortest g-vector is nearly equal to 2, $f''(g)$ decreases and changes its sign. For the present case the quantity corresponding to Eq.(9) becomes negative. We note here that the first term in Eq.(9) comes from $f''(g)$.

It has been proved that the isotropic structures become unstable if the shortest reciprocal lattice vector is nearly equal to and slightly greator than 2, in the intermediate region of density. For the above mechanism, the planar structure is more favored than the filamentary one, because the former structure produces more effectively shorter reciprocal lattice vectors in accordance with Fig.2, where the lowest branch on the right side has a steeper slope than the opposite one.

For the three cubic structures the shortest reciprocal lattice vectors are numerically given by

$$2.280/Z^{1/3} \qquad \text{bcc,}$$

$$2.031/Z^{1/3} \qquad \text{sc},$$

$$2.216/Z^{1/3} \qquad \text{fcc}.$$

For sc we have the g-vectors closest to the Fermi diameter. However sc is already at a minimum position in the rhombohedral family. Then, it is most possible to have a form distorted from fcc whose shortest vector is the one next closest to the Fermi diameter. This observation is also in accord with the numerical calculation for hydrogen with $Z = 1$.

However, the above mechanism no longer works for $Z \gtrsim 1.5$. It is because the shortest g-vector is now smaller than the Fermi diameter even for the isotropic stucture and accordingly any distortion does not produce further energy gain. Thus the planar structure does not occur for the region of interest.

The characteristic behavior of $\tilde{v}(g)$ around $g \sim 2$ may be connected with the Kohn anomaly. However it is clear by our analysis that the curvature of $\tilde{v}(g)$ in the vicinity of $g = 2$ is more responsible for the instability of lattice than the singularity itself just at $g = 2$. This conclusion is in accord with Stroud and Ashcroft,[19] who studied the phase stability in binary alloys by calculating the second order energy in the pseudopotential scheme.

The dielectric function $\varepsilon(g)$ with inclusion of the exchange= correlation effects increases the convexity of the effective coupling $\tilde{v}(g)$ near $g = 2$ as shown in Fig.3. This is a common

feature of the various kinds of current dielectric functions. Thus the exchange and correlation effect would enhance the formation of the anisotropic structures.

(d) Formation of the filamentary structures. — Effects of the three-point polarization

If the density decreases further, higher order terms in E_{st} become much more important. Though the magnitude of $E_n (n \geq 3)$ is rather small in the intermediate region, its strong dependence on the structure has a considerable effect on the choice of the stable structure. The most remarkable property of the higher order energy is the appearance of stronger singularities than the Kohn anomaly. These are the singular momentum dependence of the many-point polarization Π_n: the Brovman-Kagan (BK)[20] singularity.

To explain the role of the characteristic behavior of Π_n, let us consider the third order energy E_3:

$$E_3 = - \frac{1}{3} \sum_{g_1, g_2} \Pi_3(g_1, g_2) \tilde{v}(g_1) \tilde{v}(g_2 - g_1) \tilde{v}(-g_2) \ . \qquad (13)$$

In this expression the polarization Π_3 depends only on the triangle $< g_1, g_2 >$ determined by the reciprocal lattice vectors g_1 and g_2.

The momentum dependence of the function $\Pi_3^{(0)}$ is shown in Fig.4 for some families of similar triangles. Here $\Pi_3^{(0)}$ is the primary term in Π_3 and gives us a fundamental feature for the momentum dependence of Π_3 (see part II). In Fig.4, the horizontal axis is the radius R of the circle circumscribing the triangle $< g_1, g_2 >$.

The strong BK-singularity of the cusp type appears at $R = 1$ for acute triangles. For obtuse ones such a singularity does not appear. However even in the latter case the curve shown in Fig.4 has a fairly large peak near $R = 1$.

Now we look into the role of the singular behavior of Π_3 for the structural stability. The third order energy, Eq.(13), is a sum over triangles in the reciprocal lattice. Thus the structure having the triangles with $R = 1$ will be energetically favored. See Fig.5, where we plot radii R of the circumscribing circles for small triangles appearing in the reciprocal lattice of rhombohedral structures. Fig.5 also shows the ionic charge Z for which the structure described by γ has a reciprocal lattice triangle with $R = 1$.

Noticeable points observed in Fig.5 are the following. First, any small triangle does not appear in the planar structures for $Z \lesssim 2$. This is because the reciprocal lattice to the planar structure is oblate; the shortest g-vectors g_1 and g_2 are merely forming colinear configulations. For such a configulation, $\Pi_3^{(0)}$ can be reduced to a linear combination of $\Pi_2^{(0)}$ (see part III), and accordingly any singularity of the cusp type does not appear.

On the other hand, arbitrarily small triangle could appear if we distort the lattice towards the filamentary structure. Thus, for a fixed Z we can get a triangle with $R = 1$ at som value of $\gamma = \gamma_c$. For $Z = 1$, $\gamma_c \doteqdot 0.2417$. The structure roughly corresponds to the bcc [111] structure as called by Nagara et al. ($I^{4)}$), for which

- 115 -

$\gamma = 1/4$. With increasing Z, γ_c increases and the anisotropy of the corresponding structure decreases. For $Z = 2$, $\gamma_c \doteq 0.4835$, which is very close to bcc.

From the above observations we conclude that the strongly anisotropic filamentary structure should appear for hydrogen in the density region where E_3 becomes considerable. On the other hand the same mechanism does work to stabilize the bcc structure for helium. These conclusions are confirmed by the numerical calculation.

(e) Additional factors for stabilizing the anisotropic structure.

First we note that the cusp-type singularity described above also appears in the higher order polarizations Π_n $(n \geq 4)$.[11,20] For example, we consider Π_4, which is a function of the tetrahedron $[g_1, g_2, g_3]$ determined by reciprocal lattice vectors g_1, g_2 and g_3. Then Π_4 has the mentioned singularity when one of the radii of four circles circumscribing the sides of the tetrahedron $[g_1, g_2, g_3]$ coincides with the Fermi radius. The similar situation occurs for Π_n of higher order. Thus the higher order terms would enhance the mechanism for stabilizing the critical structure γ_c described in (d).

Second, Π_4 has another singularity when the radius of the sphere circumscribing the tetrahedron coincides with the Fermi radius.[11,20] This singularity is of the logarithmic divergence with positive sign. Thus the structure having such tetrahedrons in the reciprocal lattice space would energetically be unfavored.

However we do not meet such situation among the Bravais lattice structures in the case where $Z \leq 2$.

Next, we must mention the effect of the resummation.[8,9] As shown in Appendix A, by resumming the partial series including the higher order terms, the cusp-type singularity of Π_3 disappears. However this does not drasticlly change the peak structure of Π_3 near $R = 1$. Thus the characteristic role of Π_3 remains unaltered (§3).

Finally we note that the filamentary structure for hydrogen becomes unstable against the dimer formation (§4). This instability occurs only in the fourth-order without vertex correction.[4]

§3. Numerical results for the rhombohedral structures

In Figs.6, 7 we show the ground-state energy of rhombohedral structures as a function of the uniaxial parameter γ for $Z = 1$, 1.25, 1.5, 1.75, and 2. In Fig.6, the third order result with and without resummation is presented. The fourth-order result is shown in Fig.7. In the fourth-order energy, the electron-electron interaction is taken into account with the use of the effective vertex function.

For hydrogen we observe that the fcc structure becomes unstabe at $r_s \sim 0.9$ and the minimum position moves to the direction of the planar structure as r_s increases. For larger r_s ($r_s \sim 1.1$ in the fourth-order stage) the filamentary structure is more

favored. With increasing Z, the anisotropy of the filamentary structure reduces. Ror Z = 1.75, both bcc and fcc are stable throughout the density region calculated. The values of γ for the minimum structure are also plotted as a function of r_s in Fig.8.

The inclusion of the resummation effect changes the total energy by about 0.01 R_y at r_s = 1.6 for the third order energy of hydrogen with $\gamma = \gamma_c$. However the position of the minimum structure does not considerably change. Therefore the resummation does not alter our conclusion for the crystal stability.

In the resummation the cusp-type singularity for Π_3 is somewhat smoothed. The similar smoothing occurs when the effect of lattice vibration is taken into account. Here, the smoothing function is the sturcture factor $S(q)$ of ions. At this point we mention Straus and Ashcroft,[7] who treated the proton motion in a self= consistent phonon scheme in the second order structural expansion. Their calculation shows the isotropic structures to be more favored than the anisotropic ones. They also claimed the higher order terms would enhance this tendency by stronger smoothing effect. However we disagree with them. The misleading conclusion comes from a simple generalization of their second order result. For E_2, the structural stability depends sensitively upon the curvature of the shielded interaction $\tilde{v}(q)$ in the close vicinity of $q = 2$ as pointed out in §2(c). However, in the higher order terms the situation is quite different as seen before.

We have studied the crystal stability for crystals of virtual atoms with atomic number $1 \lesssim Z \lesssim 2$. The results for these virtual crystals may serve to get some predictions about solid mixtures of helium and hydrogen, which may be treated as an average crystal with an average atomic number

$$Z = (1-c) + 2c \qquad (14)$$

with c denoting the concentration of helium. This is a reasonable approach, where the scattering effect may then be taken into account as corrections. On this basis Straus et al[21] studied the above solid mixture by the structural expansion up to the third order.

However, the convergence of the expansion series becomes slower with increasing Z. It may simply be shown that our expansion parameter is proportional to $Z^{1/3} r_s$. Accordingly larger discrepancy might be expected with approaching Z = 2, unless the pressure is extremely high. It may be of interest to look into the higher order effect on the mixtures. According to our examination, however, the scattering contribution has proved very large. Then any reliable prediction would not be obtained until the mentioned effect is taken into account. We mention here that small difference of the cohesive energy might produce a large temperature effect.

B. Monomer-dimer transition in the system of hydrogen

§4. Higher order effects on the

monomer-dimer transition

(a) Monomer-dimer transition in the bcc [111]-model

In the sub-part A, the lowest structure of hydrogen system
was pointed out to be bcc [111] structure in the rhombohedral family,
where the two protons in the unit cell of bcc are lying along a
body-diagonal with equal separation. This structure has an out-
standing nature, where for twelve nearest reciprocal lattice vectors
g we have the structure factor $S(g) = 1$ for six g's and $S(g) = 0$
for the remaining g's. For our lattices the structure factor may
be given by

$$S(g) = \cos\left(\frac{1}{2}\, g\cdot\rho\right) , \tag{15}$$

where ρ denotes the vector to the nearest protons. Now, we have
$S(g) = 1$ because the six g-vectors are perpendicular to ρ. And we
have $S(g) = 0$ because the other g-vectors have $g\cdot\rho = \pi$. If the pro-
tons displace alternatively along the [111] direction, we have no
longer $S(g) = 0$ for the vectors mentioned above. Even for this case
we have still $S(g) = 1$ for the other six g-vectors. Then, for the
displacement considered the ground-state energy may be lowered.
This produces a monomer-dimer transition as described before.[4]
Referring to the above model, the ground-state energy has been

studied up to fourth order,[4] where the vertex function has not been taken into account. With the use of the vertex function, the result might change considerably particularly in the third order. The previous study has shown that the third order result does not produce the monomer-dimer transition unless the density is extremely low ($r_s \sim 3$). We shall look into what happens by taking account of higher order terms successively up to fifth order.

(b) Numerical results

We calculate the ground-state energy E of the hydrogen system for bcc [111] structure as a function of the proton displacement. In the monomer phase the proton separation will be denoted by $\bar{\rho}$ along [111] axis.

In Table I, contributions of various terms to E are compared with the previous result[4] up to fourth-order. The present calculation includes the higher order effects with respect to the electron-electron interaction in the effective vertex approximation described in part II. In Ref.4) these effects were taken into account by expanding them in terms of the shielded internal line. The expanded terms are written as $E_n^{(m)}$ in Table I, where m is the number of the electron-electron lines in the corresponding diagrams. The secon-order enrgy up to $E_2^{(2)}$ is almost identiacl with the present result. The third-order energy up to $E_3^{(1)}$ shows fairly good agreement with the present one.

A remarkable point arises in the fourth-order energy. The exchange-correlation contribution to E_4, which is simply neglected

in Ref.4, is considerably large. However this contribution partly
cancels that from the H-diagram $E_4{}^H$, which may be considered as a
term representing the higher-order screening effect and is also
neglected in Ref.4. Thus the total $E_4{}^{tot}$ of the fourth-order energy
in the present calculation has a fairly close value to that of the
previous one. We also note that a good cancellation between
the contributions from anomalous terms and that from the chemical
potential shift is maintained in the present calculation, and ac-
cordingly the resultant contribution δE is small.

The energy of the dimer phase may be represented as a function
of Δ defined by $\Delta = (\bar{\rho}-\rho)/\bar{\rho}$. The numerical results are well ap-
proximated by

$$E = A + B\Delta^2 + C\Delta^4 \tag{16}$$

as in Ref.4, where A, B and C are function of r_s. The monomer=
dimer transition may be analysed by this fitting form.[4] The
transition occurs when B vanishes. For the region of r_s where B<0,
the system favors the dimer phase.

In Table II we show contributions of various terms to the
constants A, B and C up to fifth-order. We notice a strong Δ-de-
pendence of the higher order terms, which comes largely from the
higher order contribution to B with slow convergence. The
constant A is fairly well convergent even at $r_s = 1.8$. On the other
hand the contribution to B from E_3 is even larger than that from
E_2 at $r_s = 1.4$. Contributions from E_4 and E_5 are also rather large.

These results may indicate that our expansion scheme would break down in the dimer phase. However it is expected that the transition point might well be described in our scheme.

The value of r_s at the transition is estimated to be 1.50 with transition pressure $P_c = 1.2$Mbar in the fourth-order stage. This result is not far from the previous one as expected from the above discussion on Table I. By including the fifth-order result we get $r_s = 1.40$ for the transition point with $P_c = 2.3$Mbar. However some cautions are needed for the fifth-order result. In the fifth-order energy, we have not included the H-type two-ring contribution (Fig. 9a), which would largely cancell the exchange= crrelation contribution. In the fifth order we also have the three-ring H-diagram (Fig. 9b), which has a negative contribution. These corrections would possibly lower the transition pressure as a resultant.

Here we emphasize that both the exchange-correlation effect and the long-range screening effect must be taken into account properly. Neglect of the former effect[22] brings us an under-estimation, while neglect of the latter[10] produces an overesti-mation in the fourth order energy.

As mentioned in (a), the transition occurs at fairly reasonable value of r_s even for the third order stage, with the vertex factor taken into account. The transition point r_s^* is given in Table III for each order of approximation. Though the scheme of extra-polation is somewhat arbitrary, the true value of r_s^* may be around

1.4. The fifth order result for the transiton pressure is close to
the value supposed currently. However the transition pressure is
very sensitive on the order of approximations, as seen in Table ·
III. Both of the above critical data may change by taking account
of the zero-point motion effect of protons. The study of this
effect is left as a future problem, though a preliminary attempt
is given in Appendix B.

Appendix A

Examination of the resummation effect

In part A we have seen that the most stable structure of hy-
drogen in the rhombohedral family is almost identical with the
bcc [111] structure[4] in the density region where the monomer=
dimer transition might occur.[4] It is numerically proved that the
resummation has only a minor effect on the determination of the
stablest structure. The method of resummation is formally given
in part II as a cluster expansion. Here we shall go into the
details of its calculation.

In the cluster expansion, the third order term for the thermo-
dynamical potential is written as

$$\tilde{\Omega}_3 = - \sum_{i<j<k} \sum_{k \in BZ} \sum_{\zeta_\ell} \ell n \frac{D_3(\{i,j,k\})D_1(\{i\})D_1(\{j\})D_1(\{k\})}{D_2(\{i,j\})D_2(\{j,k\})D_2(\{k,i\})} \quad , \quad (A.1)$$

where D_n is the $n \times n$ determinant defined in II§5, whose diagonal
elements are of the form

$$\varepsilon_{k+g} - \zeta_\ell \qquad (A.2)$$

and the off-diagonal elements are the effective external field

$$\tilde{\Sigma}_{g,g'} = \tilde{w}(g'-g)T(g'-g) \ . \qquad (A.3)$$

Here $\varepsilon_p = p^2/(\alpha r_s)^2$, $\zeta_\ell = (2\ell+1)\pi i/\beta + \mu$ with $\beta = 1/k_B T$ and μ the
chemical potential. And $\tilde{w}(g)$ is the shielded external field and

T(g) the effective vertex function (II). In Eq.(18), i,j and k in braces stand for the reciprocal lattice vectors and the summation over the quasimomenta k is to be taken in a Brillouin zone.

To evaluate $\tilde{\Omega}_3$ and higher order terms, we meet the quantity

$$I_n(k;\{1,2,\cdots,n\}) = -\sum_{\zeta_\ell} \ell n\, D_n(\zeta_\ell,k;\{1,2,\cdots,n\}) \ . \qquad (A.4)$$

Now by the definition we can write D_n as

$$D_n(\zeta,k) = \overset{\sim}{\prod_{j=1}} [\varepsilon^{(j)}(k) - \zeta] \ , \qquad (A.5)$$

where $\varepsilon^{(j)}(k)$ $(j=1,\cdots,n)$ is the j-th root of the characteristic equation

$$D_n(\zeta,k) = 0 \ . \qquad (A.6)$$

Thus Eq.(A.4) becomes

$$I_n(k;1,\cdots,n) = -\sum_{j=1}^{n} \frac{1}{\beta} \sum_{\zeta_\ell} \ell n[\varepsilon^{(j)}(k) - \zeta_\ell] \ . \qquad (A.7)$$

By using the contour integration as described in Ref.11, we get

$$I_n(k;1,\cdots,n) = \sum_{j=1}^{n} [\varepsilon^{(i)}(k) - \mu]f(\varepsilon^{(j)}(k)) \qquad (A.8)$$

at zero temperature, where $f(\varepsilon)$ is the Fermi factor. Here we note that the form (A.8) is owing to the choice of the branch cut of the logarithm as stated in II§5. However the final result (A.10) below is independent of the choice.

We shall below evalutate $\tilde{\Omega}_3$. Though the sum in Eq.(A.1) is taken over momenta in the first Brillouin zone, the summation may be replaced by that over whole momentum space. By such procedure we rewrite the sum over i,j,k in Eq.(A.1) as the corresponding sum over triangles $<g_1,g_2>$ which are not congruent to each other with respect to lattice translations. Thus we obtain the following expression for $\tilde{\Omega}_3$:

$$\tilde{\Omega}_3 = \sum_{<g_1,g_2>} \tilde{\Omega}_3(g_1,g_2) , \qquad (A.9)$$

$$\tilde{\Omega}_3(g_1,g_2) = 2 \sum_p \{ I_3(p;\{0,g_1,g_2\})$$

$$- I_2(p;\{g_1,g_2\}) - I_2(p;\{0,g_1\}) - I_2(p;\{0,g_2\})$$

$$+ I_1(p) + I_1(p+g_1) + I_1(p+g_2) \} . \qquad (A.10)$$

Here the factor 2 comes from the spin summation and the summation over p is to be performed in the whole momentum space. In Eq.(A.10) we put

$$I_1(p) = (\varepsilon_p - \mu) f(\varepsilon_p) . \qquad (A.11)$$

The first term of Eq.(A.10) is essentially the two-wave approximation, where the one-wave contributions must be subtracted since they were already counted in $\tilde{\Omega}_2$.

In the simple perturbation series, terms corresponding to $\tilde{\Omega}_3(g_1,g_2)$ is obtained by expanding the logarithmic term of Eq.(A.1)

with respect to the external field $\tilde{\Sigma}$. Then the primary term

becomes

$$\Omega_3(g_1,g_2) = N\ \Pi_3^{(0)}(g_1,g_2)$$

$$\times\ \{\ \tilde{\Sigma}_{g_1}\ \tilde{\Sigma}_{g_2-g_1}\ \tilde{\Sigma}_{-g_2} + \tilde{\Sigma}_{g_2}\ \tilde{\Sigma}_{g_1-g_2}\ \tilde{\Sigma}_{-g_1}\ \}\ ,\qquad\qquad \text{(A.12)}$$

with

$$\tilde{\Sigma}_g \equiv \tilde{\Sigma}_{0,g} = \tilde{w}(g)T(g)\ .$$

The remaining terms reduce to the higher order anomalous terms in
which only the many-point functions of the form

$$\cdot\ \Pi_n^{(0)}([g_1]^{k_1},\ [g_2]^{k_2},\ [0]^{k_3}) \qquad\qquad \text{(A.14)}$$

appear (see part III).

　　Now we turn to the effect of the resummation. Figure 10
shows the values of $\tilde{\Omega}_3(g_1,g_2)$ in comparison with those of $\Omega_3(g_1,g_2)$
in the case when $\langle g_1,g_2\rangle$ is a regular triangle. We first notice
the striking difference of the behavior near $R = 1$ with R the radius
of the circle circumscribing a triangle $\langle g_1,g_2\rangle$; the cusp-type
singularity in $\Omega_3(g_1,g_2)$ ceases to exist in the resummed result
$\tilde{\Omega}_3(g_1,g_2)$. However a shoulder remains in $\tilde{\Omega}_3(g_1,g_2)$ at $R = 1$ and the
global feature of $\Omega_3(g_1,g_2)$ does not drastically change.

　　The difference of the two curves in Fig.10 reduces with in-
creasing R. This fact permits us to use the unresummed quantity
$\Omega_3(g_1,g_2)$ instead of the resummed one $\tilde{\Omega}_3(g_1,g_2)$ for large triangles.

For the bcc [111], the smallest triangle has the circumscribing circle with $R \doteq 1.034$. For the shown case in Fig.10, the discrepancy is about 20% at the position of the mentioned triangle. However this discrepancy must somewhat be reduced by properly taking account of the effect of the chemical potential shift as discussed in II§5. Therefore we use the simple perturbation result throughout our numerical calculation.

Appendix B
An attempt for treating the phonon
effect on the monomer-dimer transition

The structural expansion of the dynamical matrix would be less convergent than that of the energy itself. Therefore it is essential to evaluate the higher order effects for the phonon problem. Unfortunately, the full calculation of the higher order dynamical matrix is much more difficult than the energy itself. Thus some ingeneous method is needed to treat the dynamical matrix.

Let us consider a crystal having two identical atoms in each unit cell. The relative position of two atoms in a unit cell will be denoted by ρ. Then the structure dependent part of the total energy E_{st} may be written as a function of ρ

$$E_{st} = E_{st}(\rho) . \qquad (B.1)$$

This energy may be expanded in a Fourier series

$$E_{st}(\rho) = \tilde{E}_{st}(0) + \sum_{g}{}' \tilde{E}_{st}(g) e^{ig \cdot \rho} , \qquad (B.2)$$

with g the reciprocal lattice vector. The above form is evident from the product of structural factors included in the structural expansion. In the structural expansion, we can get $\tilde{E}_{st}(g)$ more easily than $E_{st}(\rho)$.

Let us now look for the way for calculating $\tilde{E}_{st}(g)$. For this purpose we expand $\tilde{E}_{st}(g)$ as

$$\tilde{E}_{st}(g) = \sum_{n \geq 2} \tilde{E}^{(n)}(g) , \tag{B.3}$$

where n denotes the number of the structure factors included in a summand. Here the Madelung energy is to be included in $\tilde{E}^{(2)}(g)$. It is proved that $\tilde{E}^{(n)}(g)$ may be obtained by summing over reciprocal lattice points by the same way as for $E^{(n)}(\rho)$, but with the multiplicity of summation reduced by one. Furthermore, in the summation there appears no structure factor. It is also proved that $\tilde{E}^{(n)}(g)$ has the full symmetry of the Bravais lattice. And hence we have only to caluculate $\tilde{E}_{st}(g)$ once for each independent class of g.

Now we write down the final result for $\tilde{E}^{(2)}$ and $\tilde{E}^{(3)}$, in the following:

$$\tilde{E}^{(2)}(0) = \frac{1}{2} \left[\frac{1}{2} \sum_{g}{}' \tilde{v}(g) - \frac{1}{N} \sum_{q}{}' v(q) \right] , \tag{B.4a}$$

$$\tilde{E}^{(2)}(g) = \frac{1}{4} \tilde{v}(g) , \tag{B.4b}$$

and

$$\tilde{E}^{(3)}(g) = -\frac{1}{4} v(g) \sum_{g_2 \neq g}{}' v(g_2-g) v(-g_2) \Pi_3(g,g_2) , \tag{B.5a}$$

$$\tilde{E}^{(3)}(0) = \frac{1}{3} \sum_{g}{}' \tilde{E}^{(3)}(g) . \tag{B.5b}$$

The fourth-order term becomes somewhat complicated :

$$\tilde{E}^{(4)}(g) = \tilde{E}^{(4,a)}(g) + \tilde{E}^{(4,b)}(g), \quad g \neq 0 , \qquad (B.6a)$$

$$\tilde{E}^{(4)}(0) = \frac{1}{4} \sum_{g}{}' E^{(4,a)}(g) + E^{(4,b)}(0) , \qquad (B.6b)$$

with

$$\tilde{E}^{(4,a)}(g) = \frac{1}{8} \tilde{v}(g) \sum_{g_3}{}' \tilde{v}(-g_3) \sum_{g_2 \neq g, g_3} \tilde{v}(g_2 - g_3) \tilde{v}(g_3 - g)$$

$$\times \, \Pi_4(g, g_2, g_3), \quad g \neq 0 , \qquad (B.7)$$

$$\tilde{E}^{(4,b)}(g) = \frac{1}{32} \sum_{g_3 = g}{}' \tilde{v}(-g_3) \tilde{v}(g_3 - g) \sum_{g_2 \neq g}{}' \tilde{v}(g_2) \tilde{v}(g - g_2)$$

$$\times \, [\, 2\Pi_4(g, g_2, g_3) + \Pi_4(g - g_3, g_2, g_2 - g_3) \,] , \qquad (B.8)$$

Here in Π_4 the H-diagram contribution must be added after symmetrization. The properties of $E^{(n)}(g)$ mentioned beore can be seen explicitly in the above expressions.

In Fig.11 we plot the Fourier coefficients $\tilde{E}^{(3)}(g)$ for bcc ($\gamma = 0.5$) and the other two rhombohedral structures ($\gamma = 0.58, 0.67$). The dependence of $\tilde{E}^{(3)}(g)$ on g is quite similar for these three structures. As an application of the result, a rough sketch is made for $E(\rho)$ in Fig.12 for bcc up to the third order. The

calculation is not complete: the vertex factor is simply neglected
and the lattice summation is truncated at $g \simeq 6$. However some
general feature of the optical phonon may be obtained from Fig.11:
The transverse mode is softer than the longitudinal one.

Appendix C

Multiple summation in the reciprocal lattice

In the structural expansion, the n-th order contribution to the ground-state energy is usually written as a sum over (n-1) independent reciprocal lattice vectors. For example, the fourth= order energy is written as[11]

$$\Omega_4 = \frac{N}{4} \sum_{g_1,g_2,g_3}' \Pi_4(g_1,g_2,g_3)$$

$$\times \tilde{w}(g_1)\tilde{w}(g_2-g_1)\tilde{w}(g_3-g_2)\tilde{w}(-g_3). \qquad (C.1)$$

It is a formidable task, however, to execute such multiple sum- mation as encountered in Eq.(C.1). In fifth order, we have $\sim 10^4$ terms even if the summations are confined to the shortest g-vectors, for instance, in bcc lattice.

However, if we utilize the symmetric properties of the summand, terms to be counted can be drastically reduced. We shall describe here the procedure of such reduction particularly for the fourth= order energy. Generalization to the fifth-order one is straight- forward.

We first note that in the summand of Eq.(C.1), Π_4 is symmetric under the interchange of the vectors g_1, g_2 and g_3, while the pro- duct of $\tilde{w}$-terms changes to different forms. To avoid the above trouble, we symmetrize the summand of Eq.(C.1) with respect to

interchange of g-vectors:

$$\Omega_4 = \frac{1}{4!} \sum_{g_1,g_2,g_3}' \Omega_4(g_1,g_2,g_3) \ , \tag{C.2}$$

$$\Omega_4(g_1,g_2,g_3) = N \ \Pi_4(g_1,g_2,g_3)$$

$$\times \{ \ \tilde{w}(g_1)\tilde{w}(g_2-g_1)\tilde{w}(g_3-g_2)\tilde{w}(-g_3)$$

$$+ \tilde{w}(g_2)\tilde{w}(g_3-g_2)\tilde{w}(g_1-g_3)\tilde{w}(-g_1)$$

$$+ \tilde{w}(g_3)\tilde{w}(g_1-g_3)\tilde{w}(g_2-g_1)\tilde{w}(-g_2) + c.c. \} \ . \tag{C.3}$$

In the reduction of summation the first step is to utilize the permutation symmetry of Ew.(C.3). Number the reciprocal lattice vectors as $g^{(i)}$ such that $|g^{(i)}| \leq |g^{(j)}|$, $i < j$. Then Eq. .2) reduces to

$$\Omega_4 = \frac{1}{4} \sum_{i<j<k} \Omega_4(g^{(i)},g^{(j)}g^{(k)}) \ , \tag{C.4}$$

by considering the factor 3!, the number of permutations.

The next step is to utilize the translational and rotational symmetry of the lattice. For this purpose we note that the summand in Eq.(C.4) is a function only of the tetrahedron $[g^{(i)},g^{(j)},g^{(k)}]$ determined by g-vectors $g^{(i)},g^{(j)}$ and $g^{(k)}$. Thus the most efficient summation would be attained if we rewrite Eq.(C.4) as a sum over

different tetrahedrons with a suitable multiplication factor for each tetrahedron. Here the mentioned factor proves to be the number of the congruent tetrahedrons appearing in the reciprocal lattice with one vertex at origin. Since the complete reduction to such form is difficult in general cases, we shall below utilize partially the rotational symmetry as the second step and the translational one as the third step.

As the second step we fix $g^{(k)}$ with k the largest number among the rotationally equivalent g-vectors, and perform the summation over i and j. The resultant is multiplied by the number of g= vectors which is rotationally equivalent to $g^{(k)}$, where we divide the above resultant by the number of equivalent vectors in the triplet.

_ The third step is to utilize the translation symmetry. We choose one of the vertices of a tetrahedron, and count the contribution from tetrahedrons with the chosen vertex at origin, by taking account of the factor 4. A convenient choice is the vertex at which the largest number of the shortest g-vectors meet as the edges of tetrahedrons. Additional multiplication factor arises for tetrahedrons with equivalent vertices in conformity with the above choice. The factor proves equal to the inverse of the number of vertices satisfying our condition.

- We finally note that an additional manipulation is needed for the molecular phase, where the structure factor depends upon the direction of g-vectors with respect to the molecular axis. Even for this case the presented method remains effective if we replace

the terms in braces of Eq.(C.3) by its average. Here the average
is to be taken over configurations which are generated from the
one by rotations of the lattice symmetry.

Appendix D

Numerical integration for $\Pi_4^{(0)}$

In the expression for $\Pi_4^{(0)}$,[11] there appears an integal of the form (Eq.(5.14) of Ref.11)

$$I = \int_{R_m}^{R} \frac{dx}{(x^2+\delta)^{1/2}} f(x;s,r) \; ,$$

$$R_m = \text{Max}(s^2, -\delta) \; , \tag{D.1}$$

with

$$f(x;s,r) = \arcsin \left[\frac{r}{s} \left(\frac{x^2-s^2}{x^2-r^2} \right)^{1/2} \right] . \tag{D.2}$$

We propose the following form for the case when $s^2 + \delta \leq 0$:

$$I = \int_{0}^{\sqrt{\mu^*}} \frac{dt}{(t^2-\delta)^{1/2}} f([t^2-\delta^2]^{1/2};s,r) \; , \tag{D.3}$$

$$\mu^* = \delta + R^2 \; . \tag{D.4}$$

Equation (D.3) obtained by a simple change of the variable, $x^2 + \delta = t^2$, may be thought trivial. In this form, however, the computation time is largely reduced. It is because the denominator in the integrand of Eq.(D.3) no longer vanishes at the lower limit of the integration, while it is not the case for Eq.(D.1).

The reduction has proved very important for calculation of the fourth and higher order energy, since the main part of the computation time is devoted to this integral.

In Eq.(5.14) of Ref.11, the case $s = 0$ is excluded. For the excluded case Eq.(5.14) of Ref.11 reduces simply to

$$F_2(r_i, r_j) = \frac{\pi - \theta_{ij}}{2\pi} F_0 \ , \tag{D.5}$$

where

$$F_0 = 2\pi \left\{ \frac{R}{\sqrt{\mu^*}} - \frac{1}{2} \ell n \left| \frac{\sqrt{\mu^*} + R}{\sqrt{\mu^*} - R} \right| \right\} \ , \tag{D.6}$$

and $\pi - \theta_{ij}$ is the angle between the two sides of the tetrahedron, which is defined in Ref.11. The other notations follow Ref.11.

In the actual computation, we use the following expression for I.

$$I = f(R;s,r) \left\{ \frac{1}{2} \ell n \left| \frac{\sqrt{\mu^*} + R}{\sqrt{\mu^*} - R} \right| - \frac{1}{2} \ell n \left| \frac{(R_m^2 + \delta)^{1/2} + R_m}{(R_m^2 - \delta)1/2 - R_m} \right| \right\}$$

$$+ J \ , \tag{D.7}$$

where the remainder J of minor contribution is written as

$$J = \int_0^{(R^2 - s^2)^{1/2}} dz \frac{z}{(z^2 + s^2)^{1/2} (z^2 + s^2 + \delta)^{1/2}} g(z;R,s,r) \tag{D.8}$$

with

$$g(z;R,s,r) = \arcsin \left[\frac{r(s^2-r^2)^{1/2}}{s^2} \cdot \frac{Rz-(R^2-s^2)^{1/2}(z^2+s^2)^{1/2}}{(R^2-r^2)^{1/2}(z^2+s^2-r^2)^{1/2}} \right]$$

(D.9)

for $s^2 + \delta > 0$, and

$$J = \int_0^{\sqrt{\mu^*}} \frac{dt}{(t^2-\delta)^{1/2}} g([t^2-\delta^2-s^2]^{1/2};R,s,r)$$

(D.10)

for $s^2 + \delta \leq 0$.

References

1) E.G. Brovman, Yu. Kagan and A. Kholas, Zh. Eksp. Teor. Fiz. 61 (1971), 2429 [Soviet Phys. -JETP 34 (1972), 1300].

2) E.G. Brovman, Yu. Kagan and A. Kholas, Zh. Eksp. Teor. Fiz. 62 (1972), 1492 [Soviet Phys. JETP 35 (1972), 783].

3) E.G. Brovman Yu. Kagan, A. kholas and V.V. Pushkarev, ZhETF Pis. Re. 18 (1973), 269 [JETP Lett. 18 (1973), 160].

4) H. Nagara, H. Miyagi and T. Nakamura, Prog. Theor. Phys. 64 (1980), 731.

5) S.V. Iordanskii, O.V. Lokutsievskii, E.B. Vul, L.A. Sidorovich and A.M. Finkel'stein, ZhETF Pis. Red. 17 (1973), 530 [JETP Lett. 17 (1973), 383].

6) F.E. Harris and J. Delhalle, Phys. Rev. Lett. 39 (1977), 1340.

7) D.M. Straus and N.W. Ashcroft, Phys. Rev. Lett. 38 (1977), 415.

8) V.V. Avilov, Zh. Eksp. Teor. Phys. 77 (1979), 2331 [Soviet Phys. -JETP 50 (1979), 1122].

9) H. Beck and D. Straus, Helv. Physica Acta 48 (1975), 655.

10) Yu. Kagan, V.V. Pushkarev and A. Kholas, Zh. Eksp. Teor. Fiz. 73 (1977), 967 [Soviet Phys. -JETP 46 (1977), 511].

11) T. Nakamura, H. Nagara and H. Miyagi, Prog. Theor. Phys. 63 (1980), 368.

12) H. Miyagi, H. Nagara and T. Nakamura, Prog. Theor. Phys. 63 (1980), 1509.

13) H. Miyagi and H. Nagara, Prog. Theor. Phys. 64 (1980), 747.

14) H. Miyagi, Prog. Theor. Phys. $\underline{65}$ (1981), 66; also private communication.

15) For instance, N.W. Ashcroft and N.D. Mermin, <u>Solid State Physics</u>,(Säunders College, Philadelphia, 1976).

16) V. Heine and S. Weaire, Solid State Physics $\underline{24}$ (1970), 249.

17) D. Weaire and A.R. Williams, Phil. Mag. $\underline{11}$ (1969), 1105.

18) H. Nagara, H. Miyagi and T. Nakamura, Prog. Theor. Phys. $\underline{56}$ (1976), 396.

19) D. Stroud and N.W. Ashcroft, J. of Phys. F $\underline{1}$ (1971), 113.

20) E. G. Brovman and Yu. Kagan, Zh. Eksp. Teor. Fiz. $\underline{63}$ (1972), 1937 [Soviet Phys. -JETP $\underline{36}$ (1973), 1025].

21) D.M. Straus, N.W. Ashcroft and H. Beck, Phys. Rev. $\underline{B15}$ (1977), 1914.

22) J. Hammerberg and N.W. Ashcroft, Phys. Rev. $\underline{B9}$ (1974), 409.

Table I   Minute description of contribtuions to the ground-state
energy for representative cases in comparison with Ref.4)
(in units of Rydberg)

	$r_s = 1.4$			
	ρ/bohr 1.50		ρ/bohr 1.31	
	previous[†]	present	previous[†]	present
E_{eg}	0.3684	0.3684	0.3684	0.3684
E_M	-1.1261	-1.1261	-1.0939	-1.0939
E_2	-0.2125	-0.2117	-0.2236	-0.2226
$E_2^{(0)}$	-0.1864		-0.1959	
$E_2^{(1)}$	-0.0160		-0.0170	
$E_2^{(2)}$	-0.0101		-0.0107	
E_3	-0.0734	-0.0808	-0.0850	-0.0915
$E_3^{(0)}$	-0.0608		-0.0691	
$E_3^{(1)}$	-0.0136		-0.0159	
E_4	-0.0199	-0.0280	-0.0250	-0.0365
$E_4^{(0)}$	-0.0199		-0.0250	
E_4^H		0.0091		0.0127
δE	+0.0014	0.0023	0.0012	0.0021
E_4^{tot}	-0.0185	-0.0189	-0.0238	-0.0238
E^{tot}	-1.0631	-1.0675	-1.0579	-1.0617

† Ref.4

Table I cont'd

<center>$r_s = 1.8$</center>

	ρ/bohr = 1.70		ρ/bohr =1.23	
	previous[†]	present	previous[†]	present
E_{eg}	0.0762	0.0762	0.0762	0.0762
E_M	-0.8543	-0.8543	-0.6986	-0.6986
E_2	-0.2178	-0.2167	-0.2709	-0.2685
$\quad E_2^{(0)}$	-0.1871		-0.2321	
$\quad E_2^{(1)}$	-0.0180		-0.1227	
$\quad E_2^{(2)}$	-0.0127		-0.1161	
E_3	-0.0995	-0.1099	-0.1661	-0.1851
$\quad E_3^{(0)}$	-0.0791		-0.1298	
$\quad E_3^{(1)}$	-0.0204		-0.0363	
E_4	-0.0359	-0.0549	-0.0810	-0.1253
$\quad E_4^{(0)}$	-0.0359		-0.0810	
$\quad E_4^{H}$		0.0224		0.0541
$\quad E$	0.0017	0.0032	0.0012	0.0024
E_4^{tot}	-0.0342	-0.1293	-0.0798	-0.0688
E^{tot}	-1.1296	-1.1339	-1.1392	-1.1449

[†] Ref.4

Table II, Values of fitting constants A, B and C to reprocuduce the ground-state energy in the form $E = A + B\Delta^2 + C\Delta^4$

	$r_s = 1.0$			$r_s = 1.2$			$r_2 = 1.4$		
	A	B	C	A	B	C	A	B	C
E_{eg}	1.1786	0	0	0.6617	0	0	0.3684	0	0
E_M	-1.5745	1.584	3.62	-1.3157	1.539	1.84	-1.1277	1.322	1.54
E_2	-0.2152	-0.469	0.23	-0.2133	-0.461	0.21	-0.2114	-0.457	0.21
E_3	-0.0603	-0.418	0.23	0.0724	-0.435	0.00	-0.0804	-0.486	-0.11
E_4^{tot}	-0.0093	-0.139	-0.03	-0.0118	-0.286	0.05	-0.0164	-0.222	-0.03
E_4	-0.0139	-0.187	-0.04	-0.0195	-0.273	0.00	-0.0278	-0.346	-0.10
E_4^H	0.0034	0.051	0.00	0.0059	0.081	0.03	0.0091	0.124	0.04
δE_4	0.0012	-0.003	0.00	0.0018	-0.005	0.01	0.0023	-0.007	-0.03
E_5 a)	-0.0022	-0.060	-0.15	-0.0037	-0.101	-0.26	-0.0057	-0.155	-0.41
E^{tot}(upto 4th)	-0.6805	0.557	4.05	-0.9515	0.445	2.10	-1.0675	0.148	1.60
E^{tot}(upto 5th)	-0.6827	0.496	3.89	-0.9552	0.343	1.83	-1.07317	-0.007	1.18

a) without contribution from H-diagram

Table II cont'd

	$r_s = 1.6$			$r_s = 1.8$		
	A	B	C	A	B	C
E_{eg}	0.1901	0	0	0.0762	0	0
E_M	-0.9866	1.142	1.50	-0.8762	0.986	1.50
E_2	-0.2093	-0.451	0.20	-0.2071	-0.446	0.20
E_3	-0.0891	-0.554	0.03	-0.0967	-0.608	0.06
E_4^{tot}	-0.0196	-0.265	-0.08	-0.0234	-0.263	-0.30
E_4	-0.0353	-0.433	-0.15	-0.0442	-0.495	-0.38
E_4^H	0.0128	0.177	0.15	0.0172	0.242	0.05
δE_4	0.0029	-0.008	0.01	0.0034	-0.010	0.02
E_5 [a]	-0.0082	-0.220	-0.59	-0.0114	-0.297	-0.81
E^{tot} (up to 4th)	-1.1146	-0.129	1.65	-1.1275	-0.333	1.46
E^{tot} (up to 5th)	-1.1064	-0.350	1.05	-1.1386	-0.630	0.65

Table III   Transition pressure P_c, the value of r_s and the ground=

   state energy E per electron at the transition point, for

   each order of the approximation.

		2nd	3rd	4th	5th
P_c	a)	~ -0.1	0.06	1.19	2.33
r_s		~ 4	1.75	1.50	1.40
E	b)	~ -0.8	-1.105	-1.098	-1.073

a)   units in Mbar

b)   units in Ry

Figure Captions

Fig.1. Madelung energy for the rhombohedral structure as a
   function of γ in logarithmic scale.

Fig.2. Magnitudes of the small reciprocal lattice vectors in
   the rhombohedral structure as a function of γ.

Fig.3. Screened Coulomb matrix element $\tilde{v}(g)$ as a function of
   g for r_s = 2. The solid line is based on the dielectric
   function given in Ref.14, and the dotted line on that of RPA.
   The broken line represents the bare Coulomb matrix element.

Fig.4. Curves for $\Pi_3^{(0)}(g_1,g_2)$ vs. R, the radius of the circle
   circumscribing the triangle $\langle g_1,g_2 \rangle$.

Fig.5. Magnitudes of R for small triangles in the reciprocal
   lattice of the rhombohedral structure as a function of γ.

Fig.6. Ground-state energy as a function of γ for the rhombo-
   hedral structure. Figures 6a to 6e correspond respectively
   to Z = 1, 1.25, 1.5, 1.75, 2. The solid lines are the
   unresummed result and the broken lines the resummed one both
   up to third order without vertex correction.

Fig.7. Ground-state energy as a function of γ for the rhombo-
   hedral structure. (a) Z = 1 for r_s = 1.5 (b) Z = 1.5 for
   r_s = 1.31 (c) Z = 2 for r_s = 0.99 . The exchange-correlation
   effects are taken into account by the effective vertex function
   T(g).

Fig.8. Distortion parameter γ as a function of r_s for the ex-
tremum structures. The solid lines stand for the stablest
structure. (a):fcc, (b):sc, (c):bcc, (d): planer structure,
(e):filamentary structure.

Fig.9. H-diagrams to appear in fifth order.

Fig.10. Contribution $\tilde{\Omega}_3(g_1,g_2)$ to the third order thermodynamical
potential $\tilde{\Omega}_3$ in the cluster expansion as a function of R (solid
line) in comparrison with the unressumed one (broken line) for
the regular triangles $<g_1,g_2>$.

Fig.11. Fourier coefficient $\tilde{E}_3(g)$ plotted against reciprocal
lattice vector g, referring to the rhombohedral system.

Fig.12. Equi-energy curves for various molecular configulations
in the bcc lattice (third order result). The equi-energy curves
are drawn for positions of a proton in the unit cell when another
is at the origin of the same cell. Here $\Gamma = (0,0,0)$, $K = (-\frac{3}{8},$
$\frac{3}{8},0)$, $L = (\frac{1}{4},\frac{1}{4},\frac{1}{4})$, $W = (0,\frac{1}{2},\frac{1}{4})$ in units of the length of cube edge.

Fig. 1

Fig. 2

$\tilde{v}(g)$

$r_s = 2$

Fig. 3

- 152 -

Fig. 4

Fig. 5

- 154 -

Fig. 6a
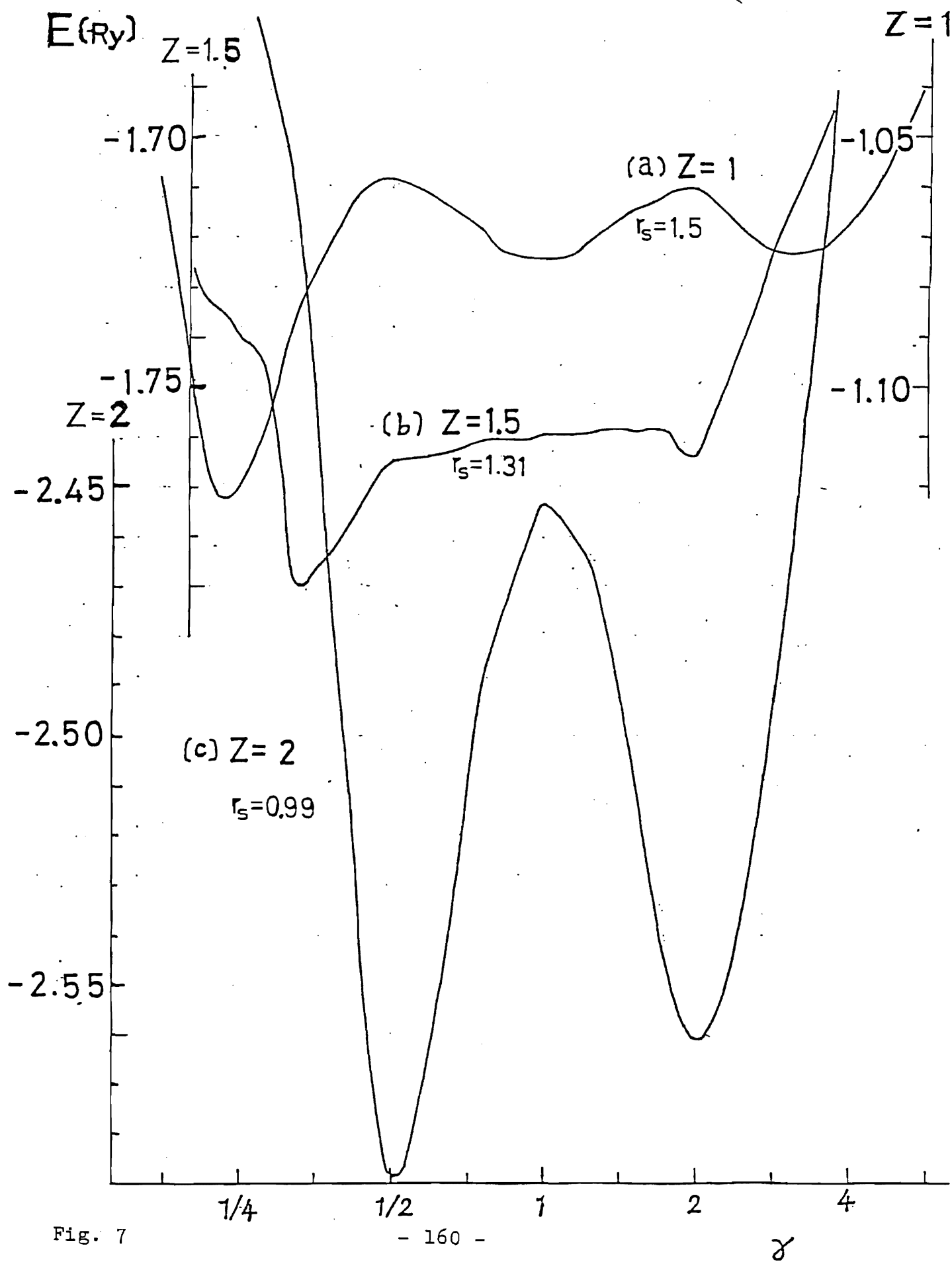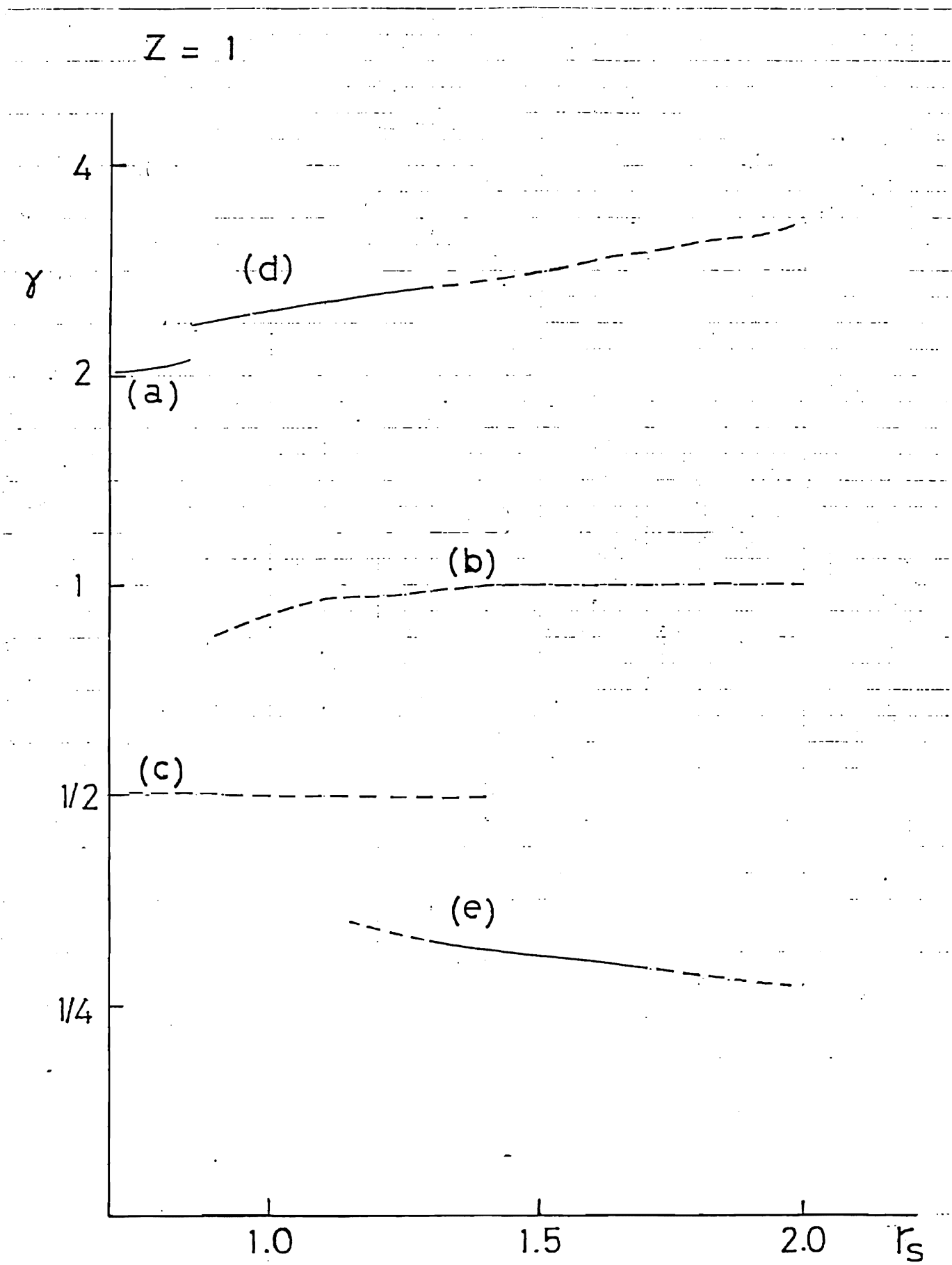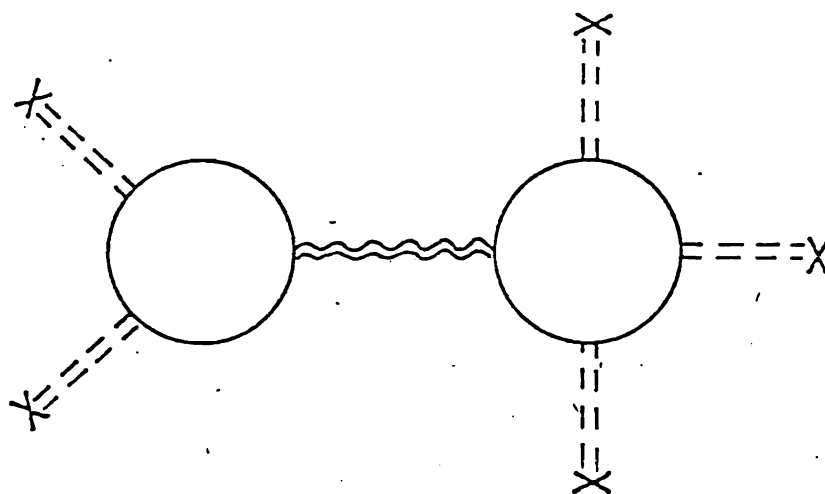
Fig. 6b

Z = 1.5

$r_s = 0.83$
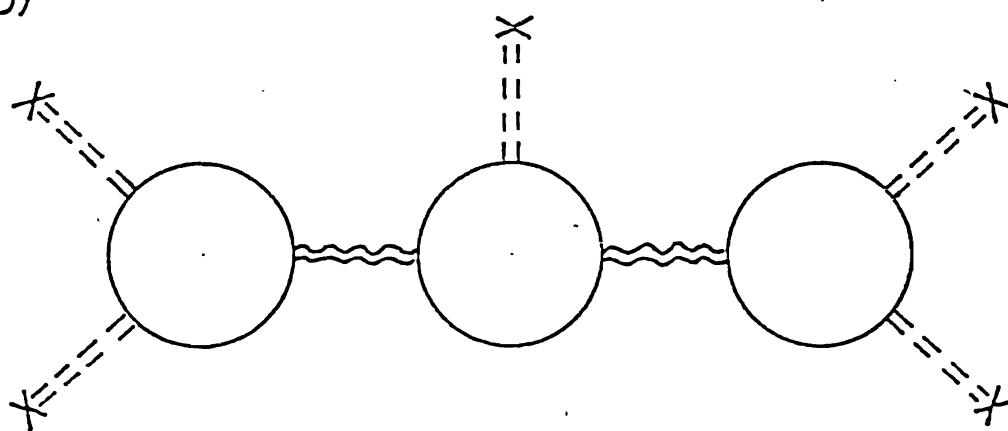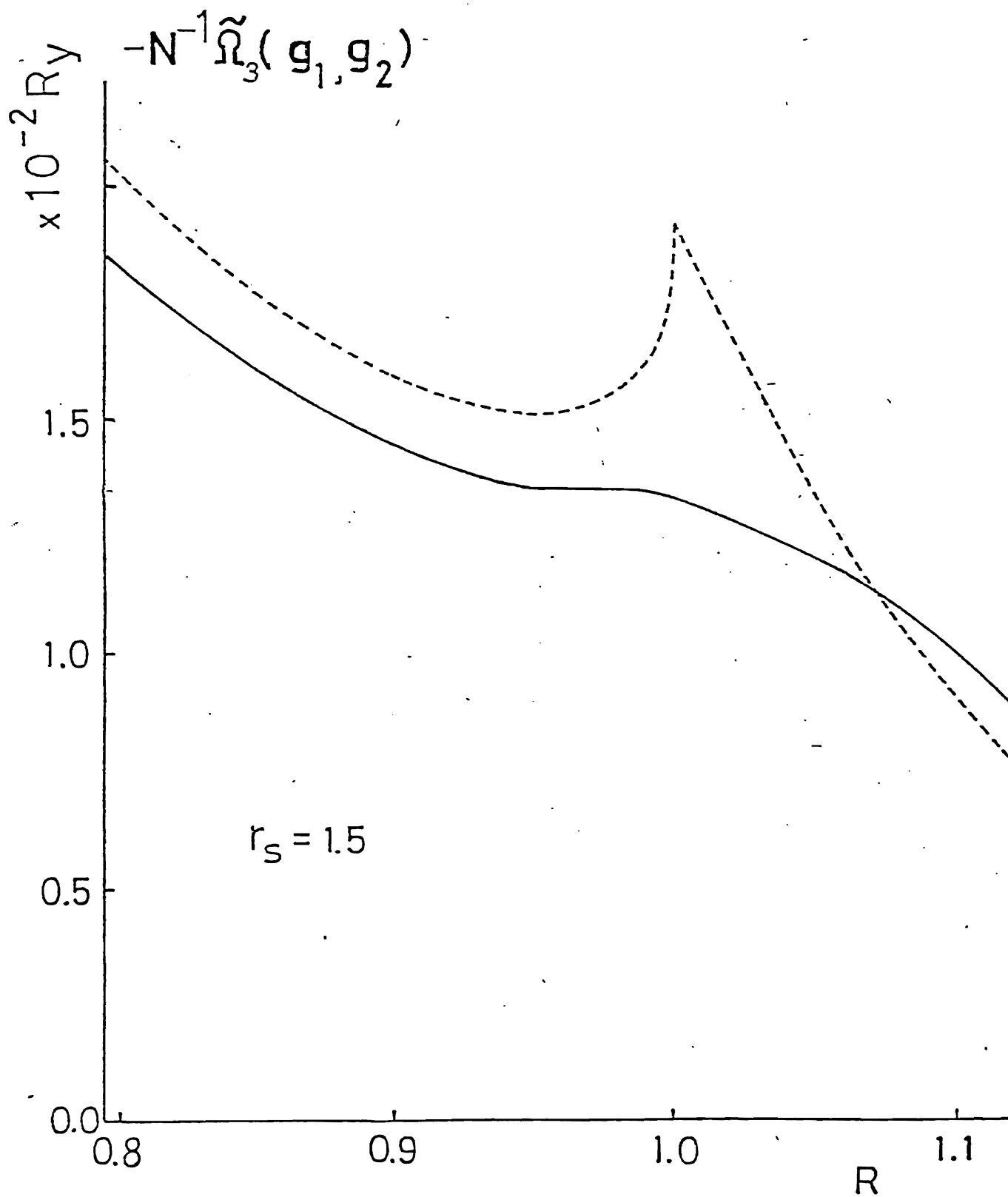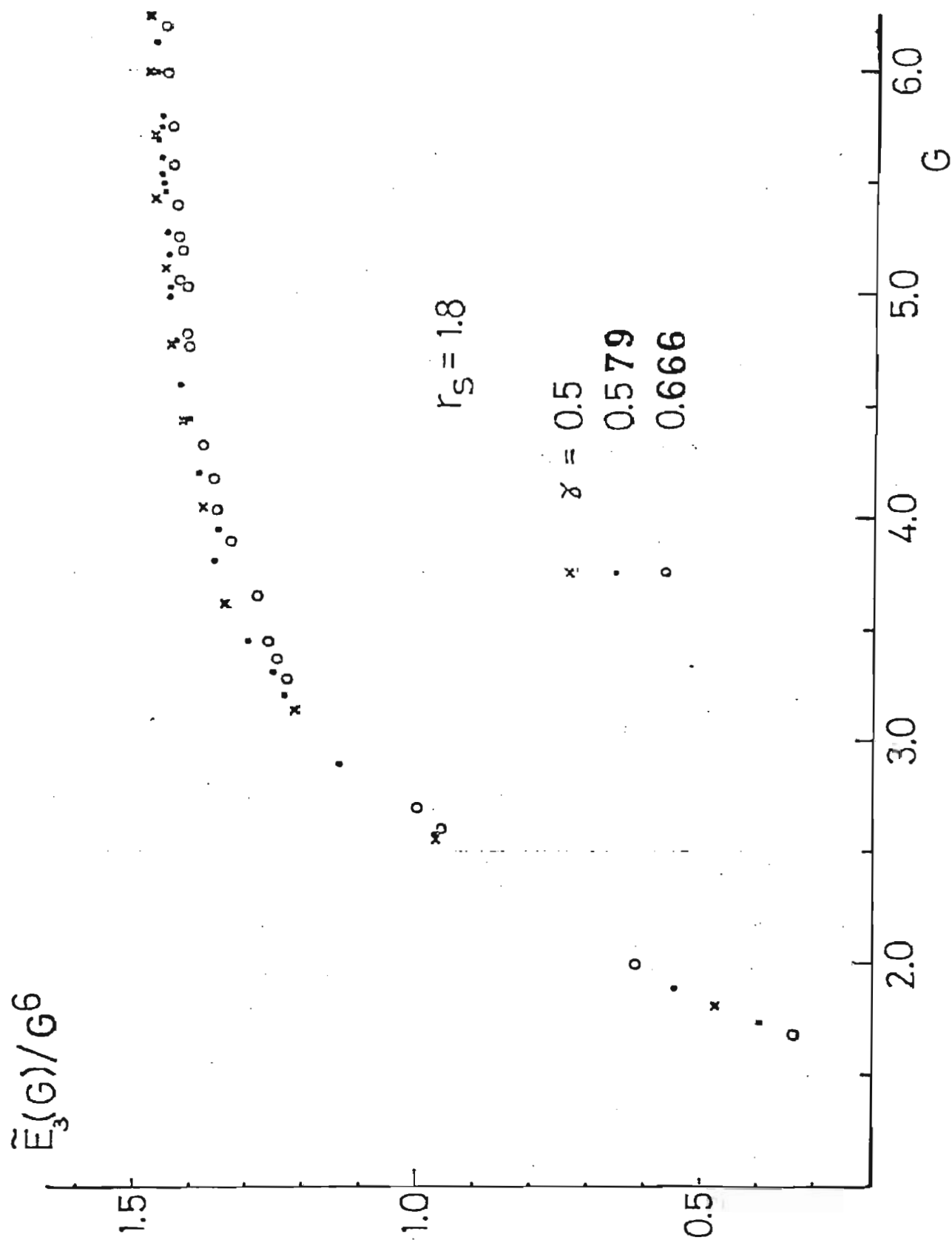
1.01

1.18

1.40
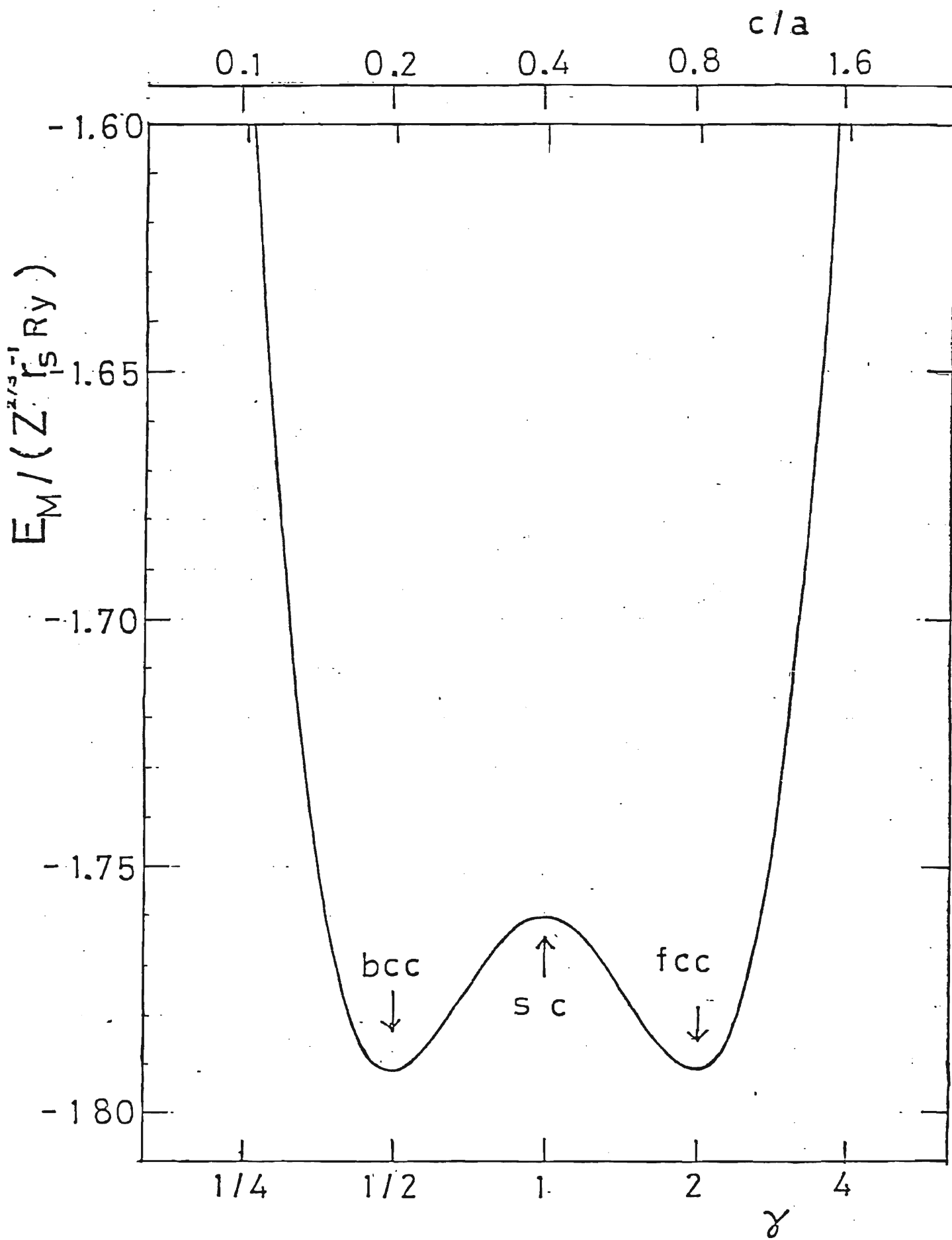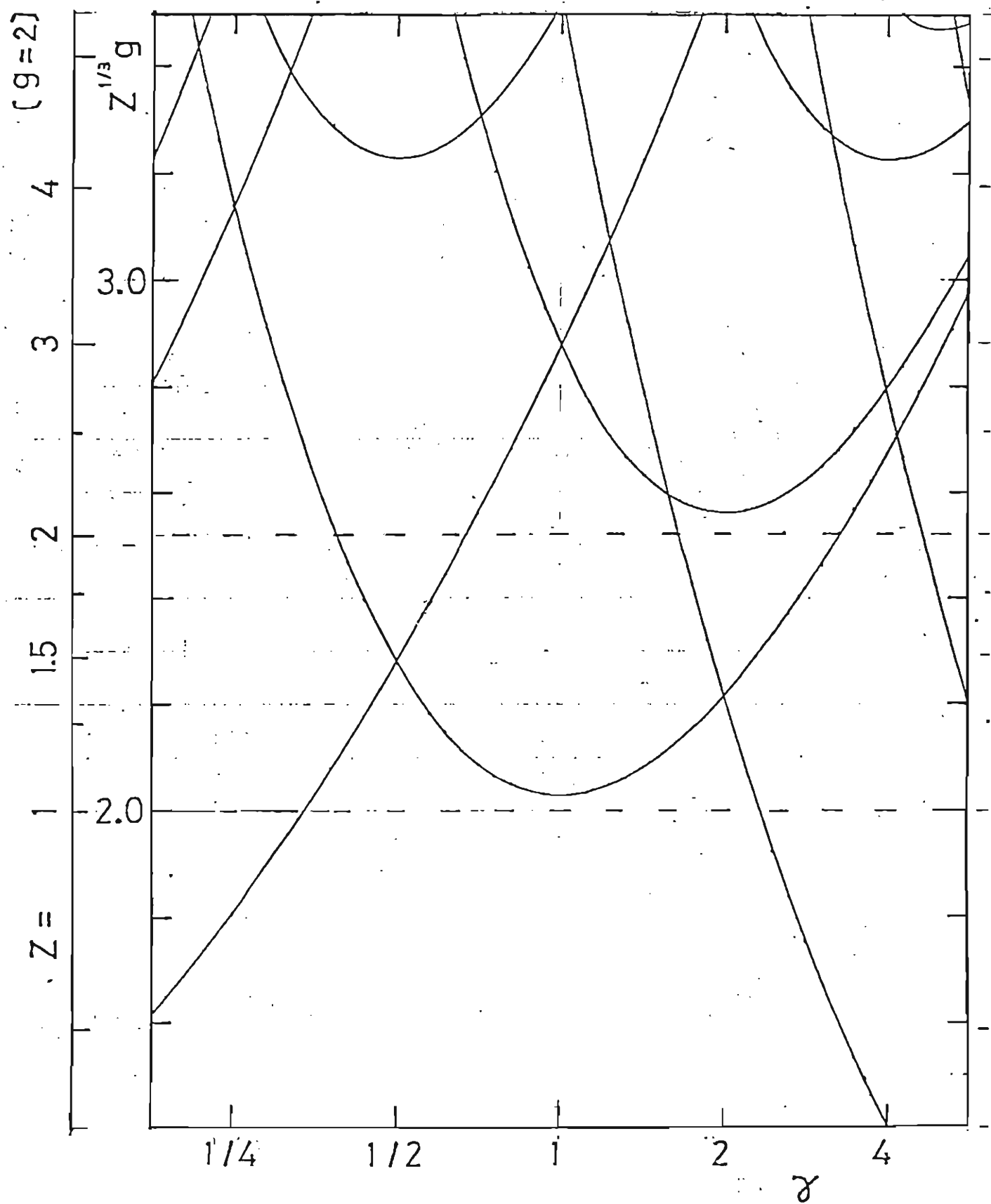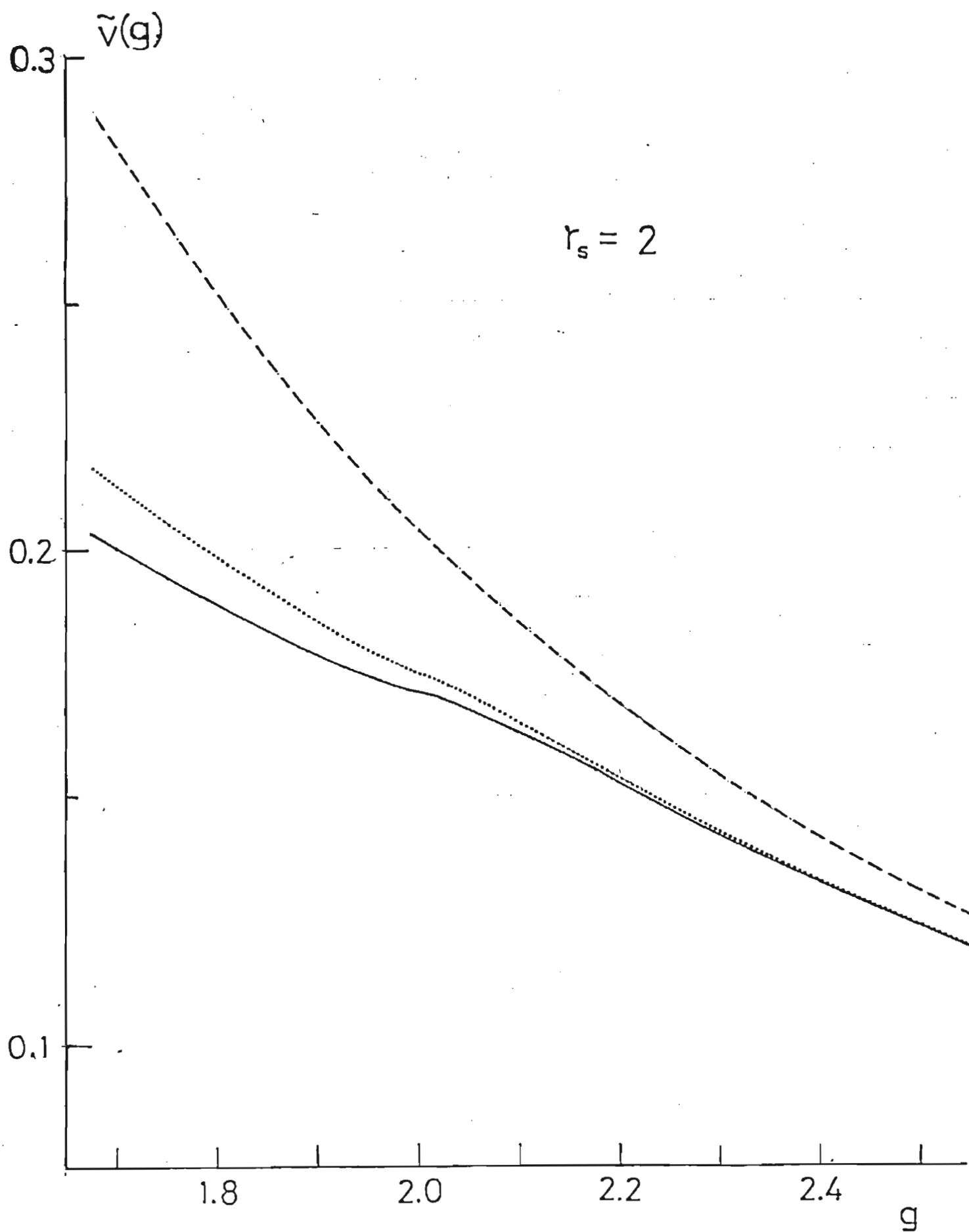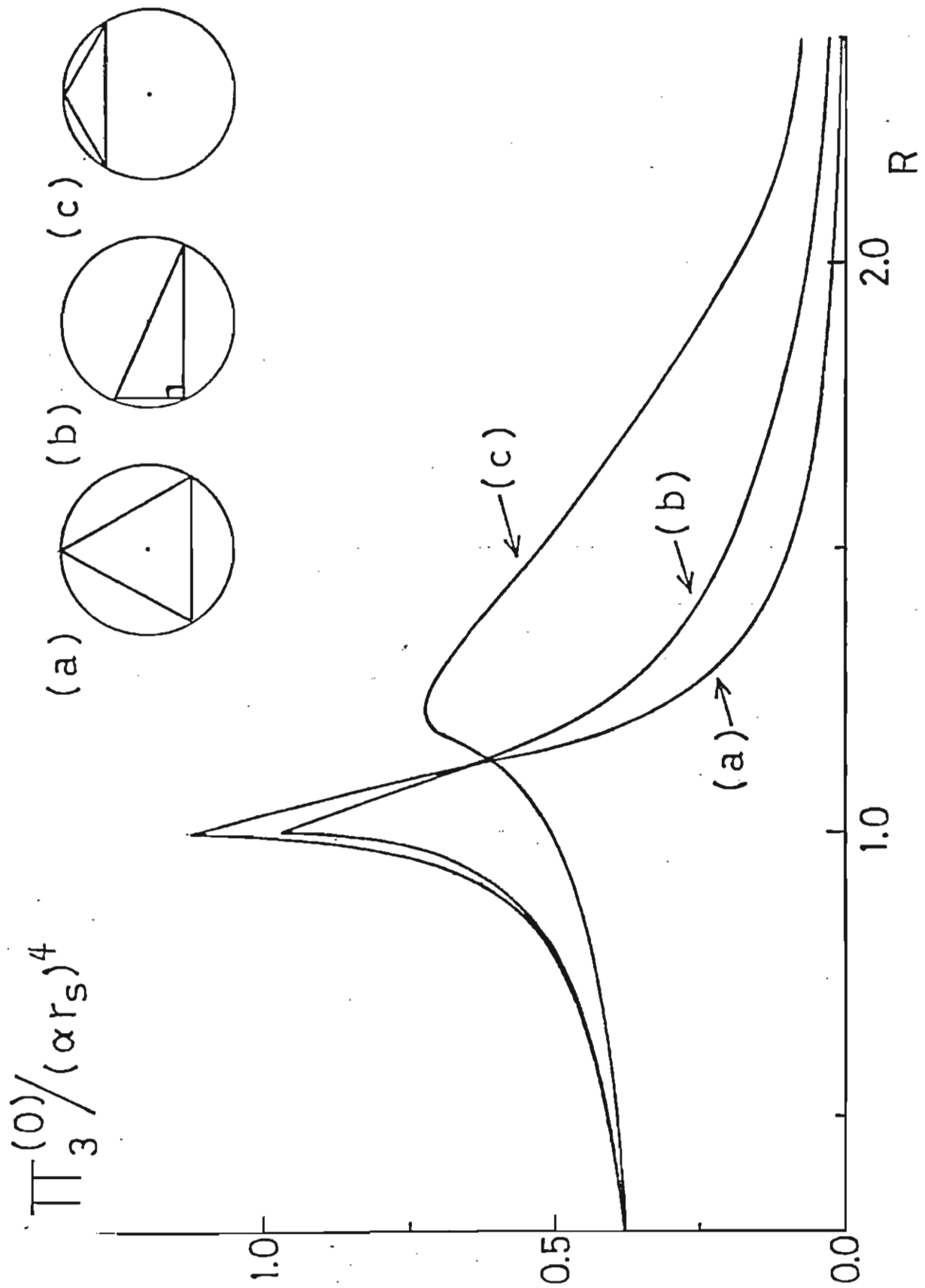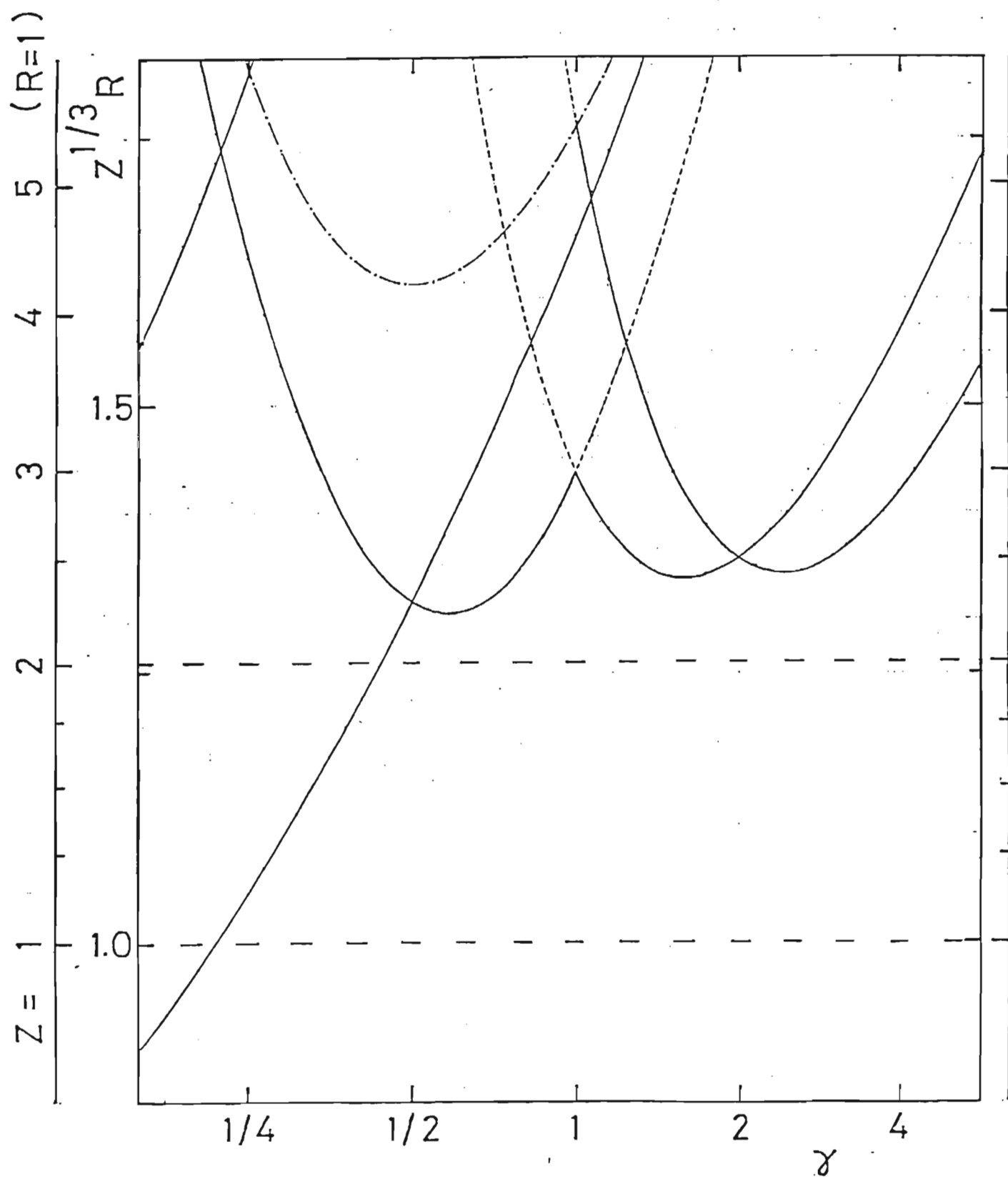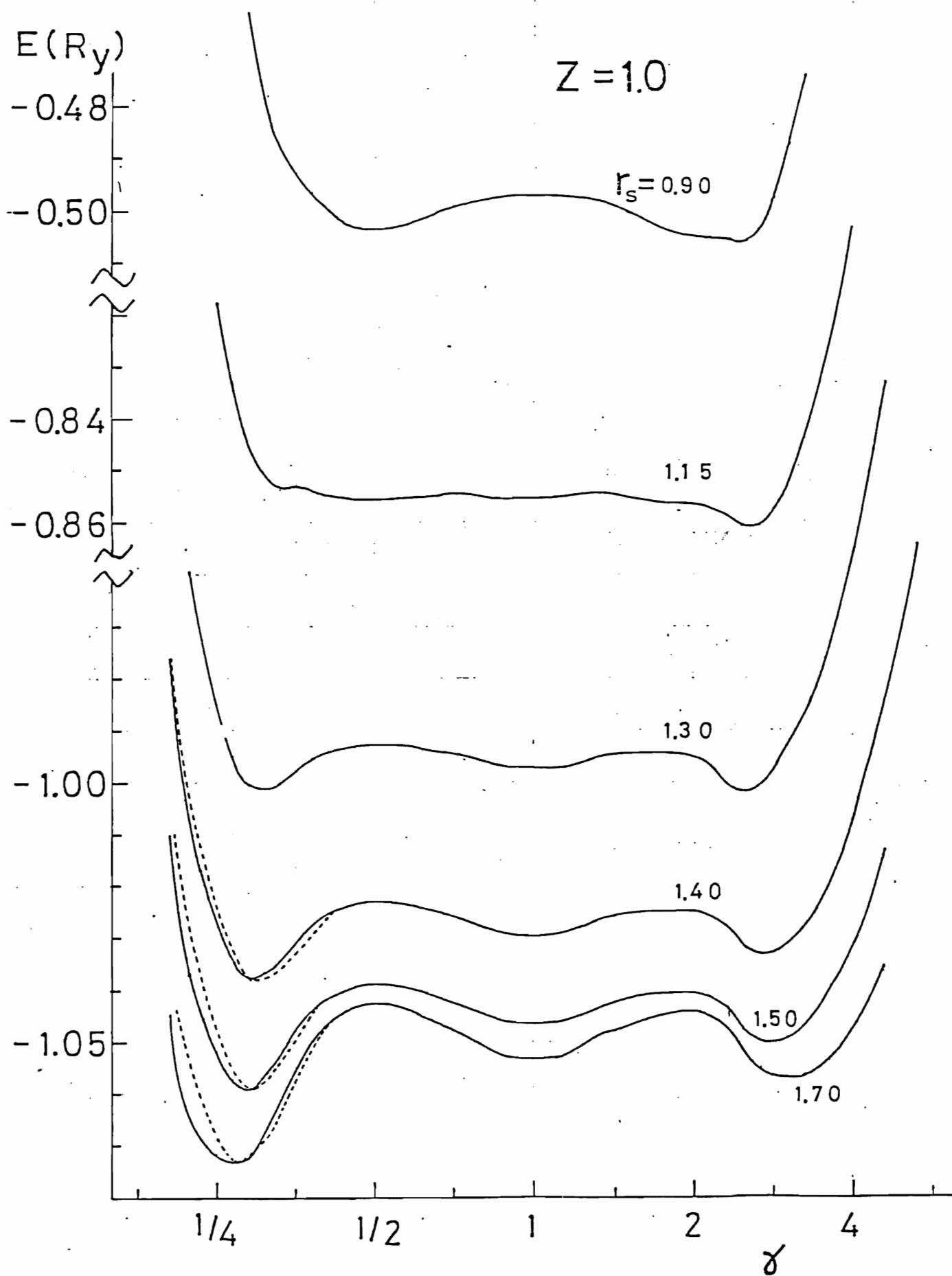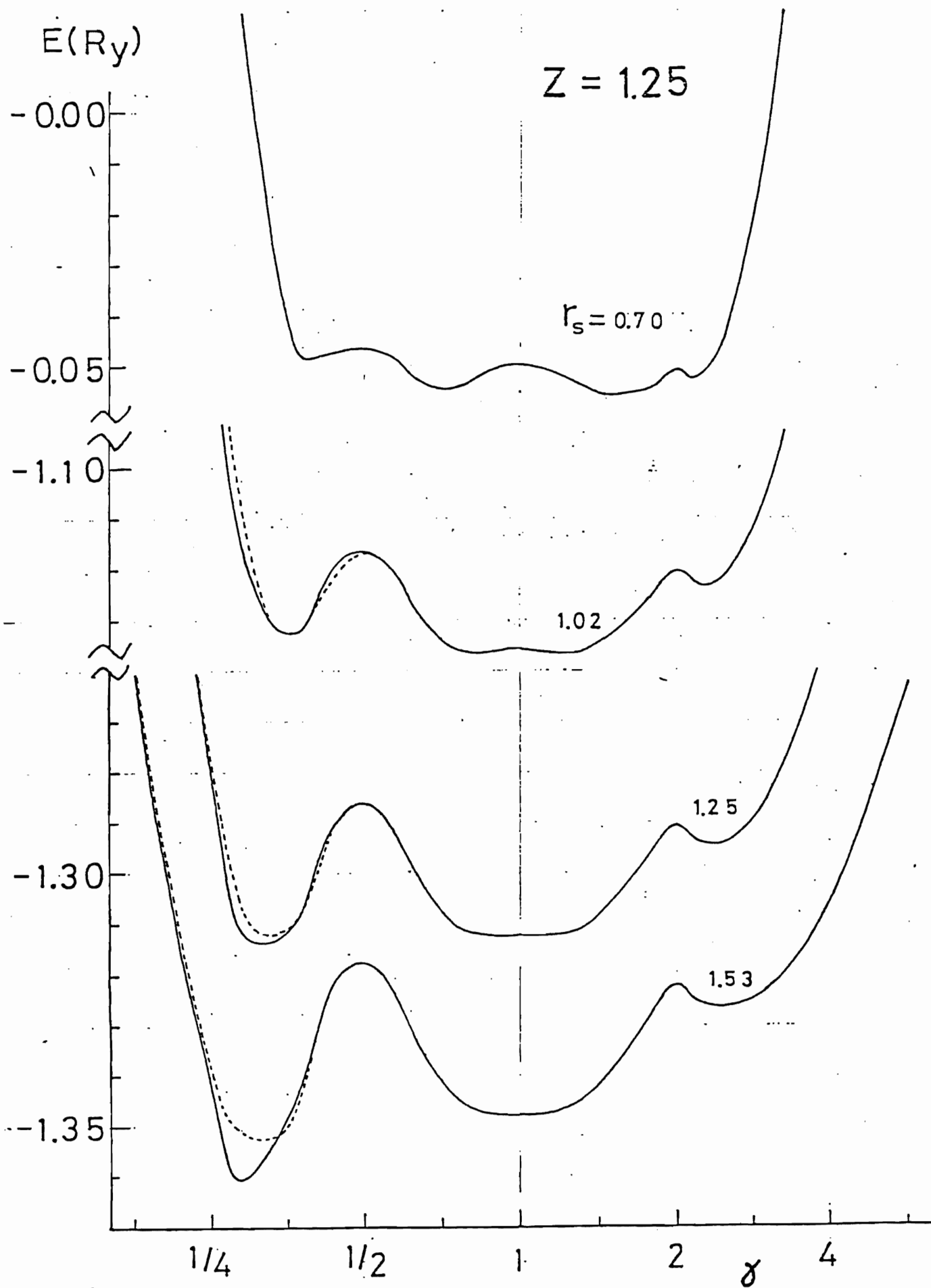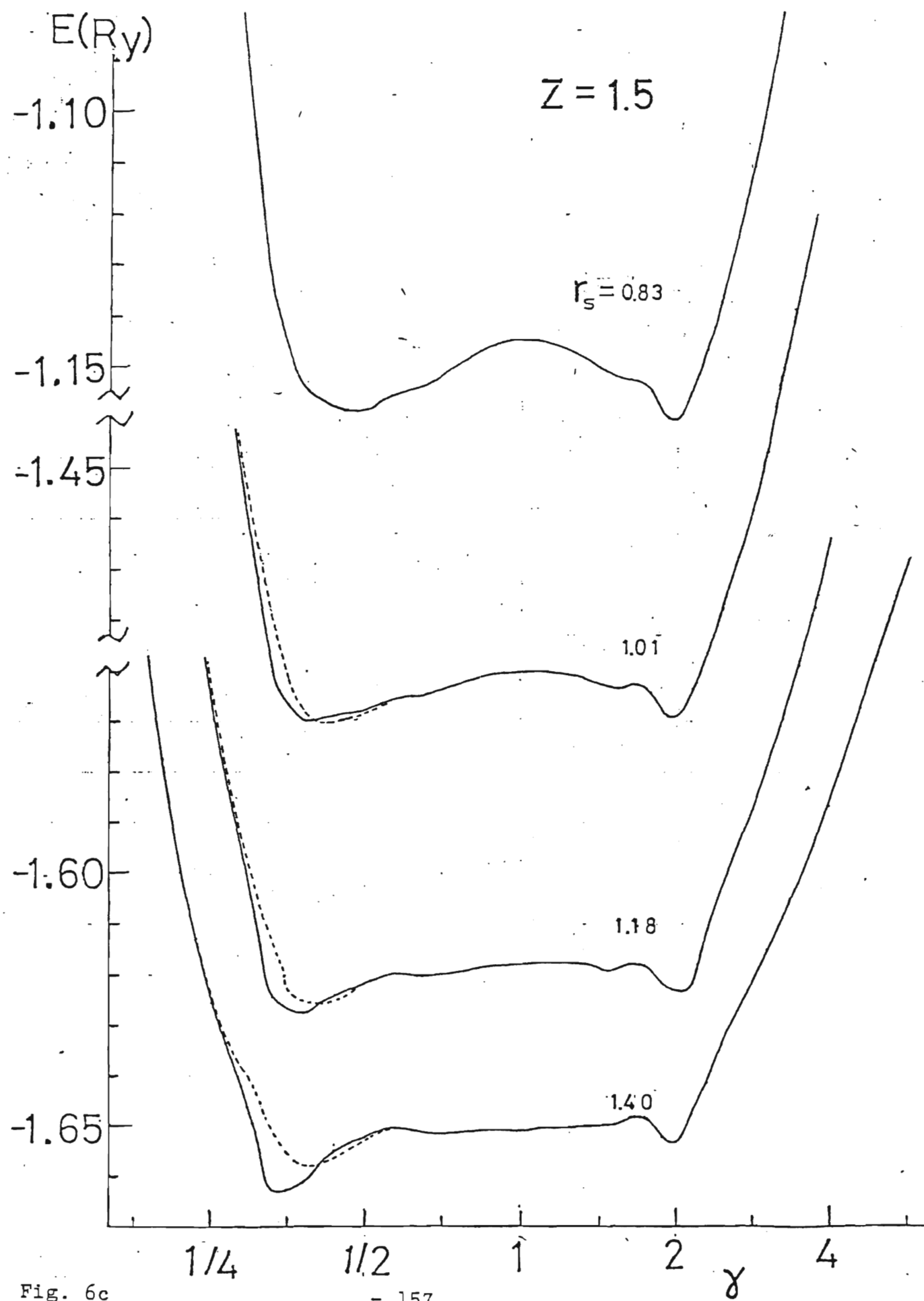
Fig. 6c
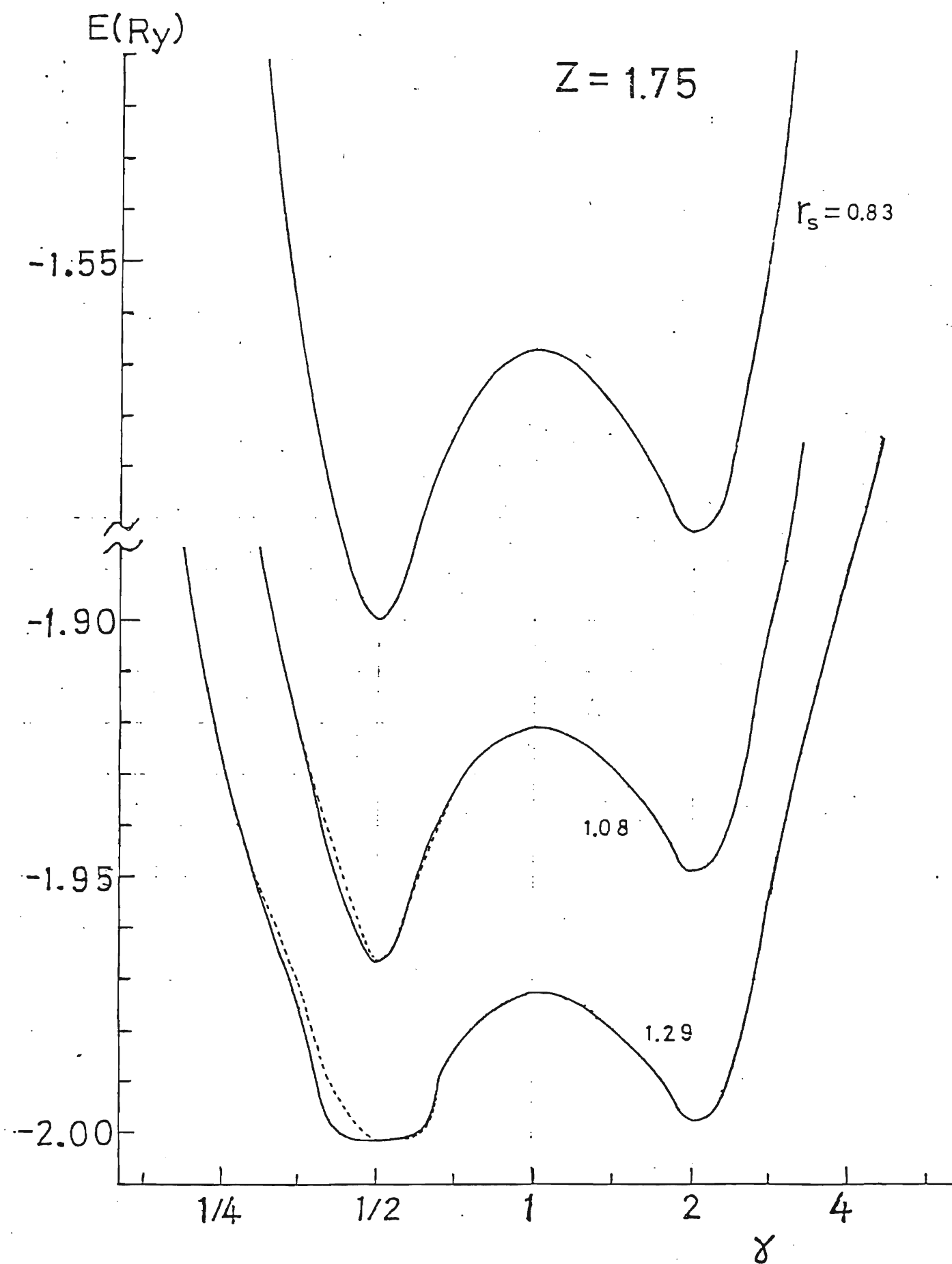
Fig. 6d
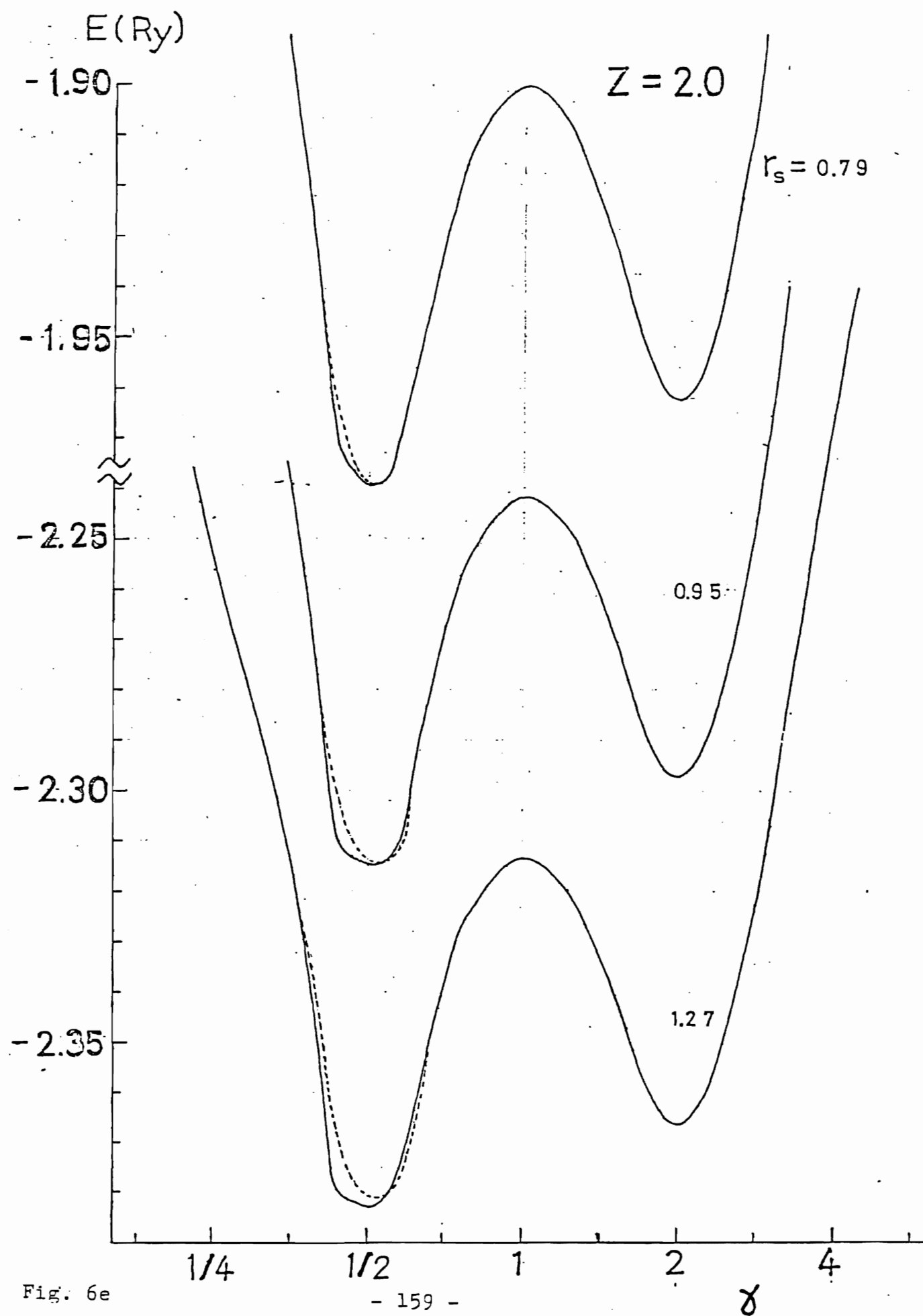
Fig. 6e

Fig. 7

Fig. 8

(a)

(b)

Fig. 9

Fig. 10

Fig. 11

Fig. 12a   - 165 -

Fig. 12b
- 166 -